VOLUME 81 NUMBER 5

THE ASTROPHYSICAL JOURNAL

AN INTERNATIONAL REVIEW OF SPECTROSCOPY AND ASTRONOMICAL PHYSICS

Founded in 1895 by GEORGE E. HALE *and* JAMES E. KEELER

Edited by

EDWIN B. FROST
Yerkes Observatory of the University of Chicago

FREDERICK H. SEARES
Mount Wilson Observatory of the Carnegie Institution of Washington

HENRY G. GALE
Ryerson Physical Laboratory of the University of Chicago

OTTO STRUVE
Yerkes Observatory of the University of Chicago

JUNE 1935

THE UNIVERSITY OF CHICAGO PRESS
CHICAGO, ILLINOIS, U.S.A.

June 1935 Vol. 81, No. 5

THE ASTROPHYSICAL JOURNAL

AN INTERNATIONAL REVIEW OF SPECTROSCOPY AND ASTRONOMICAL PHYSICS

Founded in 1895 by GEORGE E. HALE *and* JAMES E. KEELER

The Astrophysical Journal is published by the University of Chicago at the University of Chicago Press, 5750 Ellis Avenue, Chicago, Illinois, during each month except February and August. ¶ The subscription price is $6.00 a year; the price of single copies is 75 cents. Orders for service of less than a half-year will be charged at the single-copy rate. ¶ Postage is prepaid by the publishers on all orders from the United States, Mexico, Cuba, Porto Rico, Panama Canal Zone, Republic of Panama, Dominican Republic, Canary Islands, El Salvador, Argentina, Bolivia, Brazil, Colombia, Chile, Costa Rica, Ecuador, Guatemala, Honduras, Nicaragua, Peru, Hayti, Uruguay, Paraguay, Hawaiian Islands, Philippine Islands, Guam, Samoan Islands, Balearic Islands, Spain, and Venezuela. ¶ Postage is charged extra as follows: for Canada and Newfoundland, 30 cents on annual subscriptions (total $6.30); on single copies, 3 cents (total 78 cents): for all other countries in the Postal Union, 80 cents on annual subscriptions (total $6.80), on single copies, 8 cents (total 83 cents). ¶ Patrons are requested to make all remittances payable to The University of Chicago Press, in postal or express money orders or bank drafts.

The following are authorized agents:

For the British Empire, except North America, India, and Australasia: The Cambridge University Press, Fetter Lane, London, E.C. 4. Prices of yearly subscriptions and of single copies may be had on application.

For Japan: The Maruzen Company, Ltd., Tokyo.

For China: The Commercial Press, Ltd., 211 Honan Road, Shanghai. Yearly subscriptions, $6.00; single copies, 75 cents, or their equivalents in Chinese money. Postage extra, on yearly subscriptions 80 cents, on single copies 8 cents.

Claims for missing numbers should be made within the month following the regular month of publication. The publishers expect to supply missing numbers free only when losses have been sustained in transit, and when the reserve stock will permit.

Business correspondence should be addressed to The University of Chicago Press, Chicago, Illinois.

Communications for the editors and manuscripts should be addressed to: Otto Struve, Editor of THE ASTROPHYSICAL JOURNAL, Yerkes Observatory, Williams Bay, Wisconsin.

The cable address is "Observatory, Williamsbay, Wisconsin."

The articles in this journal are indexed in the *International Index to Periodicals*, New York, N.Y.

Applications for permission to quote from this journal should be addressed to The University of Chicago Press, and will be freely granted.

Entered as second-class matter, January 17, 1895, at the Post-Office, Chicago, Ill., under the act of March 3, 1879.
Acceptance for mailing at special rate of postage provided for in Section 1103, Act of October 3, 1917, authorized on July 15, 1918.

PRINTED IN THE U.S.A.

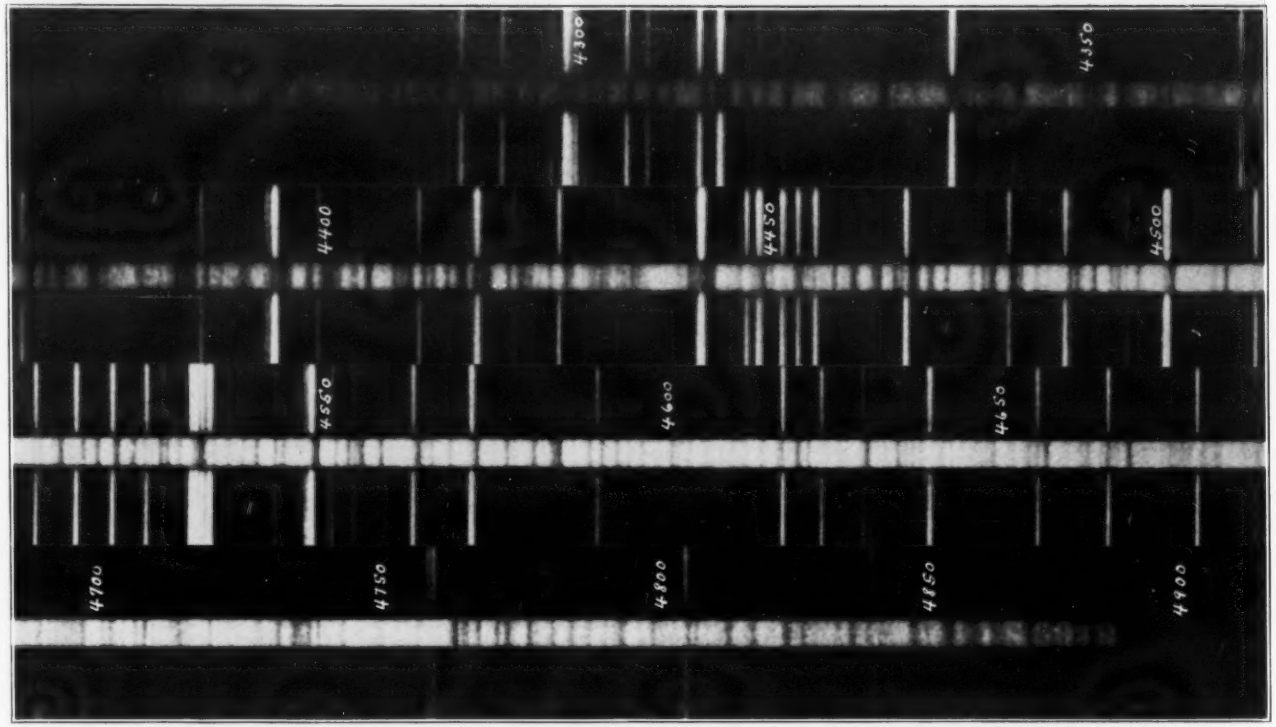

Direct Enlargement of a Spectrogram of R Coronae Borealis Taken at the Lick Observatory on July 19, 1932 (6.0 Mag.)

THE ASTROPHYSICAL JOURNAL

AN INTERNATIONAL REVIEW OF SPECTROSCOPY AND ASTRONOMICAL PHYSICS

VOLUME 81 JUNE 1935 NUMBER 5

THE SPECTRUM ANALYSIS OF THE HOT CARBON STAR, R CORONAE BOREALIS

By LOUIS BERMAN

ABSTRACT

A detailed investigation of the spectrum of the irregular variable R Coronae Borealis, in the region λλ 4300–4900 was undertaken for the purpose of studying the physical conditions of its atmosphere. The wave-lengths of approximately 650 lines were measured on the Lick three-prism spectrograms and the corresponding elements identified. Only 2 per cent of the lines belong to the non-metals. The average radial velocity of the system is +25.1 km/sec. and is slightly variable at the time of maximum light (6.0 mag.).

A calibration-curve, based upon the theoretical intensity ratios of supermultiplets, connects the observed line intensities and the absolute numbers of atoms engaged in their production. The chemical composition of the atmosphere is found to be 69 per cent carbon, 27 per cent hydrogen, less than 0.3 per cent nitrogen, and 4 per cent metals (chiefly magnesium and iron). (The theoretical abundance of the carbon molecule, C_2, whose appearance is feebly indicated by the Swan spectrum, is 0.00003 per cent.)

With these compositions and the value of the general atomic absorption coefficient derived from wave-mechanics, the computed optical depth of the photospheric level is 0.006. This improbably small value may result from the incomplete state of the theory at the present time and from the neglect of molecular opacity arising from dissociation.

The Russell-Adams analysis, used to determine the absolute temperature, does not reveal any marked deviation from thermodynamic equilibrium up to an excitation potential of 10 volts. The energy distribution of the continuous spectrum leads to a higher color temperature in the red than in the blue, but the difference may arise from the difficulty of drawing the true continuous background, owing to the peculiarity of the spectrum. The color temperature in the blue is found to be over 1000° higher than the effective temperature.

Finally, the physical parameters that define the state of the atmosphere are presented: spectral class, cF7p; effective temperature, 5300° K; color temperature, 6700° K (λλ 3500–4500), 7700° K (λλ 4500–6500); electron pressure at base of reversing layer, 8.3×10^{-7} atm., mean total pressure, 9.3×10^{-6} atm.; level of ionization, 9.6 volts; surface gravity, 2.7×10^{2} cm/sec.^{2}; mean molecular weight, 10 chemical units; velocity of turbulence, 10 km/sec.; number of neutral atoms above 1 sq. cm of surface, 4.4×10^{21}, corresponding number of ionized atoms, 2.3×10^{20}, corresponding total number of all particles, 4.9×10^{21}.

Among the irregular variables R Coronae Borealis (1900; $\alpha = 15^h44.5^m$, $\delta = 28°28'$) has long been of outstanding interest[1] on account of the capricious and wholly unpredictable behavior of the light of this star. Normally of the sixth magnitude, it may, occasionally, after a preliminary period of minor fluctuations, or even without any warning, suddenly drop to the thirteenth magnitude during one of its spectacular depressions. Whether the minimum is of short or long duration, the ascent to normal brightness is generally less rapid than the descent. There is some evidence that the slower the decline in light, the more protracted is the minimum.

A practically uninterrupted record of the light-curve since 1843 is now available,[2] together with a number of fragmentary observations preceding this date. Today the star is being constantly watched. Modern observations have apparently established the fact, long suspected, that even at maximum small variations of the order of 0.2 or 0.3 mag. take place continually.

An obvious prerequisite for interpretation of the light-variations is a study of the composition and conditions of the atmosphere during normal light. The present investigation presents an account of an analysis from the spectroscopic material previously available at Harvard and Mount Wilson together with additional spectrograms secured by the writer at the Lick Observatory.

A tabular list of the observational material furnished by the Harvard objective-prism plates, the Mount Wilson one-prism, and the Lick one-, two-, and three-prism spectrograms is shown in Table I. The table is self-explanatory. An asterisk in the second column denotes that no microphotometer run of that plate was secured.

On small-scale objective-prism spectrograms the spectrum of R Coronae, although obviously peculiar, admits of no easy interpretation. For example, at Harvard,[3] during periods of maximum brightness, it has at different times apparently resembled types F, G, K, or M, while Espin,[4] observing visually in 1890 and 1893 with small

[1] Since 1795 when Pigott, the English astronomer, discovered its inconstancy.

[2] Ludendorff, *Pub. Potsdam Obs.*, **19**, No. 57, 1909; Campbell, *Harvard Circ.*, No. 247, 1923.

[3] *Harvard Ann.*, **27**, 1890; **55**, 1907–1909; **56**, 107, 1912; **96**, 228, 1921.

[4] *M.N.*, **51**, 12, 1890; *A.N.*, **134**, 127, 1894; **152**, 139, 1900.

TABLE I

JOURNAL OF OBSERVATIONS

Date	Exp. Time	Mag.	Spectral Region	Note
	Harvard Series			
1888 June 9	79^m	6.2	3900–5000	A
1890 April 25	63	6.0	3900–5000	B
April 28	61	6.0	3900–5000	B
April 30	66*	6.0	3900–5000	B
1892 April 19	68	6.8	3900–5000	B
April 24	69	6.8	3900–5000	B
April 26	61	6.8	3900–5000	B
Sept. 2	56*	8.2	3900–5000	B
Sept. 12	60	7.4	3900–5000	B
Sept. 17	65	7.0	3900–5000	B
Sept. 20	59*	6.8	3900–5000	B
1893 Feb. 27	69*	6.2	3900–5000	B
1901 May 12	111	5.8	3900–6500	C
June 4	90	5.8	3900–6500	C
June 5	119	5.8	3900–6500	C
June 12	109	5.8	3900–6500	C
1914 April 21	61	5.8	3900–5000	D
	Mount Wilson Series			
1922 Feb. 5	61	6.2	3900–5000	E
Feb. 18	25	6.2	4700–6700	F
March 8	86	6.1	3900–5000	E
May 5	65*	6.1	3900–5000	E
July 5	80	6.0	3900–5000	E
1923 May 17	240*	12.3	3900–5000	G
May 24	325	11.3	3900–5000	H
June 10	350	10.2	3900–5000	I
June 24	20	8.0	3900–5000	H
	Lick Series			
1932 June 28	2, 6	6.0	3400–5000	J
July 2	10	6.0	3600–7000	J
July 5	6, 12	6.0	3600–7000	J
July 23	8, 13	6.0	3600–7000	J
July 24	10	6.0	3600–7000	J
July 24	5, 10	6.0	3600–7000	J
July 24	10	6.0	3600–7000	J
July 31	3, 14	6.0	3600–7000	J
Aug. 6	3, 10	6.0	3400–5000	J
Aug. 10	3, 8	6.0	3400–5000	J

TABLE I—*Continued*

Date	Exp. Time	Mag.	Spectral Region	Note
	Lick Series—*Continued*			
1932 June 27	160	6.0	4300–4900	K
July 4	150	6.0	4300–4900	K
July 19	180	6.0	4300–4900	K
July 29	180	6.0	4300–4900	K
Aug. 8	180	6.0	4300–4900	K
Aug. 9	180*	6.0	4300–4900	K
Aug. 27	150*	6.0	4300–4900	K
1933 Aug. 24	30	6.0	3900–5000	L

A. 8″ Bache refr.; obj. prism; disp. 5.8 mm ($H\beta$–$H\epsilon$).
B. 8″ Draper refr.; obj. prism; disp. 5.6 mm ($H\beta$–$H\epsilon$).
C. 11″ Draper refr.; obj. prism; disp. 19.6 mm ($H\beta$–$H\epsilon$).
D. 16″ Metcalf refr.; obj. prism; disp. 3.9 mm ($H\beta$–$H\epsilon$).
E. 60″ Refl.; disp. 1 mm = 33 A at $H\gamma$.
F. 100″ Refl.; disp. 1 mm = 75 A at λ 5200; 150 A at $H\alpha$.
G. 60″ Refl.; slitless spectrogram.
H. 100″ Refl.; disp. 1 mm = 75 A at $H\gamma$.
I. 60″ Refl.; disp. 1 mm = 75 A at $H\gamma$.
J. 36″ Refl.; 2-prism quartz slitless spectrograph; disp. 1 mm = 100 A at $H\gamma$.
K. 36″ Refr.; 3-prism spectrograph; disp. 1 mm = 10 A at λ 4500.
L. 36″ Refr.; 1-prism spectrograph; disp. 1 mm = 76 A at $H\gamma$.

dispersion, describes startling changes in the spectrum at times when there was little variation in light.

Frost[5] and Ludendorff[6] have remarked on the similarity of the spectrum to that of α Persei (cF5). The latter, however, noted a most important feature of the spectrum, later verified by Frost, viz., the apparent absence of the Balmer series either in absorption or in emission. Fraunhofer's G band had previously been found lacking as a distinct absorption band on the Harvard plates. Adams and Joy[7] pointed out that at maximum brightness the spectrum resembles that of the brightest Cepheids, and they accordingly classified it as cGop. On the Lick three-prism spectrograms a resemblance to α Ursae Minoris (cF8) was noted,[8] but the final classification during

[5] *Ap.J.*, **22**, 215, 1905.
[6] *Loc. cit.*; *A.N.*, **201**, 439, 1915; *Handbuch der Astrophysik*, **6**, Part II, 73, 1928.
[7] *Pub. A.S.P.*, **35**, 325, 1923. [8] *Ibid.*, **45**, 55, 1933.

the constant phase, as determined from the present investigation, is cF7p.

The confusion in classification is directly traceable, in the writer's opinion, to the scarcity of atmospheric hydrogen, coupled with the abnormal abundance of atomic and molecular carbon, the latter giving rise to the well-known system of Swan bands. This phenomenon gives the spectrum on plates of small dispersion a lumpy appearance, thus adding greatly to its complexity. In fact, so banded is the spectrum that the occasional clear gaps of the continuous background stand out like emission lines.

The situation is different with the high-dispersion spectrograms where the details are more legible. Here at maximum the spectrum is characterized by the strong enhanced lines of the metals and the rare earths. The metallic arc lines are weak; of these, *Fe* maintains the greatest strength generally throughout the spectrum. The hydrogen lines are so faint that their presence is detected only with considerable difficulty on microphotometer tracings, while two neutral carbon multiplets (E.P. = 7.45) are very strong. These are by far the greatest peculiarities of the spectrum. No strong lines of neutral *N* or *O* exist in the observed region of the spectrum. The spectral lines are sharp, deep, and of greater width than the solar lines, suggesting an extensive atmosphere.

Although approximately 650 lines were measured on the Mills spectrograms between λ 4300 and λ 4900, it is probable that the actual number of lines in that region may be as high as 1000, with the non-metals contributing not more than 2 per cent of the total.

A detailed account of the appearance of the spectrum has been arranged in the form of notes furnished mainly, excepting the Espin series, from an examination of the tracings and the original negatives.

THE ESPIN SERIES

The visual observations by the Reverend T. E. Espin[9] at Wolsingham with various spectroscopes do not permit definite identifications of wave-length, but the remarkable changes which he observed in 1890 deserve mention. They are quoted verbatim and are followed by the writer's remarks in brackets.

[9] *Loc. cit.*

APRIL 10, 1890. Mag. 6.0. Continuous spectrum, but again suspected lines, one bright one strongly suspected near the place of F but believed more refrangible. [This bright line may be the maximum apparent in the continuous spectrum at 4750.]

SEPTEMBER 8, 1890. The magnitude is still about 6. A most wonderful change has taken place in this star's spectrum. Two large absorption bands have appeared, one in the bluish-green, and one in the bluish-violet. These bands are sharply defined on the least refrangible side. . . . . Bright patches were seen far away in the violet. These may be bright lines or bright spaces. [Apparently the blue-violet band is to be associated with the Swan band at 4382 and the blue-green with 4737.]

SEPTEMBER 14, 1890. Mag. 6.0. The spectrum is apparently of the IV type since the bands fade away on the more refrangible side, but are sharply defined on the less refrangible. The band in the bluish-green was thought to be occasionally resolved into fine lines; between the two bands a bright line was suspected. [No clue as to the identity of the supposed bright line.]

OCTOBER 8, 1890. Mag. 6.0. . . . . The bands seem to have faded.

OCTOBER 10, 1890. Mag. 6.0. The star has now nearly returned to the continuous first-type spectrum observed in the spring. The big band in the bluish-green has disappeared, but the band in the violet is probably still there, but faint. The bright line previously mentioned again suspected.

THE HARVARD SERIES

Since many of the Harvard plates have already been amply described by Miss Cannon[10] during the progress of the Draper classification, they need not concern us here. The 1901 series, however, is of particular interest owing to the positive identification of the Swan bands.

MAY 12–JUNE 12, 1901. Mag. 5.8. A large number of absorption lines are visible, many of which are due to the enhanced metals. The hydrogen lines appear to be absent. The spectrum is generally depressed except at the "high spots" occurring at 4100, 4260, 4500, 4570, 5170, and 5640. The Swan bands of the -1 sequence from 4737 to 4685 cut a wide absorption swath in the spectrum as do the bands of the $+1$ sequence appearing at 5635–5501. The band at 5165 shows the greatest strength. In no instance are any of the bands comparable in intensity with those found in the N-type stars. Their complete identification followed from a study of the tracings rather than from the original plates.

Table II gives the wave-lengths of the heads and corresponding vibrational transitions of the Swan system.[11] The laboratory intensities are in parentheses.

[10] See n. 3.

[11] Kayser, *Handbuch der Spectroskopie*, **8**, 300, 1932.

PLATE VIII

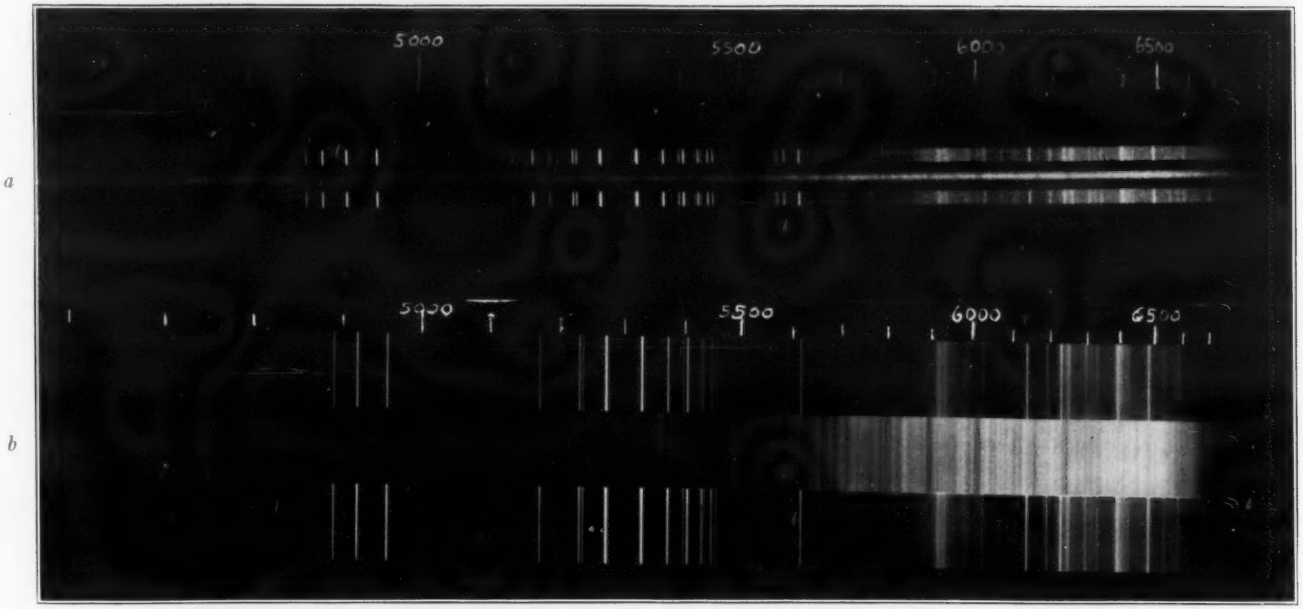

Spectrum of R Coronae Borealis Taken at the Mount Wilson Observatory on February 18, 1922 (6.2 Mag.)
a) direct enlargement; *b*) vertical enlargement

According to Jevons,[12] the dissociation potential of C_2 is 5.5 volts. The Swan spectrum arises from the electronic transition $B^3\pi$–$A^3\pi$, where $A^3\pi$ is the lowest-known state of the molecule and $B^3\pi$ is 2.4 volts higher. Professor Russell has pointed out that this is probably the resonance system of the C_2 carrier because of the enormous strength attained by the Swan bands in the spectra of the very low-temperature N-stars.

THE MOUNT WILSON SERIES

FEBRUARY 5–JULY 5, 1922. Mag. 6.0. On the red-sensitive plate secured by Merrill on February 18, the neutral lines of *Fe* and *Ca* dominate the spectrum. The D lines exhibit great strength. The Swan band at 5165, degrading to the violet, is strong, but the sharp edge that lies at 5176 is blended with the *Mg* b-triplet. Very feeble bands are suspected at 5637, 6060, and 6123, agreeing approximately with the known bands of the C_2 molecule. There is a band of moderate intensity whose head is at 5587, degrading to the violet, along which the spectrum is depressed as far as 5360, and another band of moderate intensity with its edge at 5138 but with the maximum absorption at 5129. The continuous background remains generally depressed from 5176 with diminishing intensity up to 4976. The entire appearance of the spectrum in this region raises the question whether it should not be placed at the beginning of class R. The bands appear to be displaced slightly to the red in comparison with the observed laboratory bands even after allowance for the Doppler shift in the velocity of the star. Sanford[13] finds a similar red shift of about 0.7 A in the bands of the N-type stars, compared with laboratory wave-lengths.

TABLE II

THE SWAN SYSTEM OF C_2

v' \ v''	0	1	2	3	4	5	6	7
0	5165.2(10)	5635.5(2)	6191.2(2)	.....	.....	.....	.....	.....
1	4737.1(7)	5129.3(6)	5585.5(8)	6122.1(4)	.....	.....	.....	.....
2	4382.5(3)	4715.2(6)	5097.7(1)	5540.7(7)	6059.7(5)	6677.3	.....	.....
3	.....	4371.4(4)	4697.6(5)	.....	5501.9(4)	6004.9	6599.2	6533.7
4	.....	.....	4365.2(3)	4684.8(4)	.....	5470.3(2)	5958.7	5923.4
5	.....	.....	.....	.....	4678.6(2)	.....	5542	.....
6	.....	.....	.....	.....	.....	.....	.....	5423

In the blue region the spectrum shows strong similarity to that of γ Cygni (cF8). The atomic carbon multiplets at 4762 and 4812 seem to be stronger on March 8 than on February 5. $H\beta$ is probably present as a very weak absorption line, but there is no definite trace of $H\gamma$, although $H\delta$ may be faintly present on May 5.

[12] *Report on Band Spectra of Diatomic Molecules*, p. 282, 1932.

[13] *Pub. A.S.P.*, **41**, 271, 1931.

THE LICK SERIES

JUNE 28–AUGUST 27, 1932. Mag. 6.0. The slitless spectrograms obtained with the Crossley reflector exhibit on a larger scale practically all the features noted on the earlier Harvard objective-prism photographs. The following regions of the spectrum are depressed: 3750–3790?, 3860–3910, 4060–4100, 4110–4210, 4280–4430, 4450–4480, 4500–4600, 4620–4740, 4980–5175. Some of the "dips" coincide with the Swan bands, others are apparently due to the crowding of strong lines, and still others to ill-defined and unknown banded structures.

A minute comparison between R Coronae and γ Cygni reveals a number of differences existing in the two spectra for the region covered by the Mills plates —greater than one would expect for two stars of practically the same spectral class. The results of the comparison are given below in Table III. In the first two columns appear the wave-lengths, in the next two the respective line intensities (equivalent width in 0.01 A), followed in the last column by the known principal contributing elements in the spectrum of γ Cygni.

Unless systematic errors vitiate the intensities, which are none too accurate in the vicinity of the G band, there is fair evidence that the *CH* molecule is rather inconspicuous, if present, in the spectrum of R Coronae.

A number of discrepancies in the comparison of R Coronae and γ Cygni remain unaccounted for unless they are the products of observational errors which are not deemed likely for the majority of cases. It seems reasonable to connect many of them in some manner with unknown molecular radiations.

In none of the bands was there any variation of intensity observed during the period covered by the spectrograms. There is no evidence that the bands due to the C_2 isotopes at 4745 and 4752 are present in the spectrum.

WAVE-LENGTHS AND IDENTIFICATION OF ELEMENTS

To insure good resolution of the lines and yet not prolong the exposures immoderately, the slit width of the Mills spectrograph was set at 0.002 inch. The theoretical resolving power under these circumstances is such as just to separate lines 0.15 A apart. Actually, it was barely possible to distinguish a pair of lines of separation slightly under 0.2 A, provided they were not too intense. Consideration of the type of plate used (Imperial Eclipse) will indicate that this is satisfactory performance when allowance is made for grain scattering and other instrumental and photographic imperfections. The range covered by the three-prism spectrograms is from λ 4300 to λ 4890, with the prism set for minimum deviation at λ 4500.

For about 150 A from the red end and about 50 A from the violet, the lines are unfortunately somewhat out of focus, but the resulting intensities are believed to be preferable to those obtainable with inferior dispersion in better focus. The intensities in these extreme

TABLE III

DIFFERENCES IN THE SPECTRA OF R CORONAE AND γ CYGNI

λ(I.A.)		Int.		Elem.	λ(I.A.)		Int.		Elem.
R Cor.	γ Cyg.	R Cor.	γ Cyg.		R Cor.	γ Cyg.	R Cor.	γ Cyg.	
4300.28	4300.50†	10?	20	Mn^+	4639.6–42‡‡	.....	14*	Abs.	.....
01.10	00.91	10	36	V^+	45.20	4645.27	17	07	*Ti*
02.55	02.63	25	42	*Ca*	46.37	46.21	28	40	*Cr*
04.57	04.55	10	18	*Fe*	48.86	48.80	53	38	*Ni*
05.32	05.46	15	38	Sr^+	59–60.2§§	.....	70*	Abs.	.....
06.72	06.70	15	28	*Fe*, Ce^+	62.54‖ ‖	62.54	70	30	La^+, Ti^+
09.07	09.12	07	20	Zr^+, Sa^+	62.98	62.75			
09.60	09.54	35	60	Y^+	63.66 ¶¶	63.72	65	36	Fe^+
10.49	10.47	06	14	V^+	64.50 ¶¶		08	Abs.	.....
11.20	11.08	02	03	*CH*	65.77	65.86	39	06	*Cr*
11.61	11.51	03	05	*Fe*	68.20	68.14	35	15	*Fe*
12.87	12.87	42	56	Ti^+	72–74.2***	.....	20*	Abs.	.....
14.18	14.11	50	90	Sc^+	75–80.0†††	.....	80*	Abs.	.....
17.36	17.28	08	26	Zr^+	84–85.0***	.....	60*	Abs.	.....
27.88	27.92	05	27	*Fe*	88–94.4†††	.....	50*	Abs.	.....
33.80	33.80	19	40	La^+, Pr^+	96–97.3†††	.....	40*	Abs.	.....
40.39	40.53	08	87	$H\gamma$	4701.47	4701.41	20	10	*Mn*
54.60	54.50	22	50	Sc^+	05.25	05.46	21	08	*Fe*
58.66	58.64	18	55	Y^+	11–15.8	.....	25*	Abs.	.....
60–65.0‡	.....	70*	Abs.	.....	30.20	30.13	20	10	*Mg*
70–71.5‡	.....	60*	Abs.	.....	34.20	.....	05	Abs.	.....
80–82.5‡	.....	25*	Abs.	.....	34.82	34.89	13	06	Zr^+
4408.52	4408.46	20	40	*Fe*, *V*	35.11	.....	12	Abs.	.....
10.65	10.44	05	15	*Ni*, Ce^+	35.83	35.79	15	08	*Fe*
34.00§	33.84	28	18	Mg^+, Sa^+	38.27‡‡‡	.....	45	Abs.	.....
53.30	53.33	18	09	*Ti*	42.35	.....	22	Abs.	.....
62.29	62.29	03	10	*Ni*, *Mn*	42.80	42.77	18	03	*Ti*
67.31	67.33	40	11	Sa^+	49.34	.....	19	Abs.	.....
77.39	77.44	40	06	*Y*	61.55	61.50	20	09	*Mn*
78.52	78.62	55	11	Mn^+	62.60§§§	62.60	80	50	Ti^+
82.20	82.21	50	25	*Fe*	66.69§§§	66.53	45	15	*Mn*
4500.49	4500.36	37	14	⊙	70.00§§§	70.02	40	03	*C*
06.79	06.79	40	17	Ti^+	71.80§§§	71.76	75	12	*Fe*
11.80‖	11.84	23	12	Sa^+	75.80§§§	75.87	50	07	*C*
12.84‖	12.78	28	10	*Ti*	4812.80‖ ‖ ‖	4812.75	25	03	*C*
37.74¶	37.68	29	05	Sa^+	17.34‖ ‖ ‖	17.24?	40	03	*C*
60.13**	60.28**	11	24	*Fe*	26.88‖ ‖ ‖	26.71	35	04	*C*
61.19**	60.96**	03	17	⊙	33–34.0	.....	15*	Abs.	.....
71.17††	71.04	30	19	*Mg*	40–43.3	.....	20*	Abs.	.....
74.50††	.....	10	Abs.	.....	36.20	36.29	70	30	Cr^+
77.18	77.10	28	05	*V*	50–51	.....	15*	Abs.	.....
87.50	.....	17	Abs.	.....	61.67	61.41	15	2.70±	$H\beta$
90.86	.....	15	Abs.	.....	67.70	.....	05	Abs.	.....
4632.20	4632.29	30	02	*Cr*					

* A rough estimate was made of the band intensity after allowance was made for the intervening line intensities.

† Interval from 4300 to 4314 affected by presence of G(*CH*) band.

‡ Swan sequence −2; first band apparently degrades to the violet, other two uncertain.

§ The continuous spectrum from 4431 to 4434 appears somewhat peculiar in R Coronae when compared with that of γ Cygni, suggesting that a weak band may be present in the spectrum of the former.

‖ Band lines?

¶ Shane measures unidentified band at 4540 in N-type spectra (*Lick Obs. Bull.*, **13**, 123, 1928).

** The two sets of lines may not correspond in both stars.

†† Shane finds unidentified band at 4572 in N-type stars.

‡‡ Degrades to the red. Strong unknown band appears at 4642 in N-type stars.

§§ Band seems to consist of two lines, degrades to the violet; may be violet end of −1 sequence of Swan system.

‖ ‖ Band?

*** Degrades to the violet.

¶¶ Combination apparently degrades to the violet.

††† No degradation apparent.

‡‡‡ Head of 4737 band displaced toward red by 1 A with respect to laboratory wave-length. Lines up to 4730 probably connected with this band.

§§§ Atomic carbon, $3s^3P^o-4p^3P$.

‖ ‖ ‖ Atomic carbon, $3s^3P^o-4p^3S$

regions, often given to the nearest 0.05 unit for the stronger lines, do not merit the weight of those nearer λ 4500. They should suffice, however, for the purpose of a statistical investigation.

As is well realized in stellar microphotometry, a large number of instrumental and photographic errors may creep into the final results, for example: (1) improper drawing of the continuous spectrum, (2) blending of the lines, (3) Eberhard effect, (4) scattering of light in the spectrograph, (5) grain reflection and scattering on the photographic plate, (6) intermittency effect, (7) latent-image effect, (8) variation in the Schwarzschild exponent, and (9) microphotometer errors. It is therefore desirable to minimize the systematic errors where possible and to reduce the accidental error by averaging results from a number of plates. From the assortment available, the four most suitable spectrograms were selected for detailed study.

The procedure of measuring wave-lengths was as follows: Some two hundred lines at regular intervals throughout the spectrum were first measured on the Toepfer engine, then identified on the tracings, and the remaining lines were measured on the tracings with a millimeter scale, relatively to the known lines. The dispersion for these short stretches was taken as linear with sufficient accuracy.

The total line absorptions, referred to the continuous background, are expressed in the unit now conventionally employed, i.e., in terms of 1 A of complete absorption. The integrated intensities were at first determined by measuring with a planimeter the areal amount the lines subtract from the continuous spectrum, but experience soon proved that surprisingly accurate results could be achieved by setting up carefully measured "standards" of line intensities within a small restricted region of the spectrum and then interpolating by means of a visual examination the values for the remaining lines. In every instance, unless the faintest recorded lines appeared on all the tracings, they were considered spurious. Nevertheless, the existence of lines of intensity 0.05 A or less should be regarded as doubtful.

In addition, the same procedure was applied to three of the Mount Wilson spectrograms, as a number of important lines beyond the violet range of the Mills plates were required for a more thorough analysis of the spectrum. Since these plates are not standardized,

the characteristic curve of the plate was determined from the known multiplet intensities of the iron-arc comparison spectrum. The results are not recorded here, but the comparison demonstrates that despite the smaller dispersion and lack of standardization the Mount Wilson spectrograms may be safely used when blends are not serious for a statistical survey.

The measures found in Table IV, together with a similar set from an exceptionally good three-prism spectrogram of γ Cygni (not published here), constitute the main observational data which have been utilized in the later discussions. The following sources were freely consulted for wave-length identification: "A Multiplet Table of Astrophysical Interest" (Miss C. E. Moore); "A Preliminary Table of Rowland Revised Intensities" (C. E. St. John); "A Study of the Solar Chromosphere" (D. H. Menzel, *Pub. Lick Obs.*, **17**, 1931); "The Spectrum of α Persei" (T. Dunham, Jr., *Contr. Princeton Obs.*, No. 9, 1929); and "Spectra of the Rare Earths" (A. S. King, various papers in *Ap. J.*, 1928–1933).

A knowledge of multiplet intensities, their relative behavior in sun-spots, sun, and chromosphere, the temperature class of the lines, their excitation potential, and the degree of ionization in the star's atmosphere is invaluable in estimating the percentage contribution of an element to a blended line. While the actual number of unblended lines is regrettably small, many of the lines may be safely used in a statistical capacity when proper allowance is made for blends.

An explanation of the symbols used is to be found in the key to Table IV. The wave-lengths in italics represent the solar values, with the exception of a number of unpublished lines of Fe^{+14} (denoted by "L") and the rare earths (omitting La^{+}), for which the laboratory values are given.

ELEMENTS IDENTIFIED IN THE SPECTRUM OF R CORONAE

H. An unusual feature of the spectrum is the pronounced weakness of the Balmer series. The hydrogen lines intensify, however, during minimum light.

C. The atomic carbon lines of high excitation potential (7.45 volts) belonging to two groups at λ 4762 ($3s^3P^\circ - 4p^3P$) and λ 4812 ($3s^3P^\circ - 4p^3S$) are about ten times more intense in R Coronae than in γ Cygni. Carbon is so prevalent that

[14] Kindly communicated by Professor H. N. Russell.

KEY TO TABLE IV

First column.—Measured wave-lengths in international Ångström units.

Second column.—Equivalent widths of the lines expressed in terms of 0.01 A of complete absorption. Values in parentheses denote intensities merely estimated for the most seriously blended lines. For the majority of blends it was possible to determine the intensities from the completed profiles of overlapping lines.

w slightly wide
W distinctly wide
d double
r symmetry slightly disturbed on red side
R symmetry distinctly disturbed on red side
v symmetry slightly disturbed on violet side
V symmetry distinctly disturbed on violet side

Third column.—Contributors to the line arranged in the order of decreasing importance, approximately thus:

1 overwhelming contributor, >50 per cent (unless there are two such)
2 strong contributor, 25–50 per cent
3 moderate contributor, 10–25 per cent
4 weak contributor, 10 per cent
5 trace may be present
? percentage contribution unknown but suspected to be very small, if present at all

TABLE IV

WAVE-LENGTHS IN THE SPECTRUM OF R CORONAE

I.A.	Int. (0.01 A)	Identification
4299.14	45	1*Ca* 00 1*Fe* 25 3*Ti* 25 3*CH* 14
4300.11	(65)	1*Ti*$^+$ 06 4*CH* 83 5*Cr* 98
00.28	(10)	1*Mn*$^+$22 2*Ce*$^+$33 4*CH* 32
01.10	10	1*V*$^+$18 2*Ti* 11 3*Cr* 18 4*CH* 10
01.90	45	1*Ti*$^+$93 3*Zr*$^+$78 3*Fe* 20 4*Ni* 08
02.55	25	1*Ca* 54 4*CH* 30 4*CH* 76 5*CH* 92
03.20	50	1*Fe*$^+$18
04.57	10	2*Fe* 57 4*CH* 57 4*CH* 40 4*CH* 26
05.32	15	1*Sr*$^+$ 46 3*Fe* 46 3*Ti* 47 4*Cr* 46
05.84	40	1*Sc*$^+$ 72 3*Ti* 92 4*CH* 85 ?*Pr*$^+$ 77
06.22?	05	3*CH* 15 4*V* 18
06.72	15	2*Fe* 60 2*Ce*$^+$ 73 3*CH*? 86 4*CH* 60
07.87	50	1*Ti*$^+$ 91 2*Ca* 75 2*Fe* 91 3*CH* 91
09.07	07w	2*Zr*$^+$ 94 2*Sa*$^+$ 02 3*Fe* 38 3*Ti* 07
09.60	35	1*Y*$^+$ 63 3*Ce*$^+$ 74 3⊙ 46 4*CH* 63
10.49	06	2*V*$^+$ 71 3*CH* 38 4*Ti* 38 4*CH* 56
11.20	02?	3*CH* 17 4*CH* 99
11.61	03	1*Fe* 52 3*CH*? 72 4*CH* 45 ?*CH* 52
12.87	42	1*Ti*$^+$ 88 3*Fe*$^+$ 04 4*CH* 71 4*CH* 04
14.18	50	1*Sc*$^+$ 09 2*Fe*$^+$ 29*L* 4*Ti* 36 4*CH* 09
14.92	42	1*Ti*$^+$ 98 2*Fe* 10 4*Ti* 77 4*Ti* 81
15.46?	03	1⊙ 47
15.93	05	2*La*$^+$ 87 ?*Gd*$^+$ 05
16.45?	07	2*V*$^+$ 22 5⊙ 56
16.83	40	1*Ti*$^+$ 80
17.36	08	1*Zr*$^+$ 32
18.57	(25)	1*Ca* 66 3*Ti* 66 3*Fe*$^+$ 24*L* 5⊙ 47
18.93	(10)	1*Sa*$^+$ 95 5*Sr* 00
19.52	03	1*Fe*$^+$ 72*L* 3*Fe* 46 4*Cr* 64
20.85	52	1*Ti*$^+$ 96 1*Sc*$^+$ 75 4*Ce*$^+$ 73 5*Cr* 60
21.91	06	1*V*$^+$ 02 1*Fe* 80 4*Ti* 66
22.55	08	1*La*$^+$ 51
23.50	05	2*Cr* 51 2*CH* 85 3*Fe* 37 4*CH* 37
24.17	03	3⊙ 41 4⊙ 18 4⊙ 98 4*CH*? 09
25.00	44	1*Sc*$^+$ 00 3*Fe* 00 3*Cr* 07 3*Ti* 15
25.78	37	1*Fe* 78 3*Fe* 76 3*Ni* 62
4299.14		4*Ce*$^+$ 36
4304.57		4⊙ 72
05.32		4*Ce*$^+$ 14 4*CH* 32 4⊙ 22
06.72		4*CH* 70 4*Ti* 91
07.87		3*CH* 56
09.07		3*Fe* 04 4*CH* 14
10.49		4⊙ 47
12.87		4*Mn* 51
14.18		4⊙ 22
24.17		?*Gd*$^+$ 04
25.00		4*Ni* 36

TABLE IV—*Continued*

I.A.	Int. (0.01 A)	Identification
4326.70	13w	1*Fe* 74 1*Mn*$^+$ 71 4*Ti* 36 4⊙ 92
27.13	17	1*Fe* 11 4*Ti* 97 ?*Gd*$^+$? 16
27.88	05d?	1*Fe* 93 2*Nd*$^+$ 97 4⊙ 80
28.88	07w	4⊙ 61 5⊙ 85 5⊙ 92 ?*Sa*$^+$ 03
30.30	(30w)	1*Ti*$^+$ 25 3*Gd*$^+$ 58 4*Ce*$^+$ 45 4*V* 03
30.74	(25)	1*Ti*$^+$ 71 4*Ni* 71 4*Fe* 96 ?*Eu*$^+$ 62
31.70	13	1*V*$^+$ 75 2*V*$^+$ 56 2*Fe*$^+$ 53*L* 3*Ni* 64
32.92?	04	3*Zr*$^+$ 21 4*V* 83 4⊙ 92
33.80	19R	2*La*$^+$ 77 2*Pr*$^+$ 91
37.20	(30)	1*Ti*$^+$ 26 2*Fe* 06 3*Cr* 26
37.41	(10)	1*Cr* 57 4*Mn* 41
37.90	45R	1*Ti*$^+$ 93 3*Fe* 27 3*Ce*$^+$ 78 5*Mn* 13
39.42	20	1*Cr* 72 1*Cr* 46 2*Zr*$^+$ 56 4*Ce*$^+$ 32
40.39	08W	1*Hγ* 48 4*Cr* 14 5*Ti* 03
40.88	25?	1*V* 01
41.37	36	1*Ti*$^+$ 37 4*Fe* 25 4*Gd*$^+$ 24
42.26	15R	2*Zr*$^+$ 24 2*Gd*$^+$ 21 2*Fe*$^+$ 36*L*
43.10	08	1*Fe* 27 3*Cr* 21 5⊙ 99 5*V*? 86
44.30	50W	1*Ti*$^+$ 29 2*Cr* 51 3*Mn*$^+$ 03 ?*Gd*$^+$ 34
44.74?	05	5⊙ 67 5⊙ 75 5⊙ 89
45.80	03	1*Sa*$^+$ 86 4⊙ 91 5⊙ 77
46.56	08	1*V*$^+$ 89 2*Fe* 56 3*Cr* 83 4*Ti* 56
47.20	03	2*Fe* 24 ?*Gd*$^+$ 25
47.75	05	1*Sa*$^+$ 81 2*Fe* 84
48.25	08w	1*Mn*$^+$? 49 4*Fe* 32 4*CH* 34 4*CH* 98
48.91	07	2*Fe* 95 4*Zr*$^+$ 64
49.27?	04	4⊙ 16 4⊙ 38
49.78	07	1*Ce*$^+$ 79 3*V*$^+$ 96
50.25?	03	4⊙ 16 4⊙ 25
50.83	(50)	1*Ti*$^+$ 84 4*V*? 84
50.97	(10)	1*Cr* 06
51.79	70	1*Fe*$^+$ 77 2*Cr* 77 3*Fe* 56 3*Mg* 92
52.77	20	1*Fe* 75 2*Ce*$^+$ 72 4*V* 88
53.54	04	5⊙ 44 5⊙ 52 5⊙ 65
54.16	06	1*Fe*$^+$ 36*L* 3⊙ 27 4*Cr* 95 4*Ti* 07
54.60	22	1*Sc*$^+$ 62 3*La*$^+$ 44 5*Mg*? 52 5*Fe*? 76
55.11	18	1*Ca* 10
56.03	04	4*Ni* 90 4*V* 90 4*CH* 00 5*Cr*? 14
56.59	03w	3⊙ 37 4*Cr* 74 4*Mn* 61
57.47	06	1*Fe*$^+$ 57*L* 4*Cr* 52
57.86?	03	4*Ni* 87
58.66	18W	1*V*$^+$ 72 3*Fe* 51
59.59	(08)	2*Cr* 62 3*Ni* 62 4*CH* 50
59.79	(22R)	1*Zr*$^+$ 75 4*Cr* 99 4*CH* 75
60.71	08	1*Sa*$^+$ 73 2*Fe* 81 3*Ti* 48 4*Zr* 80
26.70		5⊙ 62 5*Sr*? 48
28.88		?*Pr*$^+$ 98
31.70		5⊙ 78
39.42		5*Fe* 26
44.30		?*Pr*$^+$ 32
51.79		4*CH* 77
60.71		4*CH* 48

TABLE IV—*Continued*

I.A.	Int. (0.01 A)	Identification
4361.28	10	*1Fe⁺ 25L 5⊙ 25 5⊙ 32*
62.05	20	*1Sa⁺ 06 2Ni⁺ 10*
62.72	11	*3⊙ 54 4Cr 95 4⊙ 75*
63.22	15W	*3Cr 11 4CH 11 4CH 30 ?Mo⁺ 61*
64.18	08	*1V⁺ 17 2V⁺ 01*
64.70	17W	*1Ce⁺ 66 4La⁺ 69*
65.85	03	*3Fe 91 5V? 73*
66.35	05	*2Nd⁺? 41 3Fe⁺? 17L*
67.76	44	*1Ti⁺ 68 3Fe 59 3Fe 91 5CH 68*
68.27	10w	*2Fe⁺ 26L 2Pr⁺ 35 3Cr 30 4Ni 30*
69.47	34R	*1Fe⁺ 41 3Fe 77 4Ti 72 4CH 78*
70.97	(22)	*1Zr⁺ 99 4CH 06 5Mn? 86*
71.27	(50W)	*1Cr 29 1V⁺ 13 2⊙ 43 3Co 16*
72.25	17	*4Ti 41 4⊙ 34 5Ni? 20*
72.71	05	*3CH 74 4Fe 99 4⊙ 85*
73.67	07W	*1Fe 57 2Ce⁺ 82 3Cr 27 4Co 66*
74.20	(07)	*3Cr 18 3CH 23*
74.47	(66)	*1Sc⁺ 47 4Fe 50*
74.80	(40)	*1Ti⁺ 82 ?Dy⁺ 80*
75.09	(20r)	*1V⁺ 95 3⊙ 20 4Co 94 4Cr 34*
75.97	23	*1Fe 95 3Ce⁺ 93*
76.91	08W	*3Fe 78 3CH 24 5Cr 78*
77.52	(03)	*4Fe 38 4Cr 55*
77.89?	(02)	*3Fe 80 ?Mo⁺ 77 ?⊙ 99*
78.19	(04)	*1Sa⁺ 25 2CH 26*
79.30	(08)	*1V 24 4Co 24*
79.78	(28r)	*1Zr⁺ 77 2Mn⁺ 74 4Cr 77 5Co 07*
80.46	10	*3Mg 37 5Fe 50*
80.99	03	*3CH 73 4Cr. 12*
82.00	13w	*1Ce⁺ 17 5⊙ 89 5⊙ 00 5Mn 72*
82.81	14	*1Fe 78 4CH 78 4CH 00*
83.57	40	*1Fe 56*
84.37	35	*2⊙ 32 3Ni 54 ?Sa⁺ 30*
84.80	30	*1Sc⁺ 83 2Cr 98 2V 71 4V 73*
85.46	38r	*1Fe⁺ 39 3Fe 26 5⊙ 61 ?Nd⁺ 66*
86.86	41w	*1Ti⁺ 86 3CH 06 4Ni 46*
87.84	13w	*1Fe 90 3CH 50 4Cr 40 4Cr 50*
88.44	21v	*1Fe 42 4Ti 10 4Cr 06 5⊙ 25*
89.25	09d	*1Fe 26*
89.99	13	*1V 99 1Fe⁺ 88L 4Ni 88*
90.61	(10)	*1Mg⁺ 58 3Fe 46 4Ni 34*
90.95	(45)	*1Ti⁺ 04 3Fe 97 ?Gd⁺ 95 ?Sa⁺ 89*
91.50	(10)	*1Ce⁺ 67 4Co 57 5⊙ 48 ?Gd⁺ 45*
91.86	(07)	*3Cr 77 4Co 88 4V 07*
92.60	03	*2Fe 59*
93.27	14d	*4⊙ 04 4⊙ 28*
94.14	40v	*1Ti⁺ 07 4Ti 93 5⊙ 18*
95.07	55d	*1Ti⁺ 04 3V 25 4Fe 29 5Cr 86*
95.96	33r	*1Ti⁺ 85 4⊙ 31*
97.60?	03	*5⊙ 58 ?Gd⁺ 50*
68.27		*4V 07 4⊙ 13*
75.09		*4Ti? 49*
84.80		*4Mg⁺ 64 5Fe 68*
87.84		*?Gd⁺ 63*
95.07		*5Ti 86*

TABLE IV—*Continued*

I.A.	Int. (0.01 A)	Identification
4398.15	(30)	1V^+ 02 5⊙ 18
98.33	(20)	1Ti^+ 30 3⊙ 50
99.82	55	1Ti^+ 78 4Ni 60 4Cr 82
4400.41	(59)	1Sc^+ 40 4Fe 35
00.73	(15)	1Ti^+ 63 3V 59 4Ni 86 4Ti 60
01.27	(14)	1Zr^+ 33 2Fe 30
01.55	(10)	2Ni 55 3Fe 45
03.00?	05	1Fe^+ 88L 4Zr 96
03.30	20w	1Zr^+ 38 3⊙ 19 4Cr 50
04.39	03	2Ti 28 4Ti 41
04.77	41R	1Fe 76 3Fe 03 4Ti 93 4V 03
05.81	02	4Ti 74 4V 16 ?Pr^+ 85
06.60	05d?	1V 65
07.68	34	1Ti^+ 65 2Fe 72 3V 65
08.52	20	2Fe 43 2V 53 3V 21 ?Pr^+ 84
09.42	49v?	1Ti^+ 53 2Ti^+ 25 4Sa^+ 37 ?Dy^+ 38
10.05?	02	3⊙ 01
10.65	05	3Ni 53 3Ce^+ 64 4Ti? 77 5⊙ 86
11.07	36	1Ti^+ 08 4Cr 08
11.98	20	1Ti^+ 94 5Mn 89
13.59	(20)	1Fe^+ 60
13.86	(10)	3Cr 85 ?Pr^+ 78
14.65	13	1Zr^+ 56 3Mn 89
15.26	(60)	1Fe 14
15.57	(40)	1Sc^+ 56
16.79	38	1Fe^+ 83 4V 48 4Ti 48 4Ti 28
17.75	48	1Ti^+ 72
18.33	38	1Ti^+ 34 4Fe 43
19.00	03	2Ce^+ 78 4Cr 10 ?Gd^+ 03
19.75	04	1Mn^+ 78
20.03	33d	1Sc^+ 67 3⊙ 29 4Sa^+ 55
21.00	05	1Sa^+ 15 ?⊙ 94
21.95	29V	1Ti^+ 95 4V 58 4Ti 76 4⊙ 06
22.55	22	1V^+ 58 2Fe 58 4Ti 83
23.13	21R	1Ti^+ 27 2Fe 14 4Ni 98 4Cr 27
23.75	04	1Fe 85
24.39	11W	1Sa^+ 36 3V 59 3Cr 30 3Fe 19
25.47	23r	1Ca 45
26.80?	03	?⊙ 68 ?⊙ 89
27.27	34	1Fe 32 2Ti 11 2Fe 31 4Ti 10
27.91	18	1Ti^+ 92 3Mg^+ 99 4Ce^+ 92
29.25	09	1Pr^+ 25 2Ce^+ 27 4Fe 30
29.92	16	1La^+ 91 3Fe 20 4V 80 4Ti 06
30.66	20w	1Fe 62 3⊙ 77
31.35	40	1Sc^+ 37 4Ti 29
32.05	15W	1Ti^+ 09 4Cr 17 4⊙ 85
33.23	17	1Fe 22 2Fe 23
34.00	28w	2Mg^+ 99 2Sa^+ 91 3Fe 79 4Ti 97
35.05	41d	1Ca 97 2Fe 16
35.70	24	1Ca 69 ?Eu^+ 60
04.77		5Co 93
24.39		4Cr 07 4Ti 37
29.92		4Cr 91
34.00		4Ti 01

TABLE IV—*Continued*

I.A.	Int. (0.01 A)	Identification
4436.25	18w	*1Mn 36 2Mg+ 48 4V 15*
36.93	09	*1Fe 95 3Ni 95*
37.84	03	*2V 84*
38.42	09	*1Fe 35*
39.28	04w	*3⊙ 17*
39.88	02	*2Fe 88*
40.36	19R	*1Zr+ 48 3Fe 48 4Ti 35*
41.77	41	*1Ti+ 72 4V 72*
42.25	29	*1Fe 35*
43.18	39	*1Zr+ 00 1Fe 20 3Fe 84 4Ti 20*
43.82	60	*1Ti+ 81*
44.44	41	*1Ti+ 56 2Fe+ 57L 3Ce+ 40 3Ce+ 70*
45.41	03	*4Fe 48 4Co? 07*
46.37	17	*2Nd+ 42 2Fe+ 25L*
47.07	12w	*1Fe 14 2Fe 84 4Mn 16*
47.73	20	*1Fe 73*
49.67	31W	*1Fe+ 67L 2Pr+ 87 2Ti 15 2Ce+ 34*
50.50	52	*1Ti+ 49 3Ti 90 3Fe 32 4Fe 76*
51.56	(26)	*1Fe+ 55L 2Mn 59 3Nd+ 59 3Fe 66*
51.90	(05)	*4V 01 ?Pr+ 91 ?Nd+ 02*
52.71	10	*1Sa+ 75 4⊙ 62*
53.30	18w	*1Ti 32 3Mn 01 3Ti 71*
54.33	(25)	*1Fe 39*
54.70	(50)	*1Ca 79 2Zr+ 80 3Sa+ 66 4Fe 67*
55.27	(10)	*1Ti 32 1Fe+ 26L 2Mn 32 3Fe 03*
55.74	30W	*1Ca 90 3Mn 82 4La+ 82 4Fe? 55*
56.62	29	*1Ti+ 64 2Ca 63 3Fe 34 3Mn 04*
57.45	22v	*1Zr+ 44 2Ti 44 3Mn 55 4V 44*
58.00	14	*1Fe 09*
58.46	05W	*2Mn 26 3Sa+ 53 4Cr 54 4Cr 53*
59.09	42r	*1Fe 14 2Ni 04 3Cr 36*
60.31	24W	*1Ce+ 21 3V 30 4Mn 36*
61.07	(15)	*3Mn 09*
61.22	(45)	*1Zr+ 21 3Fe 20*
61.70	(30)	*1Fe 66 4Fe 82*
62.29	03	*3Ni 46 3Mn 01 3⊙ 20 4Fe 01*
63.07	04	*1Nd+ 02 ?Gd+ 23 5⊙ 14*
63.45	(30)	*2Ce+ 41 3Ti 41 4Ti 54 4Fe 40*
64.56	(70)	*1Ti+ 46 3Fe 78 3Mn 68 4Cr 68*
65.90	05w	*2Ti 82 4Cr 17 4Fe? 17*
66.46	55	*1Fe 56 4Ni 39 ?Gd+ 55*
67.31	40w	*1Sa+ 36 4Cr 56 ?Ce+ 54 ?Gd+ 17*
68.49	68	*1Ti+ 50 ?Pr+ 70*
69.25	43	*1Fe 38 1Ti+ 16*
70.84	68W	*1Ti+ 85 3Ni 49 3Ce+ 24 4Ti 25*
72.09	03	*4⊙ 08*
72.87	46W	*1Fe+ 93 3Mn 81 3Ce 72 4Fe 72*
44.44		*4V 20 4Ti 26*
49.67		*2Dy+ 70 4Ti 97*
50.50		*?Ce+ 74*
55.27		*3Mn 03*
62.29		*4V 36*
63.45		*5Ni 40*
64.56		*4V 78*

TABLE IV—*Continued*

I.A.	Int. (0.01 A)	Identification
4474.05	10	1*Fe*$^+$ 20*L* 3*V* 05
74.72	04	2*Ti* 86 4*V* 75
75.35?	02	4*Cr* 31
75.95	42v	1*Fe* 02 4*Fe* 08
77.39†	40	4*V* 47 ?*Pr*$^+$ 27
78.52†	55w	2*Mn*$^+$ 74 3*Sa*$^+$ 68 5*Co* 32 5*Fe* 32
79.55	(11)	2*Fe* 61 2*Ce*$^+$ 36 4*Ti* 32
80.19	(09)	2*Fe* 15 3⊙ 97 4*Fe* 28 4*Ti* 59
81.15	(41)	1*Mg*$^+$ 14 3*Ti* 28 3*Gd*$^+$ 06
81.45	(50)	1*Mg*$^+$ 34 3*Fe* 62
82.20	50r?	1*Fe* 18 2*Fe* 28 3*Ti*$^+$ 44 4*Zr*$^+$? 01
82.83	05	3*Fe* 74 4*Ti* 74 5*Cr* 88
83.47?	03	?*Gd*$^+$ 32 ?⊙ 35 ?⊙ 54
83.97	(14)	1*Ce*$^+$ 90 4*Co* 92
84.32	(10)	1*Fe* 23 4*Co* 50
85.34	(09)	2*Zr*$^+$ 42
85.65	(14)	1*Fe* 68
86.87	20W	1*Ce*$^+$ 91 1*Fe*$^+$ 69*L* ?⊙ 75 ?⊙ 01
88.28	49	1*Ti*$^+$ 33 3*Fe* 14 4 *Cr* 06 4*Ti* 32
89.18	62	1*Fe*$^+$ 19 3*Fe* 91 4*V* 91 4*Ti* 10
89.81	15	1*Fe* 75 2*Fe* 09 3*Mn* 09
90.73	(08d)	1*Fe* 78 3*Ni* 54 4*Cr* 54 4*V* 81
91.38	(55)	1*Fe*$^+$ 41 4*Cr* 66 4*Mn* 66
92.72	04w	1*Fe* 69 3*Cr* 31 4*Ti* 54
93.55	35	1*Ti*$^+$ 53 1*Fe*$^+$ 58*L*
94.51	42	1*Fe* 58 3*Zr*$^+$ 31
95.48	20	1*Ti*$^+$ 43 2*Zr*$^+$ 43 4*Fe* 58 4*Fe* 43
96.16	08	2*Fe* 96 2*Ti* 16 4*V* 06 4*Ti* 25
97.05	40	1*Zr*$^+$ 98 2*Cr*$^+$ 27 3*Cr* 86
97.69	08w?	3*Ti* 68 3*Ce*$^+$ 85 3*Na*? 73
99.09	20w	1*Mn* 90 2⊙ 15 3*Cr*$^+$ 73 4*Cr* 73
4500.49	37w	3⊙ 64 4*Cr* 29 4⊙ 37 5⊙ 51
01.38	68	1*Ti*$^+$ 28 4*Cr* 10 4*Cr* 78 5*Ni* 65
02.36	10	2*Mn* 83 3*Fe* 60 5*Cr* 27
04.68	13W	1*Cr*$^+$ 54 3*Fe* 84
06.79	40W	1*Ti*$^+$ 74 3*Cr*$^+$ 23 4*Cr* 85
08.29	62	1*Fe*$^+$ 29
09.48	09	2*Ca* 45
10.25	12W	3*Pr*$^+$ 18 ?⊙ 27
11.80	23W	1*Sa*$^+$ 84 3*Cr* 90 3*Ca* 28 4⊙ 56
12.84	28	2*Ti* 75 4*Ni* 00
14.29	22W	1*Fe* 19 3*V* 20 3⊙ 43 4*Cr* 50
15.39	71	1*Fe*$^+$ 35 3*Sa*$^+$ 11 4*Fe* 18 4*Cr* 44
16.77?	08v	?*Co*? 66
4478.52		?*Gd*$^+$ 79
4514.29		5*Ni* 91
15.39		4*Ti* 60

† These wave-lengths represent the two strongest unidentified lines in the spectrum. The elements listed are not important contributors. The former line is apparently not present, or, if present, very weak in the spectra of Polaris, α Persei, ε Aurigae, and 41 Cygni, while the latter appears definitely as a faint absorption line in these stellar spectra.

TABLE IV—*Continued*

I.A.	Int. (0.01 A)	Identification
4517.79	(15V)	*2Fe 54 3Ni 84*
18.38	(45)	*2⊙ 34 2Ti 03 4Cr 59 4Ti 70*
20.24	62	*1Fe⁺ 23 2V⁺ 54 2Ti⁺ 40 3Ni 99*
22.65	78R	*1Fe⁺ 64 2Ti 81 3La⁺ 38 4Fe 53*
23.73	10	*3Sa⁺ 93 3Fe 41 4Ni 75*
24.65	(26)	*1Ti⁺ 69*
24.98	(30)	*1Ba⁺ 95 2Fe 15 5V 17*
26.58	30W,d	*1Fe 57 2Cr 47 2Ca 94 3La⁺ 10*
27.36	20	*2Ti 33 2Ce⁺ 35 4Cr 47 4Ti 47*
28.66	45	*1Fe 63 3Ce⁺ 48 4⊙ 76 4⊙ 82*
29.54	48v	*1Ti⁺ 49 3Fe 56 3Fe 68 4Cr 86*
31.08	43R	*1Fe 16 2Co 96 2Fe 63 3Cr 74*
32.43	05	*4⊙ 32 4⊙ 58*
33.10	40	*1Ti 25 3⊙ 97 4⊙ 05*
34.08	80	*1Ti⁺ 97 2Fe⁺ 17 4Co 97 ?Mg⁺ 26*
34.80	16	*1Ti 79*
35.67	(20)	*1Ti 58 2Cr 71 4Zr 74*
36.00	(11)	*1Ti 92 1Ti 06*
37.01	05	*4Ti 22 5⊙ 91*
37.74	29	*2Sa⁺ 96 3Fe 68 4Co⁺? 96*
39.71	40	*1Ce⁺ 76 3Cr 78 4Cr 79*
40.75	05	*2Cr 71 3Cr 50 3Cr 07 4Ti 51*
41.57	52	*1Fe⁺ 52 4Fe⁺ 33*
42.85	14w, d	*1Cr⁺ 85 3Fe 71 4Cr 62*
44.07	39	*1Ti⁺ 02 3Sa⁺ 96 4Co 82*
45.18	49v	*1Ti⁺ 15 3Ce⁺ 98 4Cr 34*
46.96	17	*1Fe 03 3Ni 94 4Ni 24*
47.93	15	*1Fe 86 4Ti 86 4Ti 13*
49.60	91W	*1Ti⁺ 64 2Fe⁺ 48 2Fe⁺ 21 L 2Ti 62*
50.79	03	*1Fe 78*
52.33	40r	*1Ti⁺ 29 2Ti 46 3Fe 55 4Ti 45*
54.07	50v	*1Ba⁺ 04 3Zr⁺ 96*
55.01	40w	*1Cr⁺ 99 2Ti 49 4Ti 09 5Cr 84*
56.10	61w?	*1Fe⁺ 89 2Fe 14 5Cr 19*
57.21	11	*2⊙ 29 4Fe 93*
58.65	56	*1Cr⁺ 65 3La⁺ 47 4 Cr⁺ 78*
59.70	03	*4Ti 93 5Ni 93 ?V? 36 ?⊙ 56*
60.13	(11)	*1Fe 10 3Ti 93 4Ni 94 4Ce⁺ 29*
60.60	(11)	*2 Sa⁺ 42 4V 72*
61.19	03	*3⊙ 42 4Ce⁺ 96 5⊙ 20*
62.33	16w?	*1Ce⁺ 34*
63.76	70	*1Ti⁺ 77*
64.59	30	*1V⁺ 58 1Ni⁺? 56 3Fe 83 4Ti 23*
65.75	37R	*1Cr⁺ 78 2Fe 67 2Cr 52 4Co 67*
66.63	03	*1Fe 52 4Fe 66*
66.98	03	*1Fe 88 2Fe 00*
18.38		*4Ti 02*
22.65		*?Eu⁺ 60*
26.58		*3Ti⁺? 41 4Cr 10 4Cr 46*
31.08		*4Cr 70*
40.75		*4Cr 72 5Ti 88*
49.60		*4Co 67 4V 65*
55.01		*5⊙ 30*
59.70		*?⊙ 81*
64.59		*4Fe 70*
65.75		*?Ce⁺ 85*

TABLE IV—*Continued*

I.A.	Int. (0.01 A)	Identification
4568.37	45	1*Ti*+ *33*
69.37	18	3*Co*+? *30* 4*Cr 52* 5*Cr 62* ?*Ce*+ *30*
71.17	30w	1*Mg 10* 2*Cr*+ *30* 4*Cr 10* 4*Ti 93*
72.02	73	1*Ti*+ *98* 3*Ce*+ *28* 4*Cr 20* 4*V 81*
72.86	04	1*Cr*+ *87*
74.50	(10)	1*Zr*+ *49* 2*Fe 73* 3*Fe 23*
75.02	(15)	1*La*+ *91* 4 *Cr 12*
76.32	55	1*Fe*+ *34*
77.18	28W	3*V 19*
78.55	22d	1*Ca 56* 4*Cr 74*
79.58	10	1*Fe*+ *52L* 3*Fe 34* 5*V 19*
80.17	(40W)	1*Fe*+ *05L* 1*Fe*+ *27L* 2*Cr 06* 2*La*+ *06*
80.48	(30)	1*Ti*+ *47* 3*V 42* 3*Fe 59* 4*Ni 59*
81.42	32	1*Fe 52* 1*Ca 40* 3⊙ *20*
82.85	51	1*Fe*+ *84*
83.81	81d	1*Fe*+ *84* 2*Ti*+ *42* 4*Cr 90*
84.86	08	1*Fe 83* 1*Fe 73* 4*Cr 95* 4*Cr 09*
85.89	19d	1*Ca 88* 3⊙ *98*
87.50	17v	4*Fe 14* 5⊙ *40* 5⊙ *60* 5⊙ *73*
88.19	49	1*Cr*+ *21* ?*Cr*+ *40*
89.93	57	1*Ti*+ *96* 3*Cr*+ *89* 4*Cr*+ *96*
90.86	15w	2⊙ *79* 4*Cr 68* ?⊙ *95*
92.14	40	1*Cr*+ *06*
92.71	15?	1*Fe 66* 3*Ni 53*
93.55	(22)	1*Fe 50*
93.88	(10)	1*Ce*+ *94* 2*V 13* 3*Cr 83*
95.72	40V	1*Fe*+ *69* 3*Fe 37* 3*Sa*+ *30* 4*Ni 95*
97.79	(16)	2⊙ *76* 2*Gd*+? *88*
98.40	(16)	1*Fe*+ *54L* 2*Fe 13* 3*Fe 37* 4*Fe 75*
4600.19	46	1*V*+ *21* 3*Ni 37* 3*Cr 11*
00.90	(10)	1*Cr 76* 3*Fe 94* 3*Cr 02*
01.25	(16r)	1*Fe*+ *38* 4⊙ *15* 4⊙ *28*
02.34?	05	1*Fe 01* 4*Zr*? *54*
02.85	20	1*Fe 95*
03.90	05	4*Fe 96* 4⊙ *86*
04.93	(18)	1*Ni 00* 1*Fe*+ *03L*
05.50	(20W)	2*La*+ *79* 2⊙ *60* 3*Mn 36*
06.59	10	1*Ce*+ *41* 2*Ni 22* Sa+? *51*
07.69	(20)	1*Fe 66* 3*Sr 34*
07.98	(05)	1*Y*+ *98* 2*Fe*+ *25L*
09.29	(35V)	1*Ti*+ *27*
09.82	(08)	4*Cr 91*
10.56?	03	3⊙ *19* 4⊙ *60*
11.11	(15)	2*Fe 19* 5*V 94*
11.28	(20)	1*Fe 30* 4*Fe 28*
12.36	05	4*Dy*+ *27* 4⊙ *47*
13.22	(30)	1*Fe 22* 2*La*+ *37* 2*Cr 37*
13.95	(25)	1*Zr*+ *92* 4*V 92*
14.13	(10)	1*Fe 21*
16.10	(12)	1*Cr 13*
16.29	(18)	1*Ti*+? *23* 3*Co*+? *27*
16.67	40	1*Cr*+ *63*
4580.17	4*Co 16*	
84.86	?*Sa*+ *84*	
98.40	4*Cr*? *44*	

TABLE IV—*Continued*

I.A.	Int. (0.01 A)	Identification
4617.20	07W, d	1*Ti 28*
18.87	69	1*Cr*$^+$ *79 3Fe 79*
19.67?	10	2*Fe 30 3Ti 54 4La*$^+$? *90 4Cr 54*
20.52	47	1*Fe*$^+$ *52*
21.40?	04	2*Cr*$^+$? *48*
21.79	07	1*Cr 89* 1*Cr 96 4*⊙ *62*
22.34	05	3*Cr 45 4Cr 76* ?⊙ *13* ?⊙ *26*
23.29	05	2*Ti 10* 3⊙ *59*
24.56	03	1*Cr*$^+$ *57 4V 42*
25.16	35	1*Fe 05 3Ce*$^+$ *90 4Fe 44 4Cr? 32*
26.07	(30)	1*Cr 18* 1*Fe*$^+$ *91L 2Fe*$^+$ *15L 4Cr 92*
26.58?	(10)	2*Fe*$^+$ *76L 3Mn 54 4V 49*
27.34	05	1⊙ *37*
28.19	35W, d	1*Ce*$^+$ *15 4Cr 46*
29.36	87	1*Fe*$^+$ *34 2Ti*$^+$ *34 2Ti 34 3Zr*$^+$ *08*
30.08	07	1*Fe 13* ?*Zn 81*
30.60?	03	2⊙ *57*
31.43	05	1*Fe 49 2Fe*$^+$ *40L*
32.20	(30W)	2*Cr 15*
32.86	(15)	1*Fe 93 3Fe 82*
34.15	60	1*Cr*$^+$ *08*
35.34	31	1*Fe*$^+$ *35*
36.34	35	1*Ti*$^+$ *33*
37.53	(25w)	1*Fe 51 4Cr 77 4Cr 18 5Ti 18*
38.03	(20)	1*Fe 02*
40.32	35W	1*Fe 29 2Ti 95 4Ti 44 5V 11*
41.10	(10)	2*Fe*$^+$ *84L* 3⊙ *22* 5⊙ *98*
41.58	(15)	4⊙ *52* 4⊙ *68*
43.50	23d	1*Fe 48*
45.20	17	2*Ti 20 4La*$^+$ *32*
46.37	28W	1*Cr 17* 3⊙ *64 4V 38*
47.53	(24)	1*Fe 44 3La*$^+$ *50*
47.95	(15)	1⊙ *96 4Cr 12*
48.86	53V	1*Fe*$^+$ *93L 2Ni 66 4Cr 86*
49.85	04	2*Fe 86 2Ti 02* 3⊙ *65*
50.63?	06	3⊙ *32* 4⊙ *55* 4⊙ *81* 4⊙ *95*
51.24	20	1*Cr 29*
52.15	26	1*Cr 17 2Fe*$^+$ *28L*
54.55	45w	1*Fe 51* 1*Fe 62* 1*Fe 63 4Ce*$^+$ *31*
55.71	63	1*Ti*$^+$ *71 4Ti 66 4Ni 66 4Ti? 79*
57.14	82	1*Fe*$^+$ *98* 1*Ti*$^+$ *21*
58.30?	05	1*Y 30*
59.49	33W	3⊙ *54* 4⊙ *38* 4⊙ *77*
60.58	44W	1⊙ *43* 3⊙ *91* 4⊙ *73* 5⊙ *63*
61.92	06	2*Fe 98 3Zr*$^+$ *79*
62.54	(30)	1*La*$^+$ *52*
62.98	(40)	1*Ti*$^+$ *76 2Fe 18*
63.66	65	1*Fe*$^+$ *71 3La*$^+$ *80 4Cr 32 4Cr 82*
64.50	(08)	2*Fe*$^+$ *23L 4Ni 32* 4⊙ *55*
64.92	(12)	1*Na 80 3Cr 80* 4⊙ *18*
19.67?	4*V 79*	
29.36	4*Co 34*	
54.55	4*Cr 74*	
63.66	4*Co 42*	

TABLE IV—*Continued*

I.A.	Int. (0.01 A)	Identification
4665.77	39R	*3Cr 90 5⊙ 68 5⊙ 83*
66.90	(50)	*1Fe+ 76 3Ni 99 4⊙ 90*
67.49	(20)	*1Fe 46 2Ti 60 3Ni 77 4Ti 58*
68.20	35W	*1Fe 16 3Na 57 4Ti 38*
69.30	30	*1Fe 18 3Cr 33 3Sa+ 39 3Sa+ 66*
70.40	82	*1Sc+ 42 2Fe+ 17L 3⊙ 18 4V 56*
71.24	28w?	*2⊙ 42 3Mn 69 4⊙ 05 5⊙ 22*
72.40	20	*1⊙ 34*
73.12	25	*1Fe 17 2Fe 84 3Fe 28*
74.00	10	*2⊙ 10*
74.44	(04)	*2Sa+ 60 3Fe 31 3Fe 66*
74.84	(06)	*2Ni 76 4Y 88*
75.57	26w	*3Ni 61*
76.33	35	*5⊙ 02 5⊙ 17 5⊙ 24 5⊙ 36*
77.38	10	*3⊙ 60 4Ti 43 4Ti 93*
78.04	(10)	*1⊙ 18*
78.40	(10)	*2Fe 42*
78.84	(25)	*1Fe 86*
79.15	(15)	*2Fe 23*
79.54	(10)	*4⊙ 58 5⊙ 42*
79.99	(20)	*1Zn 14 3Ce+ 12 4Fe 98*
80.40	(20)	*2Fe 31 3Fe 49 4Cr 49*
80.85?	(05)	*2Cr 86*
81.84?	05	*1Ti 92*
82.26	50	*1Y+ 35 3Fe 11 4Fe 57 4Co 35*
83.54	08	*1Fe 57*
84.53	(30)	*1Ce+ 61 3Ti 50 4Cr 61*
84.99	(30)	*1Ca 28 2Zr+ 22 3Ti 04 ?Pr+ 93*
86.30	(10)	*2Ni 22*
86.63?	(08)	*4⊙ 63*
87.38	10	*1Fe 39 3Fe 31*
88.29	12	*1Fe 19 4Ti 38 4Fe 38 4Zr 48*
88.81	20	*3⊙ 69 4⊙ 06*
89.49	16	*1Cr 36 1Fe 50*
90.90	(15V)	*3La+? 20 4Ti 80 ?⊙ 98*
91.45	(40)	*1Fe 43 2⊙ 60 3Ti 35*
93.07	20W	*3Co 20 4⊙ 85 5⊙ 98*
94.19	(15W)	*1S 12 2Fe 87 4Cr 95*
94.75	(15)	*1Fe 86 3⊙ 45 3Cr 16*
95.31	06	*1S 45 5⊙ 60 5⊙ 75 5⊙ 86*
96.66	(15W)	*1S 31 4Ti 93 5⊙ 51 5⊙ 63*
97.33	(25)	*2Fe+ 32L 3Cr 06 4Cr 40 5⊙ 30*
98.56	45d	*1Sc+ 28 3Cr 47 3Cr 62 4Co 41*
99.36	12	*1⊙ 34*
4700.14	06	*1Fe 16*
01.47	20	*2Mn 17 3Ni 36 3Ni 54*
03.00	(50)	*1Mg 00 3Zr+ 02*
03.70	(06)	*1Ni 82 4Nd+? 60*
4669.30	*3Ce+ 52*	
70.40	*4Ce+ 74 ?Nd+ 56*	
76.33	*5⊙ 54*	
96.66	*5⊙ 76*	
98.56	*5Ni 41*	

TABLE IV—*Continued*

I.A.	Int. (0.01 A)	Identification
4705.25	21w	1*Fe* 96 1*Fe* 46
06.67	(07)	1*Nd*$^+$ 55 4*V* 56
07.25	(20)	1*Fe* 29 3*Fe* 50
08.70	35w	1*Ti*$^+$ 67 2*Fe*$^+$ 97*L* 2*Cr* 02 3*Fe* 09
10.12	10W	1*Fe* 29 2*Mn* 72 3*Ti* 20 5*Zr* 08
11.43	07	2*Fe* 49 3*Fe* 48
12.06	05	2*Fe* 08 4*Ni* 08
13.03	13	2*Sa*$^+$ 06 3*Y*$^+$ 26 4*La*$^+$ 91
13.90	15	3*Fe* 07 4*Ce*$^+$ 00 5*Ni*? 81 5*V* 12
14.43	40	1*Ni* 42 4*Fe* 37
15.80	16w	1*Ni* 77 1*Sc*$^+$ 14
16.36	(04)	2*La*$^+$ 42
16.80	(02)	3⊙ 84
17.10	(02)	?⊙ 13
18.31	05w	1*Cr* 42
18.74?	02	4⊙ 59 4*V*? 84
19.53	20	1*Ti*$^+$ 51
19.96	05	4*La*$^+$ 90 4*Sa*$^+$ 84 4*Zr*$^+$ 80 4⊙ 14
20.95	06	1*Fe* 00
22.20	08	1*Zn* 17 5*Sr* 29
23.15	04	3*Cr* 12 3*Ti* 18 4⊙ 00
23.59	04	4*Ni* 35 4⊙ 75 5⊙ 45
24.35	04	1*Nd*$^+$ 35 4*Cr* 41
24.86	04W	2*Ce*$^+$ 10 4⊙ 86
25.61	03	3⊙ 47 4⊙ 59
26.19	04d	2*Fe* 15 4*Fe* 96
27.39	18	1*Fe* 41 2*Mn* 50 4*Cr* 16
27.90	(12)	4*Ni*? 85 4*Co*? 95
28.31	(10)	1*Fe* 55 3*La*$^+$ 38 3⊙ 17
29.06	05	1*Fe* 02
30.20	21V	1*Mg* 04
31.50	50	1*Fe* 48 4*Ni* 81
32.36	04	2*Ni* 47 5*Zr* 33
33.21	05	1*Fe* 60 1*Ti*$^+$ 95 3*Ti* 43
34.21	65	1*Fe*$^+$ 09*L* 2*Fe* 11 2*Y*$^+$? 52
34.82	(13)	1*Zr*$^+$? 92 4*Co* 84
35.11	(12)	4⊙ 32 5⊙ 00
35.83	15	1*Fe* 85
36.82	50V	1*Fe* 78
38.27	45	5*V* 34
39.40	06	1*Mn* 12 3*Ce*$^+$ 50 5*Zr* 45
40.32	10w	1*La* 25 2*Fe* 35 3⊙ 49
40.95	08	1*Fe* 08 1⊙ 95
41.50	07	1*Fe* 54
42.34	22	3⊙ 30 3⊙ 55 4*Ti* 13
42.80	18	1*Ti* 80
44.38	08	1*Fe* 39
45.20	02?	4*Fe* 14 4*Cr* 32
45.79	13	1*Fe* 81
46.55	08W	4⊙ 27
47.88?	08	1⊙ 14 4*Na*? 98
48.64	10	1*La*$^+$ 74 4*V* 55
49.34	19v	3*Co* 67 5⊙ 26
51.52	05	3*Na*? 83 4*V* 55
08.70		4*Ti* 98 4*Fe* 97

TABLE IV—*Continued*

I.A.	Int. (0.01 A)	Identification
4752.10	09	*1Cr 10 2Ni 11*
54.21	16W	*1Mn 04 4Co 37*
55.24	03	*3Cr 16 4⊙ 28*
55.90	15W	*1Mn+? 70 2Cr 12 3Fe 12 4Fe 84*
56.55	(13)	*1Ni 52*
56.81?	(05)	*5Co 73 5⊙ 03*
58.05	(07)	*1Ti 13*
58.40	(05)	*4Ni 43 4V 73*
59.32	08	*1Ti 28*
60.51	04W	*4⊙ 75 ?Mo? 22*
61.55	20	*1Mn 53 3Zr+ 68*
62.60	80	*1C 41 1Ti+ 78 2Mn 38 3Ni 60*
64.02	(22)	*1Ti+ 92 2Ni 93 3Cr 29 3Ti+? 53*
64.59	(18)	*1Mn? 76 ?⊙ 87 ?⊙ 13*
65.62	(10)	*1Mn? 87 2Fe 47*
66.69	45	*1C 62 2Mn 42 4Fe 41 5Cr 64*
68.36	11	*1Fe 33 1Fe 41*
69.07?	03	*?⊙ 04*
70.00	40	*1C 00*
71.80	(75)	*1C 72 2Fe 71 ?⊙ 47*
72.88	(15)	*1Fe 82 5Ni 89*
73.72	(07)	*2Ce+ 93 4Ni? 42*
75.80	50	*1C 89*
77.49	25	*1Cr+ 74 4Nd+ 70 4Cr 60*
78.80?	20	.....
80.00	46	*1Ti+ 99 4Co 99 5Cr 93*
80.92	09	*1⊙ 82 5V? 02*
82.28	04	*?⊙ 28*
83.60	40w	*1Mn 43 2⊙ 00*
84.78	04	*5V 45 5Zr 94 ?⊙ 71*
85.78	12	*3Fe 96 4⊙ 68*
86.63	40	*1V+ 54 2Ni 54 2Fe 82 4V 54*
87.83	03	*1Fe 84*
88.74	07	*1Fe 76 4Zr 68*
89.75	10	*1Fe 66 4Ti 79*
91.35	36	*1Ti+? 49 2⊙ 14 3Fe 25*
92.48	50R	*2Ti 52 3Cr 52*
96.03	33	*2Ti 19 3Cr 19*
98.40	40	*1Ti+ 54 3Fe 27 4Fe 74*
99.82	22W	*3Ni 82 3Ti 80 3Fe 42 3Fe 89*
4802.87	08	*1Fe 89*
05.10	50	*1Ti+ 10 2Cr+ 18 4⊙ 01*
06.50	(15W)	*1Ti+ 34 4⊙ 62*
07.03	(08)	*1Ni 00*
07.65	03	*1Fe 72 4V 54*
08.70	05	*1Fe 69*
09.38?	02	*4Fe 14 5Zr? 48 ?⊙ 27*
10.46	06	*1Zn 54*
11.25	07	*1Nd+ 34 4Ti 05 5Fe 05*
12.35	(20)	*1Cr+ 36 4Ti 25*
12.80	(25)	*1C 84*
4762.60	*4Zr 77*	
66.69	*5V 64*	
99.82	*4Ca+ 16 5Fe 14*	

TABLE IV—*Continued*

I.A.	Int. (0.01 A)	Identification
4813.41	05	*2Co 48*
14.54	04	*2Ni 59*
16.05	20	*3Ni 94 4Cr 14*
17.34	40	*1C 33*
19.34?	03	*5⊙ 34*
20.40	05	*2Ti 42 2Nd⁺ 33*
21.12	06w	*1Ti⁺ 01 3Ni 13 5Fe? 13*
23.46	(30)	*1V⁺ 31 1Mn 52*
24.10	(60)	*1Cr⁺ 14 2La⁺ 04 3Fe 14*
25.64	15	*3Nd 47 4Mn 60 4Ti 48 4⊙ 73*
26.88	35R	*1C 73 3La⁺ 85 4Mn 85*
29.13	10	*1Ni 03 2Cr 37 4Cr 36*
29.89?	03	*?⊙ 70*
31.28	10	*1Ni 18 4V 65*
32.33?	08	*2Nd⁺? 28 3Sr 05 4Cr 55 4V 43*
33.04	10	*2Fe 72 4Ni 72 4⊙ 20 5V 03*
33.69?	04	*?⊙ 58 ?⊙ 84*
34.18	06	*?⊙ 18*
34.65	05	*2Sa⁺ 63 3Fe 52 5Ni 82*
36.20	70W	*1Cr⁺ 24 3Fe 88 3Ti 13 5Cr 23*
37.41?	05	*5Ti 40*
38.09	05	*2⊙ 09*
39.00	(15)	*3Fe 52 3Ni 65 4Cr 83 4Cr 36*
39.53	(25)	*1Fe 55*
40.84	07	*1Ti 89*
41.70	08	*2Fe 80 4Cr 68*
42.62	08	*2Fe 80 3Ti 59 4Fe 73*
43.31	15w	*2Fe 15 4Ni 15 4Co 51 5Ni 51*
44.26	02	*1Sa⁺ 21 2Mn 31*
45.57	05	*1Fe 66 4V 67*
48.27	(50)	*1Cr⁺ 25*
48.90	(10)	*2Fe 89*
49.11	(20)	*1Ti⁺ 17*
50.95	15	*1Mg⁺ 10 3La⁺ 56*
52.46	04	*2Ni 56*
53.50?	10	*4Ni 29 4Cr 54 4Ni 78*
54.13?	(05)	*?⊙ 16*
54.77?	(30)	*1V⁺ 88 4Mn 63 4Fe 89*
55.35	(35)	*1Ni 42 2Fe 68*
56.02	(45)	*1Cr⁺ 20 2Ti 02*
57.32	03	*2Ni 40*
59.27	70‡	*2Fe 14 ?⊙ 31*
59.80		*1Fe 75 4V 84*
60.35		*1Cr⁺ 22*
61.00	(30)	*3La⁺ 88 3Fe 99 4Cr 19*
61.67?	(15)	*1Hβ 34 4Cr 85*
64.35	(35)	*1Cr⁺ 32 4Ni 32*
65.73	(25)	*1Ti⁺ 62*
66.15	(25)	*1Ni 28 5Zr 07*
32.33?		*4Ti 05*
36.20		*5Ni 24*
39.00		*?⊙ 12*
43.31		*5Mn 15 ?⊙ 37*

‡ Impossible to estimate contributions of the individual lines.

TABLE IV—*Continued*

I.A.	Int. (0.01 A)	Identification
4867.70	05W	*2Co 88 4Fe 54*
68.61?	08	*3⊙ 42*
70.30?	10	*2Ti 14*
71.31	(35)	*1Fe 32*
72.20	(30)	*1Fe 14 3⊙ 94 ?Sr 51*
73.60	(10)	*2Ni 45 3Ni 26 4⊙ 75 ?⊙ 87*
74.15	(30)	*1Ti⁺ 01 3⊙ 36*
76.47	37	*1Cr⁺ 41 1Cr⁺ 49*
78.20	20w?	*1Fe 23 2Ca 13*
80.15	(22)	*2Ti⁺? 32 5Cr? 05*
81.71	(20)	*1Fe 72 4V 56*
82.45	(15)	*1Ce⁺ 49*
83.70	(35)	*1V⁺ 69*
84.69	(30)	*1Cr⁺ 60*
85.30	(10)	*1Fe 44 2Ti 09*
86.34	04	*1Fe 34*
87.30	10	*2Fe 20 3Cr 01 3⊙ 37 4Ni 01*
89.10	20?	*1Fe 01 1Fe 11*

it still persists in the molecular form, as is evidenced by the appearance of the Swan bands despite the fact that these bands are on the point of disappearance in the class Ro stars. Variations in the intensity of these bands may account for much of the minor fluctuation of light during maximum.

Na. The D pair is very strong. The doublet at λ 4665, though blended with other lines, appears to be present.

Mg. The great strength of the Swan band at λ 5165 masks the b-group seriously. Several singlets of fair intensity are present in the blue region of the spectrum.

Mg⁺. The high-excitation doublet at λ 4481 is very strong. One faint doublet arising from a higher level of 9.96 volts appears to be present.

Al. The resonance pair at λ 3944 and λ 3961 exhibit great strength on the one-prism spectrograms. No other lines of the neutral or ionized atom are observable.

Si. Only one line is available (on the one-prism plates), λ 4102 ($3p^2S_0 - 4s^3P^0_1$). Other lines should be observable in the yellow.

S. Three lines near λ 4694 have been tentatively identified. These lines are also present in the spectra of the sun and α Persei.

Ca. The ultimate line at λ 4227 is very strong, with an equivalent width exceeding 1 A. A number of other lines, particularly those arising from the 4^3P^0-level, exhibit moderate intensity.

Ca⁺. The widest and most intense lines in the spectrum are those of H and K. Their combined equivalent width is more than 40 A. They are among the first lines to reverse at minimum light.

Sc. The detection of *Sc* is difficult, and the strongest available lines are badly blended.

Sc$^+$. The lines are strong and easily identifiable. They reverse at minimum.

Ti. Many lines are present, but are weak and seriously blended with the exception of the group ($a^5F-y^5F^\circ$), near λ 4512.

Ti$^+$. The lines are very strong and the intensity gradient within the multiplets is small, indicating that, like all the lines of the related iron group, they are widened by some cause far in excess of that produced by thermal agitation.

V. A number of faint lines have been identified. The strongest of them belong to the group $a^6D-y^6F^\circ$, near λ 4379.

V$^+$. The lines are not especially strong and are seriously blended.

Cr. The lines near λ 4620 ($a^5D-y^5P^\circ$) are of moderate intensity and mostly unblended. About thirty lines, including blends, have been found.

Cr$^+$. The lines are nearly comparable in strength with those of *Ti*. More than two dozen lines have been identified.

Mn. The resonance triplet at λ 4030 is strong and of total equivalent width 1.7 A. A few other lines of moderate strength, though frequently blended, have been identified.

Mn$^+$. The classified lines are inaccessible. A number of unclassified lines in Miss Moore's list are present.

Fe. The great wealth of lines in the observable region has made the Russell-Adams analysis particularly applicable. The lines are of moderate to strong intensity, with plenty of unblended ones available. In going from *Sc* to *Fe*, it is interesting to note the growing strength of the arc lines with the increasing ionization potential.

Fe$^+$. The lines are among the most prominent in the spectrum, rivaling *Ti*$^+$ in strength. They do not reverse at minimum.

Co. A few faint lines are believed to have been identified on the one-prism spectrograms, none definitely on the three-prism plates. Blends make the identification difficult.

Co$^+$. The classification does not extend to the region under investigation. Identification must be held in abeyance.

Ni. With the exception of the multiplet ($z^5G^\circ-e^5F$) near λ 4592, the lines are rather weak and badly blended.

Ni$^+$. A single classified line at λ 4362 is probably present but blended with *Sa*.

Zn. The triplet near λ 4680 is present but weak.

Sr. The ultimate line at λ 4607 is present, but is badly blended with an iron line.

Sr$^+$. The resonance pair at λ 4077 and λ 4215 have equivalent width exceeding 1 A. They reverse at minimum. λ 4305 (E.P. = 3.02) is of fair strength.

Y. Traces may be present and are so recorded.

Y$^+$. About a dozen strong lines are easily identifiable.

Zr. Same comment as for *Y*.

Zr$^+$. The enhanced lines are quite strong and a number of conspicuous multiplets have been recorded.

Ba$^+$. Two strong lines lie in the observable region, one of which belongs to the ultimate pair at λ 4554.

La$^+$. This element is well represented in moderate strength by two score lines.

The rare earths. Of the rare earths, whose term values are as yet unclassified, *Ce*$^+$ and *Sa*$^+$ appear to attain the greatest prominence in the spectrum. *Nd*$^+$ and *Pr*$^+$ are thought to be present from analogy with the spectrum of γ Cygni, although the lines are all blended. Possibly *Dy*$^+$ and *Gd*$^+$ are there, but laboratory classification is needed to settle this point.

RADIAL VELOCITY OF R CORONAE

The velocity of the system is but slightly variable. Several periods of disturbed activity have, however, occurred in the interval covered by the observations. Two sets of spectrograms by Ludendorff[15] with a decade of separation, one by the author,[16] and the most recent one by McLaughlin[17] point to this conclusion. An intermediate series by Joy and Humason,[18] from observation with a single-prism spectrograph attached to the 60-inch reflector at Mount Wilson, gives values consistently smaller by 7 km/sec., as does a still earlier one-prism set obtained by Frost[19] at Yerkes when the star was fainter than usual. The significance of these results is not clear. It is known that the systematic corrections to be applied to the Mount Wilson and Yerkes measures for objects of classes F–G, in order to reduce them to the Lick system, are only +0.3 and −0.5 km/sec., respectively.[20]

The radial-velocity determinations are presented in Table V.

Omitting the Yerkes and Mount Wilson results, we obtain +25.1 km/sec. for the velocity of the system. Their inclusion, with a weight assignment equal to one-third that of the three-prism results, yields a value of +24.5 km/sec. Until further material accrues, we shall consider the velocity to be somewhat variable, granting the possibility, however, that larger variations such as those attested by the 1922 observations, for example, may alter the results from time to time while the star is at or near maximum light.

No special effort was made to detect any small systematic differ-

[15] *A.N.*, **173**, 1, 1906; **201**, 439, 1915.

[16] *Pub. A.S.P.*, **45**, 55, 1933.

[17] Privately communicated.

[18] *Pub. A.S.P.*, **35**, 325, 1923.

[19] *Loc. cit.*

[20] *Pub. Lick Obs.*, **18**, xii, 1932.

TABLE V

RADIAL-VELOCITY OBSERVATIONS

Date	Mag.	Aver. No. of Lines Meas.	Vel. Km/Sec.	Note
1902 April 28	6.2	35	+28.2	A
1904 May 30	5.8	.....	25.4	A
1906 May 24	6.0	.....	22.0	A
June 6	6.0	.....	26.1	A
July 26	6.0	.....	21.8	A
1903 July 24	7.2	11	14	B
1905 Aug. 25	7.0	.....	13	B
1913 June 15	6.0	25	28	C
June 16	6.0	.....	23	C
June 22	6.0	.....	27	C
1915 June 7	5.8	.....	24	C
June 8	5.8	.....	24	C
June 9	5.8	.....	23	C
1922 Feb. 5	6.2	14	16	D
March 8	6.1	.....	18	D
May 5	6.1	.....	20	D
July 5	6.0	.....	18	D
1932 June 27	6.0	41	25.4	E
July 4	6.0	.....	25.0	E
July 19	6.0	.....	27.0	E
July 29	6.0	.....	24.0	E
Aug. 8	6.0	.....	24.5	E
Aug. 9	6.0	.....	25.6	E
Aug. 27	6.0	.....	21.4	E
1929 March 29	6.0	36	22.5	F
1930 April 20	6.0	.....	21.1	F
April 22	6.0	.....	21.9	F
April 25	6.0	.....	31.6	F
April 29	6.0	.....	25.7	F
1931 Feb. 27	6.0	.....	26.0	F
April 18	6.0	.....	29.7	F
June 11	6.0	.....	23.7	F
1932 May 20	6.0	.....	27.6	F
1933 Feb. 22	6.0	.....	22.5	F
May 14	6.0	.....	31.3	F
May 18	6.0	.....	29.8	F
June 15	6.0	.....	27.4	F
1934 May 18	6.0	.....	22.7	F
May 29	6.0	.....	+22.5	F

A. 13-inch Potsdam refractor; three-prism spectrograph.
B. 40-inch Yerkes refractor; one-prism spectrograph.
C. 31.5-inch Potsdam refractor; three-prism spectrograph.
D. 60-inch Mount Wilson reflector; one-prism spectrograph.
E. 36-inch Lick refractor; three-prism spectrograph.
F. 37.5-inch Michigan reflector; one-prism spectrograph.

ence in the radial velocities obtained from the neutral and the enhanced lines, similar to that observed in γ Cygni by Adams and Joy.[21]

MULTIPLET INTENSITIES

In calculating the composition of a stellar atmosphere, a knowledge of the intensity gradients within multiplet systems is prerequisite. The recent observational evidence secured by Struve and Elvey[22] has led to the conclusion that the relation between the absorption line intensities and the theoretical emission intensities varies from star to star. This relation is given by the equation $A \propto (NFf)^n$, where A is the theoretical equivalent width, N the total number of atoms in the state corresponding to the lower spectroscopic term, f the fraction of atoms in this state which are engaged in the production of a particular multiplet, and F the theoretical intensity of the line in question relative to the sum total of all the lines in the multiplet (so that NFf corresponds to the number of atoms "actively engaged" in the production of the line). The exponent n ranges from 0 to 1 under different circumstances. For faint intensities thermal agitation of the atoms governs the widths of the lines, whereas radiation damping is preponderantly active in influencing the widths of the strong ultimate lines. In the former case it is easily shown that $A \propto NFf$, and in the latter case $A \propto \sqrt{NFf}$.[23] There exists, however, a transition region, of variable extent, wherein both effects operate simultaneously in such a way as to make A nearly independent of NFf, i.e., $n \to 0$. In Figure 1 there are exhibited two curves of the type indicated in terms of a parameter a equal to the ratio of the classical damping constant and the Doppler constant for *Ni* and *Co* at λ 4500.[24]

The curves are plotted logarithmically and express the absorption as a function of the theoretical intensity.

A comparison of the observed relative intensities within a multiplet with the theoretical intensities does not yield precise information regarding the relation between A and NFf, both because of

[21] *Proc. Nat. Acad.*, **13**, 393, 1927. [22] *Ap. J.*, **79**, 404, 1934.

[23] Unsöld, Struve, and Elvey, *Zs. f. Ap.*, **1**, 314, 1930.

[24] Minnaert and Slob, *Proc. Amsterdam Acad.*, **34**, Part I, 542, 1931.

observational errors and because of physical complications. The evidence indicates that in R Coronae the line absorption is not always strictly proportional to the square root of the theoretical intensities nor to the theoretical intensities themselves. The departure from the square-root law is especially marked in the case of the enhanced lines, particularly in the Ti^{+} doublet systems where the observed

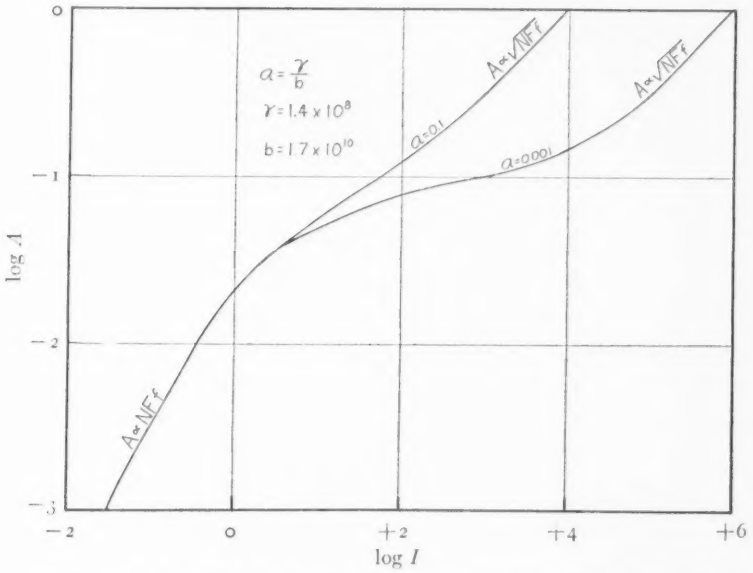

FIG. 1.—Total line absorption as a function of theoretical intensity (after Minnaert and Slob).

lines (frequently when $\Delta j = 0$) are very much stronger than prediction warrants. The gradient effect is in the same direction as that observed by Struve and Elvey[25] in α Persei and other stars.

CALIBRATION OF THE INTENSITIES

Instead of relying wholly upon individual multiplets, it is therefore more desirable, when practicable, to employ the relative intensities (or transition probabilities) of multiplet triads in order to effect the calibration. The advantage in using supermultiplets is that a larger number of lines are connected by a single set of theoretical relations and less weight is lost in the determination of zero points.

[25] *Loc. cit.*

Struve and Elvey adopted the results of an empirical method of Pannekoek and Minnaert,[26] who developed a general curve connecting the observed with the theoretical emission intensities in the flash spectrum by employing the known intensity ratios of the component lines of the individual multiplets. According to their method, the correction that was applied to the logarithms of the intensities in a multiplet was determined with the aid of Pannekoek and Minnaert's curve by the horizontal displacement of that multiplet relative to one chosen for the zero point. The present treatment is based on the theoretical work of Condon and Ufford[27] on theoretical transition probabilities in multiplets of a related group. Although the numerical results are fragmentary at the present time, it is possible, nevertheless, to sketch a fairly complete calibration-curve which may afterward be filled in by resorting to single multiplets whose observed line intensities have been well determined. I am greatly indebted to Mr. Leo Goldberg, of the Harvard College Observatory, for the numerical computation regarding the relative multiplet intensities. To the approximation used in this theory, intersystem lines ought not to appear at all. It cannot, therefore, give accurate results in the case of an element such as *Fe* I.

In Table VI are listed the multiplet triads which have been used in the preliminary calibration. In a few instances the complete triad did not lie in the observable spectral range (λλ 4000–5000).[28] The first column gives the name of the element and the electron configuration of the final and initial levels, the second column the terms resulting from the corresponding transition, and the last the relative multiplet intensities, G. In the cases marked with asterisk the values of G, here quoted, have been obtained by dividing the intensity, for transitions between two or more terms of the same type, by the number of transitions. This procedure is questionable, but the general order of magnitude may not be greatly influenced by it.

For configurations of three or more electrons, similar terms may arise by combining the spin moments of the electrons in different

[26] *Photometry of the Flash Spectrum*, p. 78, Amsterdam, 1927.

[27] *Phys. Rev.*, **44**, 740, 1933.

[28] One-prism intensities have been included, particularly when it proved necessary to complete or extend a triad.

TABLE VI

RELATIVE MULTIPLET INTENSITIES

ELEMENT Electron Configuration	TYPE	G
Sc II $3d^2-3d4p$	$a^3F-\begin{cases} z^3D \\ z^3F \end{cases}$	168 84
Ti I $3d^3(^4F)4s-3d^3(^4F)4p$	$a^5F-\begin{cases} x^5D^o \\ y^5F^o \\ y^5G^o \end{cases}$	25 35 45
$3d^3(^4P)4s-3d^3(^4P)^4p$	$a^5P-\begin{cases} y^5S^o \\ y^5P^o \\ w^5D^o \end{cases}$	5 15 25
$3d^3(^2H)4s-3d^3(^2H)4p$	$a^3H-\begin{cases} u^3G^o \\ x^3H^o \\ z^3I^o \end{cases}$	27 33 39
Ti II $3d^3-3d^2(^3F)4p$	$a^2G-\begin{cases} z^2F^o \\ z^2G^o \\ z^2H^o \end{cases}$	333* 288* 44*
V I $3d^34s^2-3d^34s(^3F)4p$	$a^4F-\begin{cases} z^4D^o \\ z^4F^o \\ z^4G^o \end{cases}$	10 14 18
$3d^4(^5D)4s-3d^4(^5D)4p$	$a^6D-\begin{cases} z^6P^o \\ y^6D^o \\ y^6F^o \end{cases}$	9 15 21
V II $3d^4-3d^3(^4F)4p$	$b^3G-\begin{cases} z^3F^o \\ z^3G^o \\ z^3H^o \end{cases}$	1269* 1357* 594*
Cr I $3d^44s^2-3d^44s(^6D)4p$	$a^5D-\begin{cases} y^5P^o \\ z^5D^o \\ z^5F^o \end{cases}$	15 25 35
Mn I $3d^6(^5D)4s-3d^6(^5D)4p$	$a^4D-\begin{cases} y^4P^o \\ z^4D^o \\ z^4F^o \end{cases}$	6 10 14
Fe I $3d^7(^4P)4s-3d^7(^4P)4p$	$a^5P-\begin{cases} z^5S^o \\ x^5P^o \\ w^5D^o \end{cases}$	5 15 25
$3d^7(^4F)4s-3d^7(^4F)4p$	$a^3F-\begin{cases} y^3D^o \\ y^3F^o \\ z^3G^o \end{cases}$	15 21 27
$3d^7(^2G)4s-3d^7(^2G)4p$	$b^3G-\begin{cases} x^3F^o \\ y^3G^o \\ z^3H^o \end{cases}$	21 27 33

ways. It is therefore essential that the state to which they converge in the ion (placed in parentheses) be known for complete identification.

The relative intensities, multiplied by suitable factors necessary for the comparison of the members of a supermultiplet widely separated in the spectrum, may now be used to calculate the observed emission intensities, I. For an individual line of a multiplet, the emission intensity relative to the total intensity of the supermultiplet, expressed in appropriate units, is given by

$$FG\left(\frac{\lambda_0}{\lambda}\right)^4 e^{-\frac{h(\nu_2-\nu_1)}{kT}} = I \propto NFf\,, \tag{1a}$$

$$\log F + \log G + 4\log\frac{\lambda_0}{\lambda} - \frac{5040}{T}\Delta E = \log I = \log NFf + \text{const.}\,, \tag{1b}$$

where F, as before, represents the theoretical intensity of the component line relative to the multiplet, G the multiplet intensity relative to the others comprising the triad, $(\lambda_0/\lambda)^4$ the frequency correction ($\lambda_0 = 4500$ A), $h\nu_2$, $h\nu_1$ the excitation potentials of the upper and lower energy-levels respectively, k the Boltzmann constant, and T the absolute temperature. In equation (1b), ΔE is the difference in excitation potential between the two states expressed in volts. T was assumed equal to 5300°, which happens to be the temperature later found for the reversing layer.

A plot of the logarithms of the theoretical intensities, log I, against the logarithms of the observed absorption intensities, log A, establishes an empirical relation between these two quantities for every atom. In default of information regarding the relative abundance of the elements and the absolute values of the oscillator strengths, Ff, the diagrams for each supermultiplet set were displaced horizontally (keeping log A fixed) with respect to each other in order to obtain the best possible superposition. Finally, by adding the results of isolated multiplets, a general curve connecting the calculated with the observed intensities was established. To fix the zero point on the horizontal scale the relation

$$A = \frac{\pi e^2 \lambda_0^2}{mc^2} \times 10^8 \times NFf = 1.8 \times 10^{-13} NFf\,, \tag{2}$$

where $\lambda_0 = 4500$ A was assumed to hold for faint lines whose profiles are defined solely by Doppler motion.

In order to compare the present results with the curves of Minnaert and Slob,[29] we must multiply our emission intensities, I or NFf, by the factor b/b_0[30] to secure their concentration co-ordinate, C, which is proportional to NFf, and the line absorption, A, by the factor $(\lambda_0/\lambda)^2(b_0/b)$ to obtain their computed A. While the first correction is relatively unimportant for the present purpose, the second one cannot be ignored. Consequently, to reduce to their scale, the following corrections were applied to the theoretical intensities, NFf, and to the observed line absorptions, A:

$$\left.\begin{aligned} NFf_c &= NFf\,\frac{b}{b_0}, \\ A_c &= A\,\frac{b_0}{b}\left(\frac{4500}{\lambda}\right)^2, \end{aligned}\right\} \tag{3}$$

where A_c and NFf_c correspond to the Minnaert-Slob values. The Doppler constants, given in their paper for $T = 5000°$, have been used with sufficient approximation.

The final results of this empirical adjustment are shown in Figure 2. The full line corresponds to Struve's theoretical curve computed on the basis of his turbulence theory with a damping constant ten times the classical value ($\gamma_{cl} = 8\pi^2 e^2 \nu_0^2 / 3\, mc^3$). The localized distribution of the neutral and ionized atoms, with the exception of *Fe*, is clearly marked.

According to the Minnaert-Slob theory, the flat part of the curve is reached for line intensities whose equivalent breadth is equal to 0.1 (see Fig. 1). The actual curve shows that this is not attained until the intensities are in the neighborhood of 0.8. The discrepancy lies in the direction of much greater observed widths for the lines than is predicted. To reach agreement with the observed curve, b_0 must be increased by a factor of 8. Hence, $a = 0.01 = \gamma_{obs}/8\, b_0$ or $\gamma_{obs} = 1.4 \times 10^9 = 10\gamma_{cl}$.

[29] *Loc. cit.*

[30] $b = \frac{2\pi}{\lambda}\sqrt{\frac{2kT}{m}}$, where the symbols have the usual meaning; $b_0 = 1.7 \times 10^{10}$. For hydrogen at 5000° and λ 4000 the value of the Doppler constant is 14.2×10^{10} compared with iron, for which the value is 1.9×10^{10}.

The observational results are in accord with those found by Struve and Elvey[31] in the intensity gradients of several stars and attributed by them to turbulence of macroscopic proportion. For stars where there is a departure from the curves of Minnaert and Slob, their modification of the theory proposes that, while the ex-

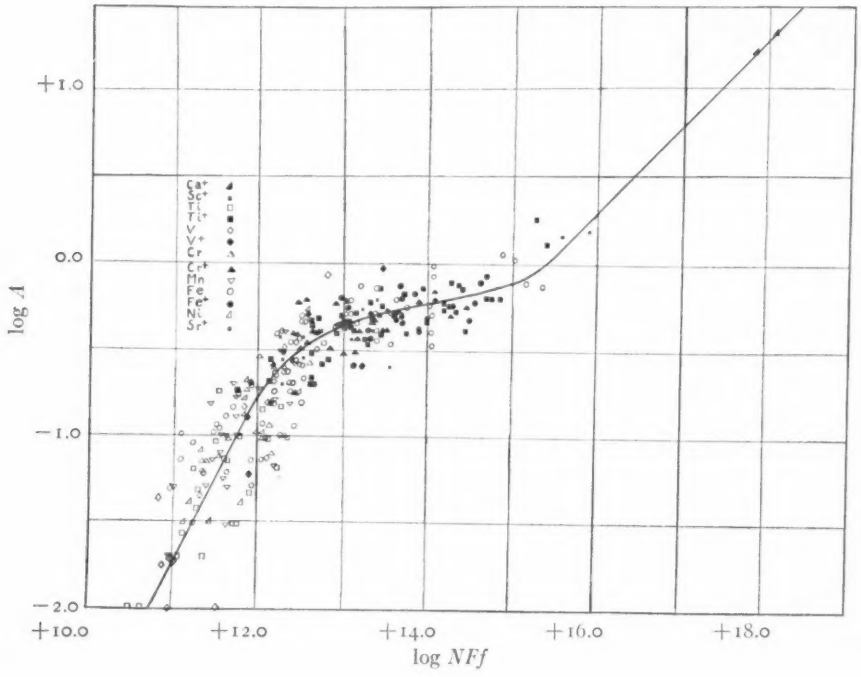

FIG. 2

tremities of the curve may still be defined by the Doppler motion of the atoms on the one hand and radiation damping on the other, the intermediate part is determined essentially by the turbulent motions of the atoms in the stellar atmospheres. The extent and height of this region above the log I axis are governed by their parameter, $b' = \lambda_0 v_0/c$, where v_0 is the Doppler effect corresponding to the most probable turbulent velocity.

Adopting Struve's suggestion,[32] we may set $b' = 8b_0 = 1.4 \times 10^{11}$

[31] *Op. cit.*, p. 409.

[32] Minnaert's and Slob's b_0 requires multiplication by $\lambda_0^2/2\pi c$ to reproduce Struve and Elvey's b'.

$(\lambda_5^2/2\pi c) = 0.15 \times 10^{-8} = v_0\lambda_0/c$, whence $v_0 = 10$ km/sec. The curve of Figure 2 corresponds to a value of Struve's parameter, $b' = 0.15$ A, exhibiting excellent agreement with the observations. The computed breadth of the strongest lines widened by turbulence corresponds to the value 0.6 A whereas the observed width is 0.8 A, in fair agreement with theory.

THE COMPOSITION OF THE ATMOSPHERE

It should be emphasized that the construction of the calibration of the intensities is independent of any theory relating to the formation of stellar absorption lines, with the exception of the aid rendered in locating the zero point on the horizontal axis. The empirical relation between the observed and the theoretical intensities, with the help of the ionization theory, should, as a first approximation, lead to a comparative census of the elements.

As a simplified approach to the problem, the following assumptions are made: (1) interlocking and redistribution in frequency when the energy-levels are not sharp may be neglected;[33] (2) collisional processes do not play a vital rôle in the formation of the absorption lines, except for their possible effect on the damping constant; (3) the vertical distribution of the neutral and ionized atoms is the same for a thoroughly mixed isothermal atmosphere; (4) the atmosphere is in thermal equilibrium with a mean electron pressure equal to exactly half the pressure at its base; (5) the atmosphere is situated above an opaque photosphere corresponding to an optical depth $\tau(\sim\frac{2}{3})$, such that the observed lines approximate those of the model atmosphere, which is assumed to be transparent to its own radiation, except in the lines.

To find the number of neutral atoms, N_0 (or ionized atoms, N_1), in the normal state, we employ the Boltzmann equation

$$N = N_0 \frac{g}{B} e^{-\frac{E}{vT}}, \tag{4a}$$

or

$$\log \frac{NFf}{Ff} - \log \frac{g}{B} = \log N_0 - \frac{5040}{T} E = \log \mathrm{D}, \tag{4b}$$

[33] Woolley, *Ann. Solar Physics Obs.*, **3**, Part II, 79, Cambridge, 1933.

where NFf is the number of atoms actively engaged in the production of the line, Ff the subdivided oscillator strength of the component line of the multiplet, g the weight of the state, B the partition function computed for the assumed temperature, $T = 5300°$, E the excitation potential corresponding to the lower state, and $v = 1/11{,}600$.

For the lines of a given element, log NFf corresponding to log A is read from the calibration-curve, and after insertion of the factors, Ff and g/B, log D is plotted against E, representing the horizontal axis. The intercept yields the number of atoms in the ground state, and the slope the inverse absolute temperature of the reversing layer. Unfortunately, of all the elements, neutral iron alone furnishes sufficient data from which to compute the desired quantities in this manner.

Pending theoretical developments, the best recourse for obtaining the absolute values of the f's is to determine them empirically from Russell's[34] investigation of the composition of the solar atmosphere. The oscillator strengths are completely known only for hydrogen at present. Incidentally, the summation of the f's for strong series is equal to unity, most of which is contributed by the principal members of the series, although this is not necessarily the case for higher series where Σf may be > 1. Adopting the Rowland calibration, one derives the values of log f by comparing the observed intensities of different multiplets arising from the same lower level with Russell's quantity, log M_{comp}, which represents the predicted total intensity for all the lines in the spectrum originating from the given level.[35] In a few instances where log M_{comp} is not given in Russell's list, it is possible to determine it in a similar manner from Menzel's[36] work on the chromosphere. For the fainter lines the estimates of log f are, naturally, much less secure, but, on the whole, individual discrepancies will tend to vanish in the mean.

Table VII lists the values of E and log D for all the elements whose line intensities could be determined from the one-prism or from the three-prism spectrograms. The adopted weights depend

[34] *Mt. W. Contr.*, No. 383, **34**, 1929.

[35] A number of intersystem combinations have been included in the results.

[36] *Pub. Lick Obs.*, **17**, 278, 1931.

TABLE VII

POPULATIONS OF ATOMS IN THE EXCITED STATES

E(Volts)	log D	Wt.†	Transition	log g/B	log f
	H log $N_0=21.08$				
10.16	11.54	1	$2^2P^o-4^2D$, etc.	+0.60	−0.92($H\beta$)
	11.32	1	-5^2D, etc.	+0.60	1.35($H\gamma$)
	11.43	2			
	C I log $N_0=21.48$				
7.45	14.40	5	$3S^3P^o-4p^3P$	0.00	1.4
	14.40	3	$-4p^3S$	0.00	1.9*
	14.40	8			
	Na I log $N_0=15.20$				
0.00	13.42	1	$3^2S-3^2P^o$	0.00	0.2
2.09	14.65	1	$3^2P^o-7^2D$	+0.47	3.8
	13.38	2	-6^2D	+0.47	1.9
	13.80	3			
	Mg I log $N_0=17.41$				
0.00	16.50	1	$3^1S-3^1P^o$	0.00	4.5
4.33	12.80	1	$3^1P^o-8^1D$	+0.48	1.2
	13.02	1	-7^1D	+0.48	0.6
	12.58	1	-6^1D	+0.48	1.3
	15.62	1	$-p^3_2P$	+0.48	4.5
	12.72	1	-5^1D	+0.48	0.7
	13.97	1	-6^1S	+0.48	−2.9
	13.45	6			

E(Volts)	log D	Wt.	Transition	log g/B	log f
	Mg II log $N_1=20.39$				
8.82	11.90	10	$3^1D-4^1F^o$	+0.70	−0.0
9.96	11.25	1	$4^1P^o-5^1D$	+0.47	0.0?
	11.53	2	-6^1S	+0.47	0.0?
	11.44	3			
	Al I log $N_0=16.30$				
0.00	16.30	1	$3^1P^o-4^1S$	0.00	0.1
	Si I log $N_0=16.85$				
1.90	15.05	½	$3p^1S-4s^3P$	−0.95	1.7
	S I log $N_0=18.57$				
6.50	12.39	3	$4^3S^o-5^3P$	−0.25	0.0?
	Ca I log $N_0=14.97$				
0.00	15.50	½	$4^1S-4^1P^o$	0.00	0.4
1.88	12.65	3	$4^3P^o-p^3_2P$	+0.95	0.6
	13.21	5	-4^3D	+0.95	0.6
	13.00	8			
2.51	13.42	2	$3^3D-6^3P^o$	+1.18	2.7
	12.22	3	-4^3F^o	+1.18	−0.8
	12.70	5			

* Value relative to $4p^3P$-state estimated from intensity rules.

† Weight arbitrarily assigned because of exceptionally good intensity determination.

TABLE VII—*Continued*

E(Volts)	log D	Wt.	Transition	log g/B	log f
	Ca I log N_0=14.97—*Continued*				
2.70	12.60	½	$3^1D-7^1P^o$	+0.70	−2.1
	12.80	1	-5^1F^o	+0.70	1.5
	11.75	1	-6^1P^o	+0.70	1.0
	12.34	2½			
2.92	13.02	1	$4^1P^o-6^1D$	+0.48	1.2
	Ca II log N_1=18.28				
0.00	18.28	1	$4^2S-4^2P^o$	0.00	0.00
	Sc I log N_0=12.70				
0.01	12.00	½	$a^2D-y^2D^o$	0.00	0.7
	12.32	1	$-z^2F^o$	0.00	0.6?
	12.21	1½			
1.43	12.05	1	$a^4F-y^4D^o$	+0.45	0.7
	Sc II log N_1=15.52				
0.31	16.33	½	$a^3D-z^3F^o$	−0.48	2.4?
	15.78	½	$-z^1D^o$	−0.48	0.2
	16.05	1			
0.60	14.39	5	$a^3F-z^3D^o$	+0.14	0.5
	14.93	7	$-z^3F^o$	+0.14	1.3
	14.92	½	$-z^3P^o$	+0.14	3.1?
	15.62	1	$-z^1D^o$	+0.14	3.8?
	14.78	13½			
1.35	15.68	1	$b^1D-z^1F^o$	−0.48	−0.7

E(Volts)	log D	Wt.	Transition	log g/B	log f
	Ti I log N_0=14.73				
0.02	13.73	2	$a^3F-z^3G^o$	−0.23	−1.4
0.83	13.36	3	$a^5F-x^5D^o$	+0.04	0.6
	13.23	6	$-y^5F^o$	+0.04	0.3
	13.27	9			
0.90	12.85	1	$a^1D-y^1D^o$	−0.80	0.6
1.06	15.21	1	$a^3P-y^3P^o$	−0.55	0.7
	14.40	1	$-v^1D^o$	−0.55	2.0
	15.35	1	$-x^3G^o$	−0.55	2.9
	14.17	1	$-w^3D^o$	−0.55	1.2
	14.78	4			
1.44	14.23	5	$b^3F-v^3F^o$	−0.23	1.6
1.50	12.86	1	$a^1G-z^1H^o$	−0.56	0.7
	13.08	1	$-y^1F^o$	−0.56	1.3
	12.97	2			
1.73	13.19	2	$a^3P-y^5P^o$	−0.32	0.8
	13.02	3	$-w^5D^o$	−0.32	0.1
	13.09	5			
1.87	12.52	1	$a^3G-v^3G^o$	−0.10	0.4
	14.00	1	$-y^3G^o$	−0.10	2.3
	12.22	1	$-y^3H^o$	−0.10	0.5
	12.91	3			
2.09	13.45	½	$z^5F^o-e^5D$	+0.04	1.0
	11.82	½	$-e^5G$	+0.04	0.2
	12.64	1			
2.15	12.76	1	$a^5D-r^5D^o$	−0.32	−0.3

TABLE VII—*Continued*

E(Volts)	log *D*	Wt.	Transition	log *g*/*B*	log *f*
	Ti I log N_0=14.73—*Continued*				
2.23	12.23	2	$b^3P-x^3S^\circ$	−0.55	−0.7
	13.31	2	$-r^3D^\circ$	−0.55	1.1
	12.77	4	.....	.....	.....
2.24	12.66	3	$a^3H-x^3H^\circ$	+0.01	0.6
	12.77	2	$-z^3I^\circ$	+0.01	0.6
	12.70	5	.....	.....	.....
2.26	12.70	1	$b^3G-x^3H^\circ$	−0.50	0.5
	Ti II log N_1=17.34				
0.58	16.43	1½	$a^2F-z^4G^\circ$	−0.63	2.0
1.08	16.08	2	$a^2D-z^4D^\circ$	−0.78	1.5
	15.86	4	$-z^2D^\circ$	−0.78	0.7
	15.90	3	$-z^4F^\circ$	−0.78	0.6
	16.02	3	$-z^4F^\circ$	−0.78	2.5
	16.66	2	$-z^4G^\circ$	−0.78	3.0
	16.05	14	.....	.....	.....
1.12	17.23	1½	$a^2G-z^2G^\circ$	−0.83	0.8
	16.13	1	$-z^2D^\circ$	−0.83	2.6
	16.64	3	$-z^2F^\circ$	−0.83	0.7
	16.43	4	$-z^4F^\circ$	−0.83	3.2
	16.63	3	$-z^4G^\circ$	−0.83	3.2
	16.60	12½	.....	.....	.....
1.16	15.40	8	$a^4P-z^4D^\circ$	−0.70	0.6
	16.50	4	$-z^2D^\circ$	−0.70	1.6
	16.25	3	$-z^2F^\circ$	−0.70	1.6?
	16.30	3	$-z^4F^\circ$	−0.70	−2.4
	15.93	18	.....	.....	.....
1.23	16.52	7	$b^4P-z^4D^\circ$	−0.70	−2.1
	16.30	4	$-z^2D^\circ$	−0.70	2.5
	16.32	2	$-z^2F^\circ$	−0.70	2.5
	16.42	13	.....	.....	.....
1.22	16.00	5	$a^2P-z^4D^\circ$	−1.00	1.4
	15.75	3	$-z^2D^\circ$	−1.00	0.3
	15.66	1	$-z^2F^\circ$	−1.00	2.2
	15.99	9	.....	.....	.....
1.57	15.63	3	$a^2H-z^2G^\circ$	−0.43	0.5
1.88	15.37	1	$b^2G-y^2F^\circ$	−0.52	1.5
2.04	15.76	4	$b^2P-z^2P^\circ$	−1.00	1.2
	15.40	2	$-y^2D^\circ$	−1.00	0.6
	14.95	2	$-z^2S^\circ$	−1.00	0.8
	15.47	8	.....	.....	.....
2.58	15.07	½	$b^2F-y^2P^\circ$	−0.63	2.3
	16.28	1	$-x^2D^\circ$	−0.63	0.3
	15.08	2	$-y^2G^\circ$	−0.63	1.1
	15.42	3½	.....	.....	.....
3.10	14.88	3	$c^2D-x^2F^\circ$	−0.78	0.4?
	15.37	1	$-y^2P^\circ$	−0.78	0.4?
	15.00	4	.....	.....	.....
	V I log N_0=14.90				
0.02	15.13	2	$a^4F-z^4D^\circ$	−0.25	2.6
	15.30	5	$-z^4F^\circ$	−0.25	2.6
	15.07	3	$-z^4G^\circ$	−0.25	−2.3
	15.20	10	.....	.....	.....

TABLE VII—*Continued*

E(Volts)	log D	Wt.	Transition	log g/B	log f
	V I log N_0=14.90—*Continued*				
0.28	14.97	3½	$a^6D-y^6D^o$	−0.22	−0.5
	13.74	5	$-y^6F^o$	−0.22	0.8
	14.16	1	$-z^6P^o$	−0.22	1.7
	14.24	9½			
1.06	14.50	3	$a^4D-y^4P^o$	−0.40	18
1.85	12.66	3	$a^4H-z^4I^o$	−0.06	0.9?
1.94	12.80	1	$b^4F-a^4D^o$	−0.25	0.4?
2.12	13.04	2	$a^4G-y^4H^o$	−0.14	1.1?
	V II log N_1=17.40				
1.43	16.00	1½	$a^3P-z^3D^o$	−0.70	1.6
1.67	16.26	1½	$a^5P-z^5D^o$	−0.48	2.3
	15.88	2	$-z^3D^o$	−0.48	3.0?
	16.04	3½			
1.80	15.55	2½	$a^3G-z^3G^o$	−0.20	1.5
2.02	15.36	1½	$b^3G-z^3F^o$	−0.20	2.0
	15.65	4	$-z^3G^o$	−0.20	2.3
	15.57	5½			
	Cr I log N_0=15.71				
0.00	14.87	1	a^7S-zP^o	−0.26	0.8
0.94	14.31	2	$a^5S-y^5P^o$	−0.41	1.0
0.98	14.77	7	$a^5D-z^5F^o$	+0.29	1.7
	14.73	8	$-y^5P^o$	+0.29	1.0
	14.75	15			
2.70	12.68	2	$a^5P-v^5P^o$	+0.07	0.8
	14.23	1	$-w^5P^o$	+0.07	−1.9
	13.20	3			

E(Volts)	log D	Wt.	Transition	log g/B	log f
	Cr I log N_0=15.71—*Continued*				
2.88	13.14	1	$z^7P^o-f^7D$	+0.21	−1.2
2.93	13.15	1	$a^3P-w^5D^o$	−0.16	1.2?
	13.46	2	$-y^3D^o$	−0.16	1.0?
	13.36	3			
3.00	12.56	1	$b^5D-x^5G^o$	+0.29	1.4
	12.09	1	$-z^5F^o$	+0.29	0.9
	12.32	2			
3.36	13.43	2	$b^3P-x^3D^o$	−0.16	1.1
	Cr II log N_1=18.21				
3.09	15.44	5	$b^4D-z^2S^o$	+0.46	3.2
3.78	14.96	2	$a^4P-z^4F^o$	+0.24	2.8
3.84	14.32	7	$a^4F-z^4D^o$	+0.60	1.3
	14.60	7	$-z^4F^o$	+0.60	1.2
	14.46	14			
4.06	14.35	7	$b^4F-z^4D^o$	+0.60	0.1
	Mn I log N_0=15.71				
0.00	16.10	1½	$a^6S-z^6P^o$	0.00	1.6
2.14	12.90	4	$a^5D-z^6D^o$	+0.70	0.2
2.29	12.63	3	$z^8P^o-e^8S$	+0.60	0.3
2.91	13.18	7	$a^4D-z^4D^o$	+0.52	0.8
	13.13	7	$-z^4F^o$	+0.52	0.6
	13.16	14			
3.06	12.87	5	$z^6P^o-e^6D$	+0.48	0.9
3.82	12.53	4	$z^4P^o-e^4P$	+0.30	−0.6?

TABLE VII—*Continued*

E(Volts)	log *D*	Wt.	Transition	log *g*/*B*	log *f*
	Fe I log N_o = 17.43				
0.08	17.92	2	$a^5D - z^7P^o$	−0.26	−4.1
	17.00	9	$-z^7F^o$		3.6
	17.17	11			
0.98	16.15	2	$a^5F - z^5F^o$	−0.10	3.3
	16.43	½	$-z^5D^o$		3.2
	16.21	2½			
1.54	16.38	3	$a^3F - y^3F^o$	−0.33	0.5
	16.47	3	$-z^3G^o$		1.1
	16.03	3	$-z^5G^o$		1.7
	16.13	7	$-y^5F^o$		2.6
	16.49	3	$-y^5D^o$		3.9
	16.73	2	$-z^3P^o$		4.2
	16.41	21			
2.20	15.32	1½	$a^5P - x^5P^o$	−0.52	1.5
	14.85	3	$-z^5S^o$		1.5
	15.10	8	$-x^5D^o$		1.0
	15.07	12½			
2.38	15.40	½	$a^3P - y^5P^o$	−0.70	3.6
	15.41	3	$-x^5D^o$		2.8
	15.04	1	$-y^3D^o$		1.5
	15.33	4½			
2.43	15.07	10	$z^7D^o - e^7D$	−0.11	0.4
2.57	14.54	½	$b^3F - y^3G^o$	−0.33	2.2
	15.07	1½	$-x^3D^o$		1.5
	15.01	2	$-w^3D^o$		2.9?
	15.98	1	$-x^5P^o$		−4.1?
	15.17	5			

E(Volts)	log *D*	Wt.	Transition	log *g*/*B*	log *f*
	Fe I log N_o = 17.43—*Continued*				
2.71	15.17	1	$a^3G - x^3F^o$	−0.22	−1.4
	14.98	1	$-w^3D^o$		1.9
	15.07	1	$-1S^o$		2.0
	14.22	1	y^3G^o		1.8
	14.86	4			
2.83	14.80	1	$b^3P - 44^o$	−0.70	1.9
	14.37	1	$-z^5S^o$		1.2
	14.52	½	-7^o		1.0
	14.57	1	$-w^3D^o$		0.7
	14.56	1½	$-x^3F^o$		1.4
	14.10	½	-10^o		1.1
	14.93	1½	$-y^3P^o$		1.3
	14.60	1	-16^o		1.1
	16.20	½	-19^o		1.6
	14.51	1	-20^o		1.6
	15.30	6	$-x^3D^o$		1.1
	14.77	4	$-w^3D^o$		1.9
	14.92	19½			
2.85	14.89	1	$z^7F^o - e^5F$	+0.03	2.6
	16.28	1	$-e^5D$		3.4
	14.28	4	$-e^7D$		0.5
	14.71	6			
2.95	14.84	1	$b^3G - 43^o$	−0.22	1.8
	13.00	½	-41^o		2.1
	14.50	3	$-z^3H^o$		1.5
	14.92	3	$-x^3F^o$		2.1
	14.58	1	$-w^3D^o$		2.7
	14.14	3	$-y^3G^o$		1.2
	14.51	11½			
2.98	15.36	3	$z^7P - e^5D$	−0.33	−3.0

TABLE VII—*Continued*

E(Volts)	log D	Wt.	Transition	log g/B	log f
	Fe I log N_0=17.43—*Continued*				
3.25	14.48	1	z^5D^o-19	−0.26	−2.2
	13.86	½	−59		1.4
	13.86	½	−17		1.0?
	13.22	½	−28		1.0?
	13.56	½	−58		0.7
	13.98	½	−29		1.7
	14.16	1	−22		1.4
	15.20	2	$-e^3F$		2.7
	14.31	8	$-e^5F$		0.5
	14.33	14½			
3.38	14.06	½	z^5F^o-4	−0.10	1.7
	14.40	1½	$-f^5D$		0.6
	14.02	1	$-e^3D$		1.3
	14.50	½	−3		2.4
	13.55	½	−13		1.4
	13.58	1	−6		1.0
	13.60	1	−18		0.7
	13.30	½	−23		1.0
	13.10	½	−57		1.0
	15.22	½	−8		1.8
	14.10	1	−14		1.3
	14.40	½	−56		0.6
	14.08	½	−16		1.6
	13.80	1	−17		1.2
	13.61	1½	−9		0.9
	13.48	½	−25		1.3
	13.76	1	−11		1.1
	14.70	½	−28		0.4
	14.60	½	−59		0.7
	13.97	½	−19		2.8
	13.91	½	−31		2.1
	14.54	1	−22		2.7
	14.60	5	$-e^3F$		2.1
	13.90	3	$-e^5F$		−0.8
	14.11	24½			

E(Volts)	log D	Wt.	Transition	log g/B	log f
	Fe I log N_0=17.43—*Continued*				
3.64	14.66	6	$z^5P^o-f^5D$	−0.52	−1.5
	13.97	2	−3, 4		1.0
	13.97	2	−2		1.2
	14.72	2	−7		2.6
	13.12	2	−17		0.4
	14.12	1	−20		1.0
	14.52	1	−59		2.1
	14.43	2	−26		2.1
	14.27	1	−27		2.1
	13.48	1	−29		1.3
	13.82	1	−19		1.4
	13.56	1	−31		0.8
	13.37	1	−32		0.6
	14.30	2	−22		1.4
	13.20	1	−33		0.4
	14.13	26			
3.90	13.83	2	$z^3F^o-e^3G$	−0.33	1.2
	13.70	1	$z^3D^o-f^3D$	−0.47	0.9
	12.81	1	−50		1.6
	13.57	1	−55		0.9
	13.55	5			
4.15	13.81	2	$y^5D^o-f^3D$	−0.25	1.5
	13.67	1	−49		1.7
	12.87	1	−40		1.4
	13.56	1	$-e^3G$		2.0
	12.45	1	−50		0.9
	13.36	6			
4.22	13.60	1	$z^3P^o-f^3D$	−0.10	2.0?
	13.40	2	$y^5F^o-f^3D$		−1.6
	13.47	3			

TABLE VII—*Continued*

E(Volts)	log *D*	Wt.	Transition	log *g*/*B*	log *f*
	Fe II log $N_1 = 19.84$				
2.68	17.44	2	$b^4P - z^4F^\circ$	−0.70	−2.8
	16.56	6	$-z^4D^\circ$		1.9
	16.78	8			
2.82	17.41	10	$b^4F - z^4F^\circ$	−0.23	2.0
	17.27	8	$-z^4D^\circ$		2.0
	17.35	18			
2.88	17.04	3	$a^6S - z^4D^\circ$	−1.00	2.6
	17.90	1	$-z^4F^\circ$		3.1
	17.25	4			
	Co I log $N_0 = 15.94$				
0.15	15.55	1	$a^4F - z^6G^\circ$	−0.15	3.2
	16.45	1	$-z^6F^\circ$		4.0
	16.00	2			
0.43	14.91	½	$b^4F - z^4F^\circ$		
0.98	14.53	1	$a^2F - y^4G^\circ$	−0.45	2.0
	15.12	½	$-y^4F^\circ$		2.1
	14.95	1	$-z^2F^\circ$		1.1
	13.45	½	$-z^2G^\circ$		0.9
	14.59	3			
1.95	14.22	1½	$b^4P - x^4D^\circ$	−0.52	1.0
2.92	13.48	1	$z^6F^\circ - e^6F$	−0.10	0.8
3.17	13.14	3	$z^6D^\circ - e^6F$	−0.13	−0.2?

E(Volts)	log *D*	Wt.	Transition	log *g*/*B*	log *f*
	Ni I log $N_0 = 16.99$				
1.67	14.72	1	$b^3D - y^1D^\circ$	−0.88	−2.5
3.30	13.71	5	$z^5D^\circ - e^5F$	−0.18	1.0
3.44	13.43	8	$z^5G^\circ - e^5F$	+0.07	0.5
	14.13	2	$-f^3D$		2.2
	13.57	10			
3.60	14.23	2	$z^3P^\circ - f^3D$	−0.63	1.4
	14.08	½	$-g^3D$		2.0
	13.67	1	$-f^1D$		1.4
	14.05	3½			
3.65	13.32	1	$z^3F^\circ - g^3D$	−0.26	1.8
	12.36	2	$-f^3F$		1.2
	12.68	3			
3.72	13.59	1	$z^3D^\circ - g^3D$	−0.40	1.8
	13.90	3	$-f^3F$		1.3
	13.82	4			
4.15	12.43	1	$z^1G^\circ - f^1F$	−0.63	0.7?
	Ni II log $N_1 = 18.52$				
4.02	14.50	½	$a^2G - z^2D^\circ$	+0.26	3.0
	14.80	1	$-z^4F^\circ$		
	14.70	1½			
	Zn I log $N_0 = 15.23$				
4.02	11.41	3	$4^3P^\circ - 5^3S$	+0.95	−0.3

TABLE VII—*Continued*

E(Volts)	log D	Wt.	Transition	log g/B	log f
	Sr I log $N_0=11.60$				
0.00	11.60	½	$5^1S-5^1P^o$	0.00	−0.0
	Sr II log $N_1=15.13$				
0.00	15.77	1	$5^2S-5^2P^o$	0.00	0.0
3.03	11.61	1	$5^2P^o-6^2S$	+0.48	0.1
	V II log $N_1=15.48$				
0.00	16.53	½	$a^1S-z^1P^o$	−1.23	1.0
0.10	15.60	5	$a^3D-z^3P^o$	−0.05	2.2
0.40	15.87	½	$a^1D-z^3F^o$	−0.53	0.3
	13.53	1	$-z^1D^o$	.....	0.7
	16.53	1	$-z^3P^o$	.....	1.7
	15.20	2½	.....	.....	.....
1.01	14.11	4	$a^3F-z^3D^o$	+0.09	0.5
	Zr II log $N_1=15.38$				
0.54	14.61	½	$a^2D-z^4G^o$	−0.78	0.6
0.73	13.98	½	$a^2P-z^4D^o$	−1.00	0.3
	15.32	1	$-z^4F^o$	.....	0.1
	14.87	1½	.....	.....	.....
0.75	16.93	1	$a^2F-z^2D^o$	−0.63	0.9
	15.45	1½	$-z^4F^o$	.....	0.3
	16.13	2	$-z^2F^o$	.....	0.3
	14.23	3	$-z^4G^o$	.....	0.9
	14.99	7½	.....	.....	.....
0.99	14.11	2	$a^2G-z^2F^o$	−0.52	0.4
1.20	14.00	8	$b^4P-z^4D^o$	−0.70	−0.0?
1.50	13.84	3	$a^2H-z^4D^o$	−0.44	−0.4
1.75	13.15	½	$b^2D-y^2F^o$	−0.78	0.0?
2.40	13.03	2	$b^2F-x^2F^o$	−0.63	0.0?
	13.31	1	$-x^2D^o$	.....	0.6
	13.12	3	.....	.....	.....
2.45	13.80	1	$b^2P-x^2D^o$	−1.00	0.5
	Ba II log $N_1=16.28$				
0.00	15.80	1	$6^2S-6^2P^o$	−0.40	0.0
2.60	14.30	1	$6^2P^o-7^2S$	+0.08	0.6
	La II log $N_1=14.66$				
0.00	14.35	½	$a^3F-y^1D^o$	−0.25	0.9
0.12	14.45	3	$a^3F-z^3D^o$	−0.25	1.3
0.17	13.62	1	$a^1D-y^1F^o$	−0.87	0.9
	12.97	1	$-y^1D^o$	.....	0.3
	13.30	2	.....	.....	.....
0.32	13.89	2	$a^3D-y^3D^o$	−0.39	0.3
	14.24	1	$-x^3F^o$	.....	0.3
	14.89	2	$-y^1D^o$	.....	2.0
	14.36	5	.....	.....	.....
0.70	14.04	1	$a^3P-y^3D^o$	−0.62	0.9
0.92	14.32	1	$a^1G-z^1H^o$	−0.62	0.5?
1.75	13.75	2	$z^3F^o-e^3G$	−0.25	0.1
	13.95	1	$-e^1F$	.....	0.6
	13.82	3	.....	.....	.....
1.94	12.52	½	$z^1F^o-e^1G$	−0.72	−0.0?

upon the number of lines employed in each multiplet, half-weight being given to the single-prism observations.

The rectilinear relation between log D and E, exhibited in Figure 3 for the neutral iron lines, indicates that *if* there is a departure from thermodynamic equilibrium, it is similar in R Coronae and the sun, at least up to 4.5 volts.[37] There is, as a matter of fact, little reason to suspect that marked deviation is present even as high as 10 volts, corresponding to the high-excitation lines of Mg^+, as we shall see shortly.

A least-squares solution of the observations represented in Figure 3 gives the following result:

$$\log D = (-0.95 \pm 0.03)E + 17.43 \pm 0.09 , \qquad (5)$$

whence $N_0 = 17.43 \pm 0.09$ and $T = (5305° \pm 168°)$ K. With this value of T the weighted means of the numbers of neutral and ionized atoms in the unexcited states have been computed for the other elements. The results have been placed opposite the names of the elements in Table VII.

The numbers of ionized and neutral atoms may be used to derive the mean electron pressure in the atmosphere from the ionization equation

$$\frac{N_1}{N_0} = \frac{K}{\bar{P}} ; \qquad K = 0.267 \frac{B_1}{B_0} T^{5/2} e^{-\frac{I}{\theta T}} , \qquad (6)$$

where, in the ionization constant, T is to be taken as the photospheric temperature, 5300°. In the form available for computation, equation (6) becomes

$$\log \bar{P} = 2.74 - \log \frac{N_1}{N_0} + \log \frac{B_1}{B_0} - 0.95I . \qquad (7)$$

The values of log $\bar{P}$ derived for a number of elements are given in Table VIII.

The effective electron pressure is, therefore, 4.17×10^{-7} atm. and the pressure at the base of the reversing layer is twice as much, or 8.34×10^{-7} atm. The level of ionization, corresponding to an element half-ionized, is 9.6 volts.

[37] I am indebted to Professor Russell for this conclusion.

The fact that the pressure computed from the few available high-excitation lines of ionized and neutral magnesium is in tolerable

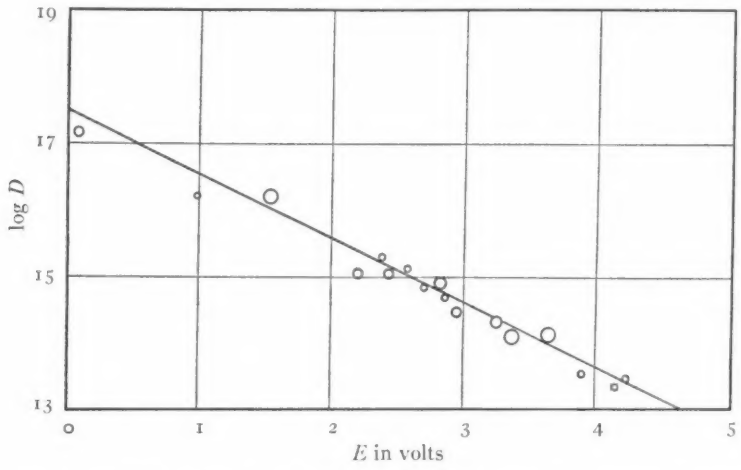

FIG. 3.—Number of excited neutral iron atoms as a function of excitation potential

agreement with the other results may be taken as an indication that there is little or no departure from thermodynamic equilibrium up to 10 volts. A damping constant ten times the classical value recom-

TABLE VIII

VALUES OF LOG $\bar{P}$

Atom	log $\bar{P}$	Atom	log $\bar{P}$
Mg	−7.17	*Cr*	−6.42
Ca	6.06	*Fe*	6.82
Sc	6.26	*Ni*	6.60
Ti	6.05	*Sr*	−5.86
V	−6.19		
Average	log $\bar{P}$ = −6.38		

mended by Struve and Elvey from their observations seems to be required here in the case of the H and K lines, since the number of ionized atoms of calcium determined from the calibration-curve leads to a value for the electron pressure in conformity with the results obtained for the other atoms.

Slightly adjusting the observed values of N_0 and N_1 to correspond to a mean electron pressure of 4.17×10^{-7} atm., we obtain the following census of the elements in the atmosphere of R Coronae. The first two columns of Table IX are self-explanatory; the next three give, respectively, the logarithmic numbers of neutral, singly ionized,

TABLE IX

CHEMICAL COMPOSITION OF THE ATMOSPHERE

Element	Atomic No.	log N_0	log N_1	log N_2	log N	Volume (in Per Cent)
H	1	21.08:	17.04:	.....	21.08:	27:
C	6	21.48	19.79	.....	21.49	69
C_2	.....	15.18	.....	.....	15.18	0.00003
N	7	.....	.....	.....	.....	0.3*
O	8	.....	.....	.....	.....	?
Na	11	15.20:	19.16:	.....	19.16:	0.32:
Mg	12	17.81	20.00	.....	20.00	2.24
Al	13	16.30:	18.98:	.....	18.98:	0.21:
Si	14	16.85:	18.09:	.....	18.11:	0.03:
S	16	18.57:	17.55:	.....	18.61:	0.09:
Ca	20	14.81	18.44	16.68	18.44	0.06
Sc	21	12.64	15.58	.....	15.58	0.00008
Ti	22	14.56	17.50	.....	17.50	0.007
V	23	14.86	17.50	.....	17.50	0.007
Cr	24	15.73	18.19	.....	18.19	0.03
Mn	25	15.71	17.92	.....	17.92	0.02
Fe	26	17.65	19.62	.....	19.62	0.93
Co	27	15.94	17.61	.....	17.62	0.01
Ni	28	17.10	18.41	.....	18.43	0.06
Zn	30	15.23:	15.47:	.....	15.67:	0.0001:
Sr	38	11.58	15.15	13.79:	15.17	0.00003
Y	39	12.31	15.48	12.82:	15.48	0.00007
Zr	40	12.59	15.38	11.00:	15.38	0.00005
Ba	56	11.39	15.90	16.36:	16.43	0.0006
La	57	10.64	14.66	12.87:	14.66	0.00001

* Upper limit.

and doubly ionized atoms per square centimeter; the sixth gives the total logarithmic number of atoms of a given kind; and the last gives the abundance of the element by volume.

In the case of *H*, *Na*, *Al*, *Si*, *S*, and *Zn*, doubt arises because of the uncertain measures of log *A;* for *Sr–La* the partition functions corresponding to second ionization are unknown, but the final tabulation is practically unaffected by this source of error. The contribution of *N* and *O* remains undetermined as there are no lines available for analysis in the observed spectral region. The cyanogen absorp-

tion band at λ 3883 appears to be too faint for positive identification on the slitless spectrograms and much fainter than the Swan bands. Hence N must be much less abundant than C.

To compute the number of carbon molecules the total pressure is required. Hence

$$\bar{p}=\frac{1+\beta}{\beta}\,\bar{P}\,, \tag{8a}$$

$$\beta=(\epsilon x_1)_C+(\epsilon x_1)_H+(\epsilon x_1)_{Mg}+(\epsilon x_1)_{Fe}\,, \tag{8b}$$

where ϵ is the relative abundance of the element by volume and x_1 the fraction ionized. The partial pressure accruing from the remaining elements may be neglected. The total mean pressure, according to equations (8a) and (8b), is 9.29×10^{-6} atm., most of which is contributed by carbon and magnesium.

The partial pressures of C and C_2 are related as follows:

$$\log\frac{\bar{P}_C^2}{\bar{P}_{C_2}}=\log K'\,; \qquad \log K'=A+\tfrac{1}{2}\log T-\frac{B}{T}\,, \tag{9}$$

where K' represents the dissociation constant. The molecular constants, A and B, have been tabulated by Russell in his paper, "Molecules in the Sun and Stars."[38] Moreover,

$$\bar{P}_C=\epsilon_C\bar{p}=\frac{N_C}{\Sigma N}\,\bar{p}\,, \tag{10a}$$

$$\bar{P}_{C_2}=\epsilon_{C_2}\bar{p}=\frac{N_{C_2}}{\Sigma N}\,\bar{p}\,, \tag{10b}$$

where ΣN is the total number of particles. Substituting in equation (9), we obtain, with $T=5300°$, $\log K'=+1.11$, on solving for N_{C_2}, $\log N_{C_2}=15.18$. Thus, omitting possible ionization of the molecule, the abundance of C_2 is comparable with that of neutral sodium.

The theoretical amount of C_2 may be compared with the observed intensity of the Swan bands. Owing to the crowding of the numerous faint lines, the total absorption of the bands was determined from the unresolved contribution of the lines as a whole; hence, corresponding

[38] *Op. cit.*, No. 490, 6, 1934.

to each approximate value of log A in Table III, log $Nf(F=1)$ was read from the calibration-curve. The results are tabulated here.

Band	log Nf	Band	log Nf
λ 4737	13.6	λ 4678	13.4
4715	12.0	4382	11.9
4697	12.3	4371	12.6
4685	12.8	4365	13.4

Roughly, then, the observed total intensity of the bands in the blue corresponds to log $Nf \sim 14.0$. If the strong band at λ 5165 blocked out three times as much energy from the spectrum as the band at λ 4737, log $Nf \sim 15.7$. This suggests that the computed abundance of C_2 is, perhaps, too low.

For the dissociation constants of other carbon compounds we find CH, log $K' = +1.93$; CN, log $K' = +0.04$; CO, log $K' = -2.00$. With log $P_H = -5.58$, log P_{CH} comes out -12.69, so that there should be only 1/17 as much CH as C_2 in the atmosphere. The weakness of the G band is thus explained. If nitrogen was as abundant as hydrogen, log P_{CN} would be -10.80. As the CN bands were not observed, nitrogen can hardly be more than 1/100 as abundant as hydrogen.

If oxygen were as abundant as hydrogen, log P_{CO} would be -8.76, so that only 1/1500 of the oxygen, and 1/4000 of the carbon, would be locked up in carbon monoxide. Since this is the most firmly bound molecule known, it appears that molecules of any sort must form but a negligible fraction of the star's atmosphere.

From the relation

$$p = \mu g \Sigma N , \qquad (11)$$

where μ is the mean molecular weight, we may derive the surface gravity, g, equal to 2.68×10^2 cm/sec.^{2}, or 0.01 times the solar value.

Using Russell's equation[39]

$$M_v = \frac{29{,}500}{T} - 5 \log R - 0.08 , \qquad (12)$$

[39] Russell, Dugan, and Stewart, *Astronomy*, **2**, 732, 1927.

we find for various assumed values of the absolute magnitude, with $T = 5300°$:

M_{vis}	log R	M_{bol}	log m_{Edd}	log g_{comp}
−1.0	1.32	−1.1	0.74	−1.90
3.0	1.72	3.1	1.12	2.32
−5.0	2.12	−5.1	1.55	−2.69

where m_{Edd} is from Eddington's mass-luminosity curve. The sun is taken as standard. An exact agreement with observation is obtained for $M = -1.4$, $\log m = 0.82$, $m = 7 \times \odot$. The data are far too uncertain to present this as a determination of the mass of R Coronae, but at least they show that the results are reasonable.

TABLE X

COMPARATIVE ABUNDANCES IN R CORONAE AND γ CYGNI

Element	R Coronae (Per Cent)	γ Cygni (Per Cent)
Hydrogen	27:	99
Carbon	69	0.5:
Metals	4	0.5

It is of interest to compare relative abundances in the atmospheres of R Coronae and γ Cygni (Table X).

The estimated hydrogen content in the atmosphere of γ Cygni may require reduction, owing to the peculiar influences operative for that element—for example, pressure, Stark, and fine-structure effects. The total number of atoms in the atmosphere of γ Cygni comes out about thirteen times that of R Coronae. The difference, however, may result from the circumstance that in the former star we view more material per square centimeter on account of the decreased opacity arising from the overwhelming abundance of neutral hydrogen atoms.

One final calculation may be performed. By definition the optical depth, τ, of the photospheric surface is given by

$$\tau = N_0 a_\nu , \qquad (13)$$

where a_ν is the atomic absorption coefficient resulting from photo-electric ionization of the atoms. It is proper to neglect the contribution of the free-free transitions to the general opacity in comparison with the former physical process.

According to Menzel,[40] the simplified absorption coefficient for the "hydrogenic" atom derived on the basis of the wave-mechanics has the value

$$a_\nu = \frac{16\pi^2}{3\sqrt{3}} \frac{Z^2\epsilon^6}{ch^3\nu^3} \frac{kT}{h} \frac{2B_1(T)}{B_0(T)} e^{-h(\nu_1-\nu)/kT}, \qquad (14)$$

the only new symbols being Z, the nuclear charge; ϵ, the electrostatic charge of the electron; and ν_1, the ionizing frequency of the radiation. Employing equations (13) and (14) for the various elements, at λ 4000, we obtain Table XI.

TABLE XI

CONTRIBUTION TO THE GENERAL OPACITY BY DIFFERENT ELEMENTS

Element	τ
Hydrogen	3×10^{-7}
Carbon	2×10^{-3}
Metals	4×10^{-3}
	$\Sigma\tau = 0.006$

The computed opacity arising from the partly ionized gases is absurdly inadequate. Moreover, the previous calculations make it doubtful whether there are sufficient molecules in the atmosphere to produce much opacity. Even if we took $M_v = -5$ in equation (12), corresponding to $\Sigma N = 2\times10^{22}$, the opacity would still be too small by a factor of 20. It is of interest to note that Russell[41] finds a value of the solar opacity equal to 0.05. He suggests that most of the opacity in the sun's external layers is produced by the interaction of the neutral hydrogen atoms and free electrons, but unpublished calculations by Menzel have indicated that the contribution from this source is insignificant.

The discordance in the observed opacity could be removed by an arbitrary charge in the zero point of the calibration-curve of the in-

[40] Private communication.

[41] *Op. cit.*, No. 477, 39, 1933.

tensities which would affect the numbers of absorbing atoms (see Fig. 2). The zero point rests upon the theoretical determination of the absorption intensities for faint lines whose widths are defined solely by Doppler broadening. Its evaluation is based upon the acceptance of a definite atmospheric model, either the Schuster-Milne or the Eddington approximation.[42]

A comparison of lines in common between R Coronae and γ Cygni, similar to the procedure adopted by Russell and Adams,[43] may be used to derive the atmospheric temperature of R Coronae, provided that of γ Cygni is known. If N_R and N_γ be the respective numbers of atoms per unit surface area, neutral or ionized, in the excited states in the two stellar atmospheres, we have

$$\log \frac{N_R}{N_\gamma} = \log \frac{N_{oR}}{N_{o\gamma}} + 5040\left(\frac{1}{T_\gamma} - \frac{1}{T_R}\right)E\,, \tag{15a}$$

or

$$Y = Y_o + SE\,. \tag{15b}$$

From a plot of Y against E, the slope, S, may be determined, and hence the temperature, T_R. The intercept yields the relative abundance of the atoms in the unexcited state in the two atmospheres. The results of the analysis, which depend upon the observed line absorptions, may be conveniently summarized according to the element, the derived slope, the total number of lines employed, and the assigned weight, depending upon the number of lines and their range in excitation potential (Table XII).

Caution must be exercised in computing the temperature in the two cases, since the intensities of the faint neutral lines follow generally along the Doppler branch of the calibration-curve, whereas most of the enhanced lines lie along the flat portion of the curve. In the former instance, $A \propto N$; and in the latter case, $A \propto N^{.13}$. Hence,

[42] According to recent calculations by Menzel and Pekeris, the discrepancy in the computed solar opacity has now been virtually removed by their application of a more exact expression than that given by eq. (14) (*Pub. A.A.S.*, **8**, 119, 1935).

[43] *Op. cit.*, No. 359, 1928.

with sufficient approximation,[44] we find, assuming Russell's revised value of $T\gamma = 5300°$ K,[45]

Neutral atoms: $S = +0.045 \pm 0.005 = 5040\left(\frac{1}{T_\gamma} - \frac{1}{T_R}\right)$; $T_R = (5570° \pm 31°)$ K,

Ionized atoms: $S = +0.006 \pm 0.002 = 655\left(\frac{1}{T_\gamma} - \frac{1}{T_R}\right)$; $T_R = (5575° \pm 94°)$ K.

The foregoing results are in satisfactory accord with the value of 5300° K derived by the absolute method.

TABLE XII

VALUES OF S

Element	S	No. Lines	Range of E(Volts)	Wt.
	Neutral Atoms			
Ca	+0.08	9	2.92	2
Ti	.06	28	2.13	4
V	.07	24	2.10	3
Cr	.03	33	3.16	10
Fe	.04	196	4.13	100
Ni	+0.10	28	2.45	5
	Ionized Atoms			
Sc	+0.10	16	1.05	0
Ti	+ .00	84	2.00	10
Cr	− .07	28	0.97	1
Y	+ .05	12	1.01	0
Zr	+ .02	27	1.86	3
La	+0.05	22	1.80	2

THE COLOR TEMPERATURE OF R CORONAE

From the description of the spectrum it is obvious that the spectrophotometric determination of the temperature is beset with difficulties, chief of which is the location of the continuous back-

[44] The relation between the observed and theoretical intensities is nearly the same for the spectrum of γ Cygni as for that of R Coronae.

[45] Privately communicated.

ground unaffected by line or band absorption. It is doubtful whether in the face of these difficulties much weight can be attached to the results.

The method employed was the usual one. Spectra of a standard comparison star, in this instance, ζ Ophiuchi, Bo, with an adopted temperature $T = 22{,}000°$ K, whose energy distribution is then known, were impressed on the same plate as those of the star whose temperature was sought. To allow for the variation of the contrast factor with wave-length, three sets of sensitometer images in the red, green, and blue regions were put on the slitless spectrograms. The difference between the true energy-curve of the known star outside

TABLE XIII

COLOR TEMPERATURE OF R CORONAE

Date	Plate No.	λλ 3500-4500	λλ 4500-6500	Wt.
1932 June 28	E 1	6500° K	.....	1.00
July 2	W 2	6500	8000° K	0.50
July 5	W 12	7000	8000:	0.25
July 23	W 18	7000	8000	1.00
July 24	W 21	6000	9000:	0.25
July 24	W 22	6500	7000	1.00
July 24	W 23	6500	7000	0.50
July 31	W 25	7000	8000	0.75
Aug. 6	J 20	7000	.....	0.25
Aug. 10	J 26	7500	.....	0.25

the earth's atmosphere and its "apparent" energy-curve as given by the plate determined the correction factor, which is a function of the instrumental constants, the type of plate used, and the wave-length. This factor, plus a small additional correction to allow for the differential effect of atmospheric selective absorption between the two stars at the time the photographs were secured, applied to the apparent energy distribution in the spectrum of the unknown star, yielded the energy gradient of the star.

The color temperatures thus derived from the observed energy distribution on the plates taken with the two-prism quartz slitless spectrograph attached to the Crossley reflector are presented in Table XIII.

The assignment of weights was based upon the quality of the spectrograms. The weighted average of the color temperature is

(6700° ± 70°) K, (λλ 3500–4500) and (7700° ± 200°) K, (λλ 4500–6500). It is not clear why there should be an observed temperature difference of 1000° between the violet and the red unless (1) the opacity in the more refrangible region is relatively larger than in the region of longer wave-lengths owing to increased line and band absorption (the so-called violet depression), (2) the observer cannot properly trace the continuous background, and (3) the energy distribution of the comparison star is affected by selective absorption in space.[46] I believe that we may accept the result that the color temperature is somewhat higher than the effective temperature.

The R- and N-type stars suggest that the cosmic abundance of carbon must be high. The connection of the R Coronae type variables with these classes is readily apparent. According to Miss Payne,[47] there are eleven R Coronae type variables with spectral classes ranging from G to R. If the classification is correct, it would appear that the objects of earlier type may be thought of as abnormally hot carbon stars. Further research on stars of even earlier class than G whose spectra indicate exceptionally weak hydrogen lines should prove interesting.

ACKNOWLEDGMENTS

It is a pleasure to express my gratitude to Director Harlow Shapley for privileges extended me in connection with the present research at the Harvard College Observatory; likewise to Director W. S. Adams, Dr. A. H. Joy, and Dr. Olin Wilson for courtesies rendered me while at the Mount Wilson Observatory; and, particularly, to Director R. G. Aitken, who graciously accorded me the use of the Lick Observatory equipment in furtherance of this investigation. I express my deepest obligation to Professor D. H. Menzel for many helpful comments and to Professor H. N. Russell whose careful preview of the manuscript led to a number of improvements and to several important additions.

JUNIOR COLLEGE
SAN MATEO, CALIF.
February 26, 1935

[46] Stebbins and Huffer find an excess color index of +0.11 for ζ Ophiuchi (*Pub. Washburn Obs.*, **15**, Part V, 232, 1934).

[47] *Stars of High Luminosity*, p. 244, 1930.

ζ AURIGAE: THE STRUCTURE OF A STELLAR ATMOSPHERE*

By WILLIAM H. CHRISTIE and O. C. WILSON

ABSTRACT

From the measures of spectrograms of ζ Aurigae taken during the 1934 eclipse a number of new and interesting results have been obtained.

By combining the measures of the light of the star made at Mount Wilson and Madison with the spectroscopic elements derived by Harper and by the authors, new elements for the system have been obtained.

A method has been devised whereby the effects of the light of the K star in the composite spectrum of the two bodies may be eliminated from measures of microphotometer tracings of the spectra. This possibility has enabled us to measure the total absorption of the continuous spectrum of the B star produced by the various elements in the atmosphere of the K star.

From a number of microphotometer tracings made from the most suitable plates, the changes in the total absorption have been measured for nearly a hundred lines in the spectra. These measures have been used to determine the effect of the B star shining through the atmosphere of the K star alone, thus affording means of obtaining the relative numbers of atoms of the various elements existing at different levels above the photosphere of the K star. These results are grouped into six distinct classes: neutral metals; *Mg; Ti*$^+$ (two groups); *H; Ca*$^+$.

Comparison of these results with theory reveals that there is, in most cases, no adequate hypothesis to account for the observed distribution. The measures of the hydrogen lines indicate that the hydrogen shell surrounding the star is of uniform density.

INTRODUCTION

The binary character of the eclipsing star ζ Aurigae was announced by Campbell[1] in 1908, although the probability of the star's being a double had previously been recognized by Miss Maury when she classified the spectrum as composite.[2] The elements of the spectroscopic orbit of the system were investigated at the Dominion and the Dominion Astrophysical observatories by Harper[3] in 1917–1924. One of Harper's spectrograms, which showed the spectrum of the K component alone, brought out the eclipsing character of the star. In 1926 Bottlinger[4] drew attention to the pressing need for photometric observations and predicted the times of the following eclipses. The minimum of 1932 was observed by Guthnick and

* *Contributions from the Mount Wilson Observatory, Carnegie Institution of Washington*, No. 519.

[1] *Lick Obs. Bull.*, **5**, 62, 1908.

[2] *Harvard Ann.*, **28**, 99, 1897.

[3] *Pub. Dom. Ap. Obs.*, **3**, 151, 1924.

[4] *A.N.*, **226**, 239, 1926.

Schneller[5] and by Hopmann,[6] whose measures confirmed the eclipsing character of the binary.

The 1934 eclipse was looked forward to by a number of observers but, unfortunately for most of them, the skies of Europe and of the Eastern United States were none too good. Mount Wilson, however, was more favored, as Table I, containing the observational data, will show; clouds interfered with observations only at the beginning and end of the eclipse.

The next opportunity for studying this remarkable system will come in April, 1937, and, although the star will then be rather far west before observations can be started in the evening, it should be possible to secure valuable data during the first half of the eclipse. A more favorable opportunity will present itself in December, 1939, when the star will be above the horizon for the greater part of the night; but we shall then have to contend with the vagaries of winter weather.

ζ Aurigae is an ideal system for the intimate study of the distribution of the elements constituting the atmosphere of a giant K-type star. The two components are so bright that spectra of moderate dispersion can be obtained in a reasonable time. Further, the brightness of the B and K components in the photographic region of the spectrum, i.e., at λ 4300, is the same, thus permitting a study of the combined spectra to the best advantage. Finally, the ratio of the diameters of the two stars is such that the B star, to a fair approximation, may be considered as a point source of light—a factor of especial value when the B star is seen through the atmosphere of the K.

These fortuitous circumstances have, for the first time, permitted actual measurements of the relative heights to which the various elements observable extend in the atmosphere of a giant K star; moreover, they permit us to learn, with fair approximation, the relative numbers of atoms existing at the various levels in the star's atmosphere. The only important data lacking are those which would give us the inclination of the orbit to the line of sight. In the case of eclipsing binaries, fairly accurate determinations of this quantity

[5] *Sitzungsberichte Preuss. Akad. der Wissenschaften*, p. 1, 1932.

[6] *Berichte über die Verhandlungen, Akad. der Wissenschaften zu Leipzig*, **85**, 117, 1933.

TABLE I

OBSERVATIONAL DATA: ζ AURIGAE

PLATE	DATE G.C.T.	J.D. 2427000+	RADIAL VELOCITIES; KM/SEC.			NO. OF LINES‡
			H and K	Hydrogen	Others	
γ 20561	1934 Aug. 21	671.00	.....	+28.5	+15.4	(2), 25
20562	21	71.02	+29.0*	24.4	15.5	(3), 17
V 530	22	72.01	25.7*	22.0	20.6*	(10), 13, 22
534	23	73.01	32.6*	20.9	17.3	(5), 40
535	24	73.99	.....	.....	17.2	34
538	25	74.99	10.9	.....	14.7	45
541	26	75.96	10.0	.....	10.1	51
γ 20574	27	76.94	.....	.....	14.5	36
V 544	28	77.98	9.6	.....	16.7	44
551	29	78.97	13.2	.....	14.7	40
560	30	80.02	11.4	.....	14.4	57
567	31	81.02	17.0	.....	16.8	42
573	Sept. 19	699.99	17.8	.....	22.4	39
577	20	700.96	.....	.....	22.1	49
583	21	01.94	.....	.....	21.6	47
γ 20592	22	02.90	.....	.....	21.6	14
V 585	25	05.94	.....	.....	24.8	27
591	26	06.95	25.9	.....	26.9	29
597	27	07.97	.....	.....	26.0	29
603	28	08.94	.....	.....	27.0	27
609	29	10.02	.....	.....	25.3	57
611	30	10.93	17.7	.....	25.5	40
612	30	11.02	.....	.....	23.5	29
615	Oct. 1	11.91	20.7*	.....	21.4	38
616	1	12.00	.....	.....	24.3*	42, 36
618	2	12.84	5.8*	18.7	20.4	(4), 43
619	2	12.91	8.4*	16.0	20.2	(4), 52
620	2	13.01	11.3*	20.8	21.5	(10), 59
621a	3	13.96	13.6*	13.2	.....	(11)
621b	3	14.04	10.9	18.5	26.1	(3), 25
622a	4	14.88	22.6*	27.7	26.0	(9), 3
622b	4	14.97	17.8*	.....	.....	.....
622c	4	15.00	16.9	.....	.....	.....
623	5	16.00	12.2*	.....	.....	.....
624	5	16.03	18.0*	.....	.....	.....
625a	5	16.06	+13.0*	+18.0	28.5	(3), 25
626	11	21.87	.....	.....	33.8	27
628	11	21.92	.....	−16.8†	.....	(9)
629	20	30.92	.....	.....	34.6	26
669	31	42.03	.....	.....	36.7	23
681	Nov. 25	66.83	.....	26.4†	.....	(6)
695	Dec. 20	91.78	.....	44.5†*	.....	(8)
696	20	91.91	.....	.....	50.2	15
700	21	92.66	.....	.....	45.9	15
701	21	92.79	.....	−44.3†	.....	(9)
702	21	793.00	.....	.....	48.8	15
734	1935 Jan. 13	815.62	.....	.....	+48.7	13

* Mean of two or more measures

† B-type component.

‡ Numbers in parentheses refer to hydrogen lines.

are usually available, but for ζ Aurigae the inclination cannot be obtained until the light-curve has been determined with the highest accuracy; even then considerable uncertainty may exist.

To meet the need for extensive data the star was observed whenever possible during the 1934 eclipse. The first night that observations were attempted, August 20, clouds interfered; however, from August 21 to August 31, inclusive, an unbroken series of spectra was obtained. The dark of the moon then followed and the telescope was being used exclusively for direct photography; but, as the star was by that time deep in eclipse, observations were less necessary. From September 25 to October 5 another unbroken run of observations was obtained, but, unfortunately, clouds prevented observation on October 6. The forty spectra taken during total eclipse and the critical periods of ingress and egress have proved excellent for the present investigation, but the knowledge of the requirements of the problem now available suggests a somewhat different procedure for the observation of future eclipses.

The majority of the spectra were made with the three-prism ultraviolet spectrograph and 10-inch camera, attached to the 60-inch telescope; the dispersion of this combination is about 19 A per millimeter at λ 3800. The exposure times range from 1 to 210 minutes, although the subsequent spectrophotometric measurement and reduction showed that much longer exposures during the total phase would have been of great value. A number of plates have been taken since the star returned to its normal aspect, some of several hours' exposure, for the purpose of determining the value of the mass ratio of the two components from measures of the B-type spectrum.

As already mentioned, there is great need for accurate photometric observations, both visual and photographic, during ingress and egress of the B star. On such observations will depend the final value of the relative diameters of the two components, the amount of extinction suffered by the B star's light on passing through the K star's atmosphere, and the inclination of the orbit plane. It would be exceedingly helpful if institutions well separated in longitude were to co-operate during the next few eclipses in determining the complete light-curve of this star.

The most complete series of photometric observations made during the 1934 eclipse of which we are aware are those by Oosterhoff,[7] made with the Schraffierkassette[8] attached to the 10-inch telescope at Mount Wilson, and by Huffer[9] with a photoelectric cell at Madison. We have combined these results to determine the phases at which the spectroscopic observations were made.

DESCRIPTION OF THE SPECTRA

The normal composite spectrum of the two bodies forming the system of ζ Aurigae is about that of a star of type gK4, upon which is superimposed the almost continuous spectrum of a star of early type, presumably a late B. The exact classification of the early-type star is practically impossible owing to the presence of the K spectrum, but we believe that B8 will not be very far wrong. Long exposures on the composite spectrum show the broad hydrogen lines of the B star extending down to about $H(19)$, the last member of the Balmer series to be recognized with certainty. To the violet of the hydrogen series, our spectra extend to about λ 3550. Numerous lines are to be seen to the very limit of the observed spectrum, which, when compared with those of a normal K-type star, we find are all attributable to the K component. It is somewhat surprising to find the K-type lines so easily visible in the extreme ultra-violet, where they are more distinct than in the region λλ 3700–4000. One would expect the continuous B spectrum to be more active in blotting out lines in the extreme ultra-violet than in the latter region; but the presence of continuous hydrogen absorption may perhaps explain the anomaly.

The Balmer lines of the B star are broad and diffuse and would be difficult to measure with accuracy even were the spectrum of the K star not present; as it is, the wings and cores are filled and distorted by the numerous strong lines originating in the K star, rendering the problem of determining the radial velocity of the B star, and hence the mass ratio, etc., of the two components, exceedingly difficult.

[7] *Mt. W. Contr.*, No. 518; *Ap. J.*, **81**, 461, 1935.

[8] *Mt. W. Contr.*, No. 476; *Ap. J.* **78**, 313, 1933.

[9] *Ap. J.*, **81**, 292, 1935.

PLATE IX

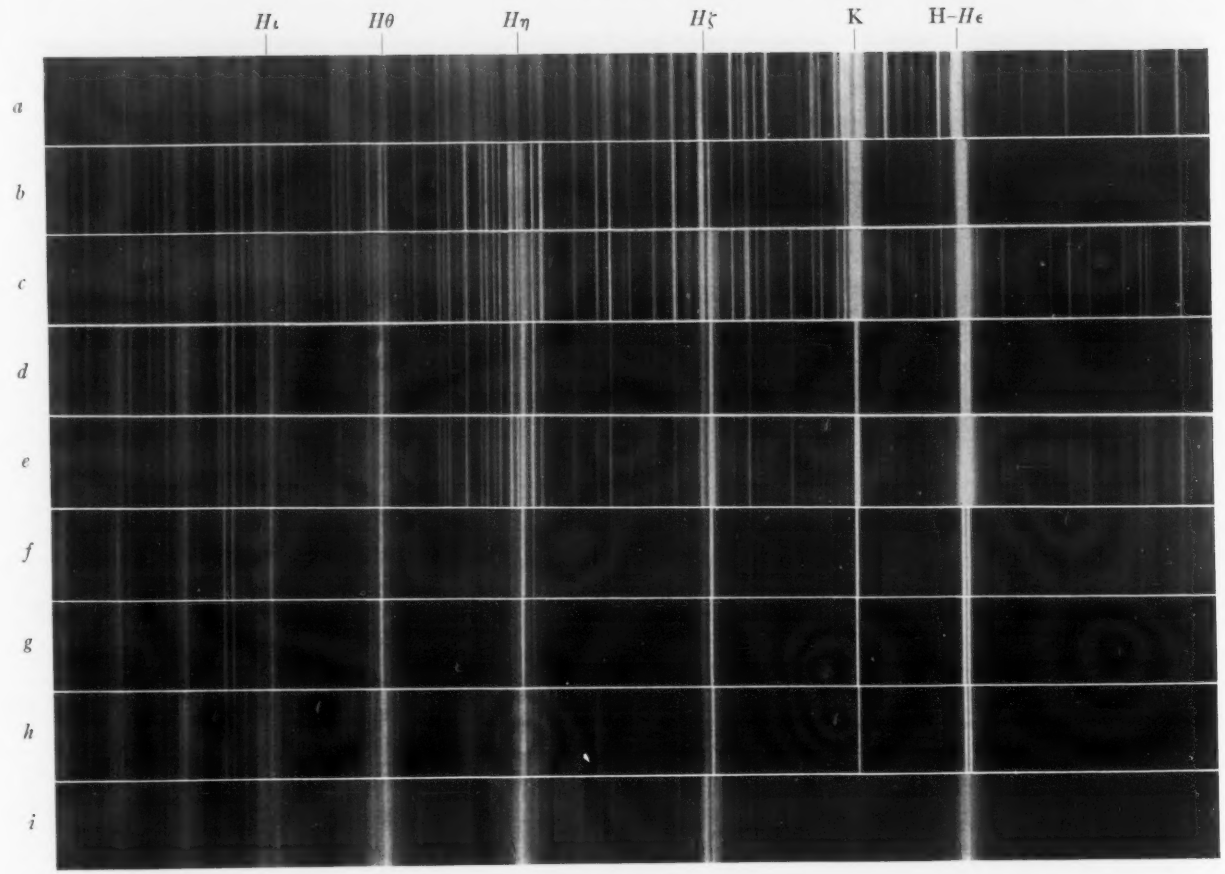

SPECTRA OF ζ AURIGAE

a) V 551, normal K spectrum; *b*) V 615; *c*) V 534; *d*) V 619; *e*) V 530; *f*) V 621; *g*) V 622; *h*) V 624; *i*) V 630, normal composite spectrum

Emission lines are seen in the cores of the strong Ca^+ lines in the spectra taken during the eclipse, as is to be expected in the spectrum of a giant K star. These lines are double and are evidently self-reversed, and there is some evidence that the amount of emission is not constant. This detail, however, must be left for a future eclipse to decide. Measures of radial velocity during the eclipse of the B star show that the velocity obtained from the central H and K absorption agrees, within the limits of error, with that derived from the normal absorption K lines.

The change in appearance of the composite spectrum, as the B star enters and leaves eclipse, is well shown in the reproduction of several of our spectra on Plate IX, and in the series of microphotometer tracings on Plate X. The first noticeable effect, as the B star approaches eclipse, is the appearance of faint lines at H and K; these lines increase in strength without widening greatly, and, at the same time, the hydrogen lines of the Balmer series show sharp central cores, whose intensity increases until eclipse takes place. This stage is followed by the appearance of strong lines of Ti^+ at λ 3759 and λ 3761; other Ti^+ lines then strengthen, accompanied by three strong *Mg* lines λλ 3829, 3832, and 3838; finally, lines of other neutral metallic elements strengthen. On emergence from eclipse, the phenomena appear in the reverse order.

No lines that can be attributed to the B star, other than the hydrogen series, have been seen in the composite spectrum. Tremblot,[10] at the Paris Observatory, reports having measured several B-type lines, namely, λλ 3705 (*He*), 3727(*O*), 3806(*Si*), 3819(*He*), 3867(*He*), 3882(*O*), 3889(*H*), and 3970(*H*), in spectra of the pair made with a four-prism spectrograph giving a dispersion of 30 A per millimeter at λ 3800. With the exception of the last two, we have not been able to identify these lines on our spectra. Numerous lines, just visible in the composite spectrum, coincide exactly with those of the normal K spectrum taken during eclipse, but with the exception of the hydrogen lines there is none that can be attributed to the B star. That the lines listed by Tremblot may exist, we certainly do not deny; but we think that further evidence is necessary

[10] *Comptes rendus*, **198**, 1977, 1934.

before their existence can finally be accepted. Unfortunately, Tremblot's plates were taken when the velocities of the two components were changing very slowly; hence, if the lines measured were misidentified K lines, there would be practically no change in wave-length during the period of observation to reveal the error. If the lines measured were actually B-type lines, the spectrum must have changed considerably in the interval between his and our observations.[10a]

MEASUREMENTS OF RADIAL VELOCITY

All the plates suitable for radial-velocity determinations have been measured with the micrometer (Table I). For phases immediately preceding and following eclipse a large number of lines was measured with the object of determining whether there is any systematic difference between the velocities derived from lines in the ultra-violet and those in the normal photographic region, i.e., to the red of the calcium lines. No such difference was found, nor were there any outstanding lines other than those of hydrogen and ionized calcium among those measured. The individual observations are shown plotted in Figures 1 and 2. The velocity computed from Harper's orbit is indicated by the dotted line in Figure 2, and the velocity-curve derived from our observations by the full line. During the ingress and egress of the B star, a distinct demarcation of the observations from the normal velocity-curve is apparent, most noticeably so for the H and K lines of Ca^+, for which in the mean it amounts to some 12 km/sec. The residuals from the other lines, excepting hydrogen, are much smaller, about 6 km/sec. If, as there is every reason to believe, this demarcation from the normal velocity is due to rotation of the K star, the discrepancy between the metallic

[10a] *Note added while in press.*—Since the foregoing was written, the neutral silicon line, λ 3905, has appeared in emission. This line was first seen by Dr. Adams on an excellent plate taken with the nine-foot camera of the 100-inch coudé spectrograph on February 16, 1935. Since that date the line has widened and increased in intensity. The excitation of this line, which evidently belongs to the K spectrum, is probably due to the radiation of the B star and was not previously visible because the sub-B point was on the far side of the K star. A careful scrutiny of our plates has failed to show any other additional lines in emission. The wave-length of this line as determined from our spectra is 3905.45; the difference from the laboratory value, −0.08 A, corresponds to a rotational value similar to that derived from the Ca^+ lines.

PLATE X

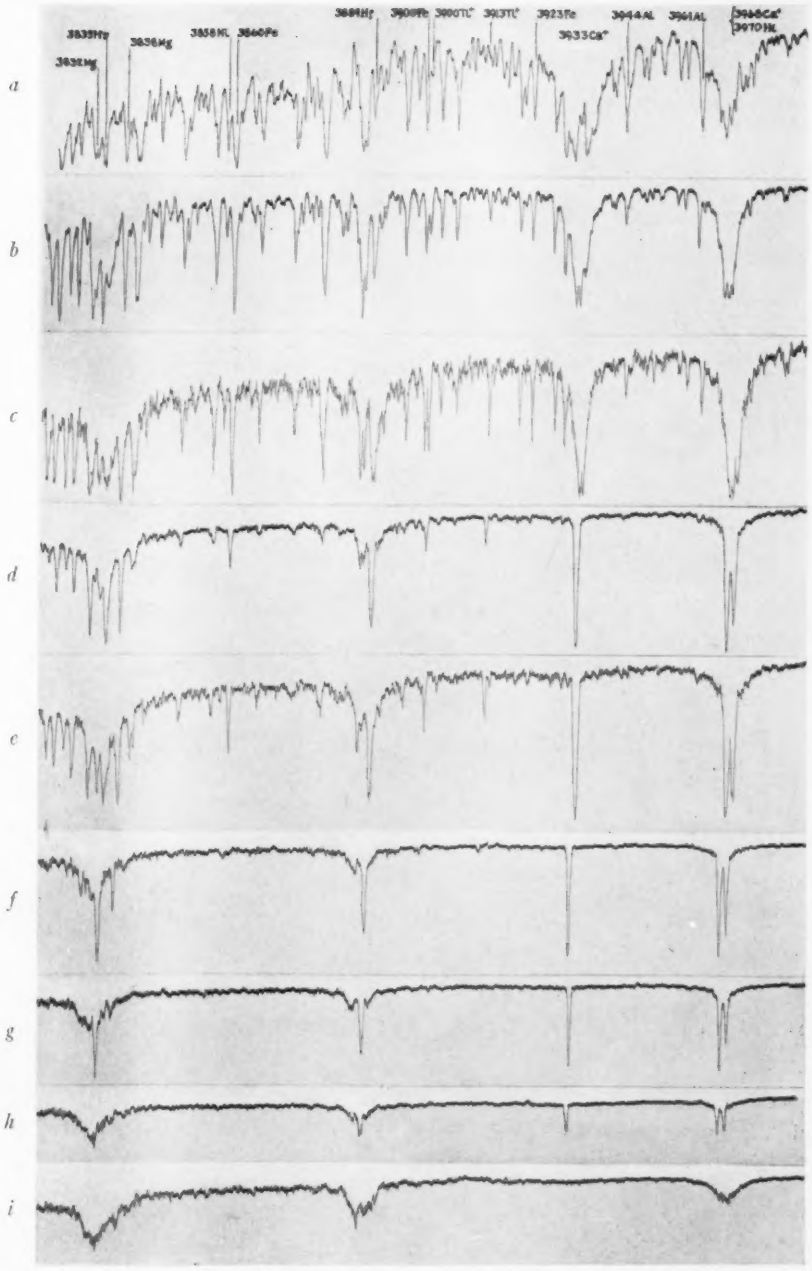

MICROPHOTOMETER TRACINGS OF SPECTRA OF ζ AURIGAE

a) V 551, normal K spectrum; *b*) V 615; *c*) V 534; *d*) V 619; *e*) V 530; *f*) V 621; *g*) V 622; *h*) V 624; *i*) V 630, normal composite spectrum

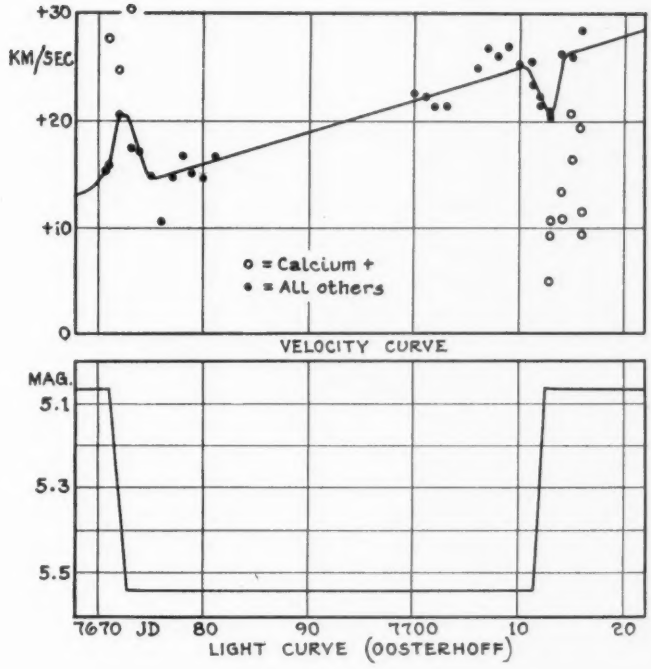

FIG. 1

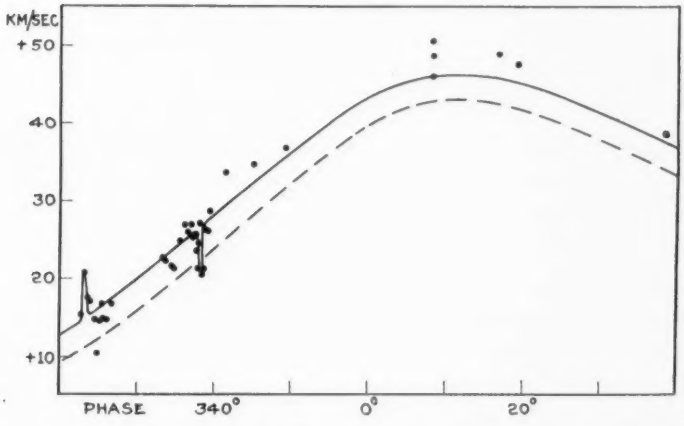

FIG. 2.—Mount Wilson radial velocities of ζ Aurigae. Dashed curve, Harper's orbit

lines and those of Ca^+ is readily explained. The metallic lines, in the spectrum formed by the light of the B star shining through the atmosphere of the K, are blended with those of the normal K; hence the rotational effect will be reduced. The strong, sharp Ca^+ lines, however, are but little affected by the normal broad H and K, the wings of which are filled, at this stage, with the B continuous spectrum. The rotational effect derived from the Ca^+ lines must, then, have some weight, although the scatter of the observations

TABLE II

ROTATIONAL EFFECT FROM Ca^+ LINES

Plate	Vel.	No. of Measures	Average Deviation	O—C
	km/sec.		km/sec.	
γ 20562	+29.0	3	1.8	+13.8
V 530	25.7	4	1.8	10.3
534	32.6	2	2.2	+21.0
615	20.7	2	3.0	− 5.1
618	5.8	2	0.8	20.6
619	8.4	2	0.0	18.4
620	1.3	2	0.7	15.2
621	13.6	2	0.1	13.2
622*a*	22.6	3	2.4	4.4
622*b*	17.8	4	2.7	9.2
623	12.2	2	2.8	15.2
624	18.0	3	2.0	9.4
625	+13.0	3	2.4	−14.4
Weighted mean, regardless of sign				±12.4

is much more than one would expect from the character of the lines. The velocities derived from the Ca^+ lines, where the rotational effect is in evidence, are given in Table II; the residuals, O−C, are computed from Harper's elements plus a correction of +4 km/sec., the source of which is described below.

The rotational velocity derived from the measures published by Beer[11] is 21.3 km/sec. The velocities of the K star used by Beer in determining this quantity were derived from Harper's orbit after T, the time of periastron passage, had been changed by nine days in order to make Harper's elements fit the observed time of eclipse. This change slightly affects the rotational value we have derived,

[11] *M.N.*, **95**, 24, 1934.

but not enough to account for the discrepancy between his measures and ours. The velocity computed from Harper's elements for October 5 is, for example, +23.4 km/sec.; Beer's velocity for the same date, +26.3 km/sec.; our adopted velocity, +27.4 km/sec. Whether the difference between the velocities of rotation as derived by Beer and ourselves is real, or is to be accounted for by some systematic difference between the two sets of measures, cannot be determined at present.

The radial velocities for the K star as determined at Mount Wilson show a systematic deviation from the values derived from Harper's elements amounting to some 4.0 km/sec. On computing the time of the middle of eclipse from Harper's elements, we find a deviation of 9.5 days from the observed value. By reducing the date of periastron by this amount, keeping the original value of $\hat{\omega}$, and recomputing the velocities, the residuals are reduced slightly; but the general run of the observations no longer follows that of the computed curve. It seems likely, as one would expect, that $\hat{\omega}$ and the other elements also need a slight revision. Since plates measured on the spectrocomparator, as Harper's were, most likely differ systematically from those measured on the micrometer, it is unwise to attempt to combine the two sets of observations in order to determine the necessary corrections. Hence it will suffice to treat the residuals as if they were wholly systematic until sufficient material is available to determine the revised elements with accuracy.

Four long-exposure spectrograms of the composite spectrum have been measured in order to determine the velocity of the B component, and hence the mass ratio of the pair. Two of these plates have been measured by one of us alone, the other two by five experienced measurers—Christie, Joy, Merrill, Sanford, and Wilson. The uncertainty in the measures of these broad, distorted, hydrogen lines is such that the average deviation of the velocity determined by a single measurer from the mean for the five is ±17 km/sec. for plate V 695 and ±8 km/sec. for plate V 701.

Although the discordances, both internal and between the different measurers, are large, the mass function derived from these measures should have considerable weight. Table III contains the mass ratios derived from the several sources, including the value of

Tremblot. Unfortunately, we do not know what correction, if any, to apply to Tremblot's determination to allow for the fact that he has used Harper's elements without any correction for the systematic difference which, for the reason stated above, most likely exists between his measures and those of Harper; hence we have had to neglect his determination in the mean. If the correction required by his velocities is of the same order as that applied to ours to make them agree with Harper's, his mass ratio would be 1:1.3. It is to be noted that a correction of +4.0 km/sec. has been added to the velocity of the system, as derived by Harper, in obtaining our mass ratios given in Table III.

TABLE III

MASS RATIOS, ζ AURIGAE

Source	m_B/m_K	Date
Tremblot	1:1.88	
V 628	1:2.17	1934, Oct. 10
681	1:1.32	Nov. 25
695	1:1.86	Dec. 19
701	1:1.85	20
Adopted mass ratio	1:1.85	

PHOTOMETRIC OBSERVATIONS

There still seems to be some uncertainty in the determination of the duration of the phases of partial and total eclipse. We have derived new values by combining the observations of Oosterhoff made with the Schraffierkassette with the photoelectric measures of Stebbins and Huffer. Numerous observations were also made by other observers during the 1934 eclipse, but since they are rather scattered we have not been able to use them in our determination of the photometric elements. Our values for these elements, although derived independently, would be identical with those of Oosterhoff had we not taken the liberty of making some allowance for the curvature which must be present in the light-curve at the beginning and end of partial eclipse. The amount of curvature permitted is limited by the observations. Figure 3 shows the critical values at the beginning and end of the eclipse combined in a single branch.

Three Königsberg observations given in Beer's[11] recent paper and one made at Cambridge are also included. It is at once evident that a partial phase of less than one day is inconsistent with the present

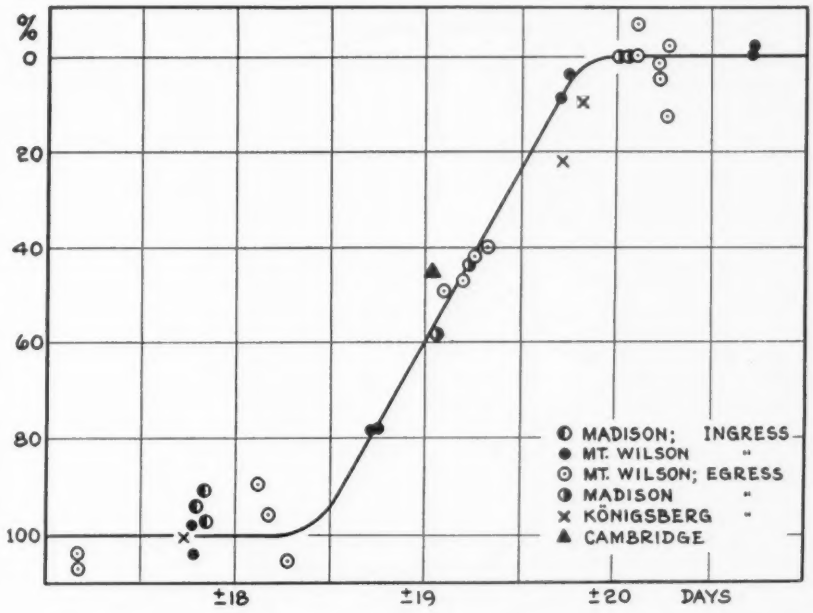

FIG. 3.—Photometric observations during partial phase, 1934 eclipse. Ordinates, per cent eclipse; abscissae, days from epoch of minimum.

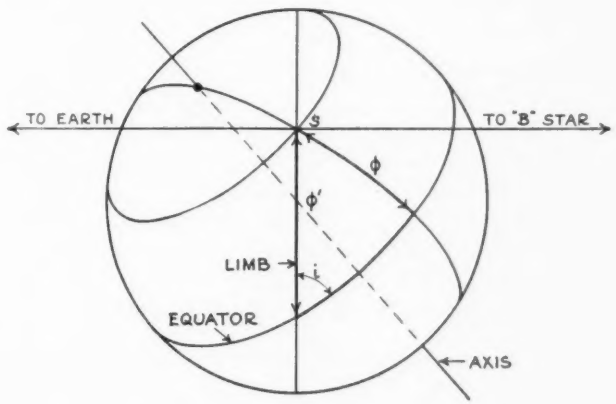

FIG. 4.—Notation of co-ordinates of K star

photometric data, especially when one considers the observations made at Mount Wilson at the beginning of the eclipse.

The photometric elements derived from the adopted light-curve are given in Table IV.

TABLE IV

PHOTOMETRIC ELEMENTS

Epoch of minimum	J.D. 2427692.70
Duration of eclipse	40.0 days
Duration of totality	36.6
Duration of partial phase	1.7

ELEMENTS OF THE SYSTEM

We are now able to apply the mass function and the eclipse data to the evaluation of other elements of the system. These are given in Table V.

TABLE V

ELEMENTS OF THE SYSTEM (ASSUMING CENTRAL TRANSIT)

P^*	$=973$ days
T^*	= J.D. 2415122.471
K_K^*	$=23.78$ km/sec.
K_B^*	$=44.0$ km/sec.
e^*	$=0.411$
$\bar{\omega}_K^*$	$=330^\circ.13$
$\bar{\omega}_B^*$	$=150^\circ.13$
γ	$=+14.73$ km/sec.
m_K	$=15.3\odot$
m_B	$=8.3\odot$
m_K/m_B	$=1.85$
R_K	$=134\times10^6$ km $=192\odot$
R_B	$=5.9\times10^6$ km $=8.5\odot$
J_B/J_K (visual)	$=260$
J_B/J_K (λ 4300)†	$=510$
ρ_K	$=2.16\times10^{-6}\odot$
ρ_B	$=0.013\odot$
(a_K+a_B)	$=8.27\times10^8$ km

* Harper's elements. † Derived from eq. (8).

Figure 4 clarifies the notation that has been used for the various co-ordinates of the K star. On the assumption that the plane of rotation coincides with the plane of the orbit, i is the angle between the

plane of the equator and the plane of the sky; ϕ is the latitude of the point, S, on the limb, at which eclipse takes place; ϕ' is the angular distance of the point S from the equator, measured along the limb. The length of the chord formed by the path of the B star across the K star, the curvature being assumed negligible, is

$$2\,R_K \sin i \cos \phi' = 268 \times 10^6 \text{ km}. \tag{1}$$

Guthnick and Schneller[5] have shown that the radius of the star as determined from the rotation effect is

$$R_K = \frac{VT}{2\pi} (\cos^2 \phi - \cos^2 i)^{-1/2}, \tag{2}$$

where V is the velocity of rotation at latitude ϕ, and T the period of axial revolution. Now

$$\cos \phi' = \left(1 - \frac{\sin^2 \phi}{\sin^2 i}\right)^{1/2}; \tag{3}$$

hence we have, from (1) and (2),

$$T = \frac{2\pi \times 134 \times 10^6}{V}, \tag{4}$$

whence $T = 785$ days. If the eclipse is central and the plane of rotation coincides with that of the orbit, and if the two periods are identical, we should find a velocity of rotation of about 9.9 km/sec. The difference of 2.5 km/sec. between the observed and computed velocities of rotation is not hard to reconcile with errors of observation; but this discrepancy is supported by the observations of Guthnick and Schneller and by those of Beer. It seems probable, therefore, that, if the effect is wholly due to rotation, we have a period of rotation for the K star of the order of 785 days or less.

Table VI gives for the critical periods of ingress and egress the distance of the B star from the limb of the K star expressed in terms of radii of the K and B stars and measured along the path of the B star.

THE SPECTROPHOTOMETRIC MEASURES

Consider the composite spectrum of the system as it appears when the light of the secondary is traversing the atmosphere of the primary on its journey to the observer. We have, first of all, the normal spectrum of the K-type star, upon which is superimposed the spectrum of the B-type secondary. In addition to its own absorption lines, the B spectrum will show others produced by the atoms in the atmosphere of the primary which happen to exist in sufficient

TABLE VI

DISTANCES OF B STAR FROM LIMB OF K

Date (G.C.T.)	J.D.	(1)	(2)	(3)	(4)
1934 Aug. 22.....	2427672.01	$+0.080R_K$	$+0.080R_K$	$+1.81R_B$	$+10.8\times10^6$ km
23.....	73.01	+ .028	.033	+0.63	+ 3.8
24.....	73.99	− .023	.009	−0.51	− 3.1
Oct. 1.....	7711.99	+ .006	.022	+0.13	+ 0.8
2.....	12.92	.056	.056	1.27	7.5
3.....	14.00	.112	.112	2.52	15.0
4.....	14.95	.162	.162	3.62	21.6
5.....	16.05	+0.219	+0.219	+4.92	+29.2

1. Distance of center of B star from limb of K.
2. Distance of center of visible area of B star from limb of K.
3. Distance of center of B star from limb of K in radii of B.
4. Distance of center of B star from limb of K in kilometers.

numbers in the line of sight at the moment. These additional lines will, in general, nearly coincide with the ordinary absorption lines in the K-type spectrum. A slight tendency toward separation of these two sets of absorption lines arises from the rotation of the primary, but is insufficient to produce more than a moderate widening. The first problem is how to deduce from the measured composite lines the total absorptions which the constituents of the primary's atmosphere produce in the spectrum of the secondary.

In accordance with the usual definition, let $r_K = I_K/I_{CK}$ be the value of r at any point, λ, within a line of the normal K-type spectrum. I_K and I_{CK} are, respectively, the intensities in the line and in the continuous background at λ. Similarly, if the K-type star, except for those portions of its atmosphere lying in front of the secondary,

could be annihilated, we should have $r_B = I_B/I_{CB}$ at λ. We actually measure a composite r which we may denote by r_{BK}. By definition,

$$r_{BK} = \frac{I_K + I_B}{I_{CK} + I_{CB}} .$$

Setting $I_{CB}/I_{CK} = a$, we find

$$r_{BK} = \frac{r_K + a r_B}{1 + a} . \tag{5}$$

For the total absorption, A, of a line, we write $A = \int\int dr\, d\lambda$. The usual expression, $A = \int (1 - r) d\lambda$, is, of course, obtained from the former by integrating with respect to r. Now, in the composite spectrum, the quantity measured is $A_{BK} = \int\int dr_{BK} d\lambda$. Differentiating equation (5), multiplying through by $d\lambda$, rearranging and integrating, we find

$$\int\int dr_B d\lambda = \frac{1 + a}{a} \int\int dr_{BK} d\lambda - \frac{1}{a} \int\int dr_K d\lambda , \tag{6}$$

or

$$A_B = A_{BK} + \frac{1}{a} (A_{BK} - A_K) . \tag{7}$$

On the right-hand side of (7), A_{BK} is the measured total absorption of the composite line, and A_K the total absorption of the line as it appears in the normal K-type spectrum when that of the companion is absent. The values of A_K are, of course, obtained by measuring plates taken during the total eclipse of the secondary. The only other unknown is a, which, from the definition, is a function of wave-length and could be computed from the temperatures and relative dimensions of the two stars on the assumption that they radiate as black bodies. This is not necessary, however, since equation (7) is still true when $A_B = 0$, which will be the case when the eclipse is entirely over. Thus from (7) we have

$$a = \frac{A_K}{A_{BK}} - 1 . \tag{8}$$

Equation (8) was applied to the measures of two excellent plates, one of which was taken on September 29, just before the end of totality, and the other on October 30, long after the atmosphere of the primary had ceased to have any effect on the light of the secondary. The results are shown in Figure 5, where each point represents the measures of one line. Aside from yielding α for use as noted above, this curve is of interest in itself. If we assume the temperature of the B-type component to be between 15,000° and 20,000°, the run of the observed values of α indicates that the tem-

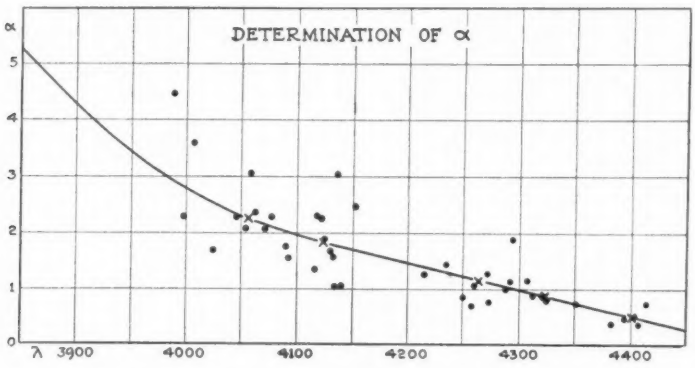

FIG. 5.—Dots, individual lines; crosses, normal places

perature of the K-type primary is of the order of only 1500°. Why this figure is so low we do not know. It is a fact, however, that, judged from the appearance of spectrograms taken during totality, the K-type spectrum is rather weak in the violet. The points of Figure 5 do not extend farther to the violet simply because the K-type lines are so nearly obliterated by the continuous spectrum of the secondary that no measures of value could be obtained there. This fact in itself indicates that our curve is at least approximately correct. The curve was continued to the violet of λ 4000 by roughly sketching it in on the basis of the foregoing temperatures. The justification of this procedure lies in the fact that where α is so large, we need only an approximate value to determine the corrections to our measured composite line intensities with ample accuracy.[12] For

[12] A. B. Wyse (*Pub. A.S.P.*, **46**, 350, 1934) has used the central intensities of four iron lines (essentially eq. [5] with $r_B = 1$) to derive the magnitude difference at about

those plates taken when only a portion of the light of the secondary was present, the a's were modified accordingly, the only assumption being that the percentage of the total light present was the same for all wave-lengths. Similarly, for those lines lying within the Balmer lines of the secondary, the appropriate a's were found by measuring the depths of the hydrogen lines at the points in question.

Our spectrograms were not subjected to a careful examination until after the end of the eclipse in October; thus it was not realized until too late that by applying the foregoing method valuable results could have been obtained as far to the red as λ 4400 at least. Since our observing program had been arranged on the assumption that only the region to the violet of about λ 4000 would be of interest, nearly all our spectrograms were too dense for photometric use to the red of this wave-length. This point should be borne in mind in observing future eclipses; graded series of exposures will greatly increase the number of lines available for study.

For the present, therefore, we confine ourselves to wave-lengths shorter than λ 4100. Our results are presented in Table VII, which lists the wave-length and source of the line as given in the *Revised Rowland*, followed by the measured intensities corresponding to the date at the top of each column. The last column contains the total absorptions as measured in the normal K-type spectrum during totality.[13] The numbers in the second line opposite each wave-length are the values of A_B deduced from those in the first line by means of equation (7). All total absorptions are expressed in angstroms of complete absorption. The wave-lengths were measured with only sufficient accuracy for identification, a relatively easy matter in a spectrum of this sort. The identifications were doubtful in but one or two cases, which are characterized in the table by the absence of the fifth digit in the wave-length.

λ 3600 between the two components on September 29 and 30 and October 1. He finds a much smaller light-ratio on the latter date than would be expected from our results, for the probable reason that r_B was not equal to unity at that time. There is also the possibility that continuous absorption at the head of the Balmer series may reduce the intensity in the B-type spectrum at the wave-length in question.

[13] Owing to the weakness of the K-type spectrum in the violet, it was necessary to use normal total absorptions as measured on a spectrogram of Arcturus, Ko, for wave-lengths short of λ 3827. These values are indicated by asterisks in Table VII.

TABLE VII

TOTAL ABSORPTIONS, ζ AURIGAE

λ	Source	Aug. 24	Oct. 1	Aug. 23	Oct. 2	Aug. 22	Oct. 3	Oct. 4	Oct. 5	Norm. K Sp.
3721.9	*H*(14)	.....	.....	.....	.....	.....	0.54	.....	.....	.....
3734.4	*H*(13)	.....	.....	.....	.....	.....	.60	.....	.....	.....
3737.1	*Fe*	.....	.....	.....	0.55	.....	.20	.....	.....	1.55*
					.42		.07			
3741.6	*Ti*+	.....	0.41	.....	.33	.....	.16	.....	.....	0.37*
			.42		.33		.14			
3745.6, 3745.9	*Fe*	.....	.97	.....	.54	.....	.23	.....	.....	1.48*
			.91		.45		.11			
3748.3	*Fe*	.....	.....	.....	.42	.....	.15	.....	.....	1.29*
					.30		.04			
3759.3	*Ti*+	.....	.88	.....	.90	.....	.77	0.46	0.23	0.82*
			.89		.91		.76	.42	.17	
3761.3	*Ti*+	.....	.79	.....	.79	.....	.67	.42	.14	0.48*
			.84		.82		.69	.41	.10	
3763.8	*Fe*	.....	.83	.....	.40	.....	.17	.....	.....	1.54*
			.72		.26		.01			
3770.6	*H*(11)	.....	.....	.....	.66	.....	.58	.46	.....	.....
3786.7	*Fe*	.....	.39	0.31	.....	0.12	.....	.....	.....	0.46*
			.39	.30		.08				
3787.9	*Fe*	.....	.60	.49	.....	.....	.....	.....	.....	0.49*
			.62	.49						
3790.1	*Fe*	.....	.64	.21	.....	.10	.....	.....	.....	0.71*
			.63	.14		.02				
3795.0	*Fe*	.....	.71	.44	.23	.22	.....	.14	.....	.....
3797.9	*H*(10)	.....	.....	.....	.81	.....	.72	.57	.....	.....
3813.0	*Fe*	.....	.71	.62	.23	.....	.....	.....	.....	0.72*
			.71	.60	.16					
3814.6	*Ti*+, *Fe*	.....	.41	.39	.19	.28	.....	.....	.....	0.46*
			.40	.38	.15	.25				
3815.8	*Fe*	.....	.68	.59	.26	.32	.....	.....	.....	1.21*
			.57	.49	.12	.18				
3820.4	*Fe*	.....	.96	.73	.46	.48	.....	.....	.....	1.72*
			.81	.57	.26	.28				
3824.4	*Fe*	.....	.63	.59	.21	.36	.....	.....	.....	1.05*
			.55	.52	.08	.25				
3825.9	*Fe*	.....	.85	.63	.33	.46	.....	.....	.....	1.42*
			.73	.50	.13	.30				
3827.8	*Fe*	.....	.56	.41	.22	.24	.....	.....	.....	0.85*
			.50	.33	.11	.14				
3829.4	*Mg*	.....	.54	.55	.31	.41	.17	.....	.....	0.55
			.54	.55	.26	.38	.09			
3832.3	*Mg*	.....	.61	.70	.55	.44	.24	.14	.....	.....
3835.4	*H*(9)	.....	.....	.....	.....	.....	.75	.53	0.15	.....
3838.3	*Mg*	.....	.84	.72	.59	.64	.40	.24	.....	0.64
			0.92	.74	.57	.64	0.33	0.12		
3840.4, 3841.1	*Fe*	.....	1.26	.82	.44	.51	.....	.....	.....	1.03
			1.33	.77	.30	.39				
3843.1	*Fe*, *Zr*+, *Sc*+	.....	0.34	.26	.07	.....	.....	.....	.....	0.25
			.36	.26	.04					
3850.0	*Fe*	.....	.66	.43	.16	.12	.....	.....	.....	0.78
			0.64	0.37	0.05	0.00				

TABLE VII—*Continued*

λ	Source	Aug. 24	Oct. 1	Aug. 23	Oct. 2	Aug. 22	Oct. 3	Oct. 4	Oct. 5	Norm. K Sp.
3850.8	*Fe*	.....	0.41	0.22	0.09	0.12	.....	.....	.....	0.47
			.40	.18	.02	.06				
3852.6	*Fe*	.....	.22	.15	.....	.....	.....	.....	.....	0.25
			.21	.13						
3856.4	*Fe*	.....	.81	.64	.28	.26	.....	.....	.....	0.77
			.82	.62	.19	.16				
3858.3	*Ni*	.....	.41	.26	.....	.11	.....	.....	.....	0.64
			0.36	.19		.01				
3859.9	*Fe*	.....	1.11	.73	.38	.36	0.32	.....	.....	1.33
			1.06	.63	.20	.16	.13			
3865.5	*Fe*	.....	0.48	.39	.12	.10	.....	.....	.....	0.62
			.44	.35	.02	.00				
3867.6	*V?*	.....	.14	.10	.07	.....	.....	.....	.....	0.26
		.....	.11	.07	.03					
3872.5	*Fe*	.....	.58	.57	.22	.10	.....	.....	.....	0.87
			.50	.51	.09	− .05				
3874.0	*Co, Fe*	.....	.32	.15	.....	.....	.....	.....	.....	0.40
			.30	.10						
3875.3	*Ti*	.....	.26	.11	.....	.....	.....	.....	.....	0.32
			.24	.07						
3876.1	*Fe*	.....	.32	.18	.....	.....	.....	.....	.....	0.35
		.....	.31	.14						
3877	?	.....	.27	.15	.....	.....	.....	.....	.....	0.36
			0.25	.13						
3878.0, 3878.6	*Fe*	.....	1.27	.92	.43	.43	.....	.....	.....	1.30
			1.26	.84	.25	.25				
3886.3, 3887.1	*Fe*	.....	1.27	.95	.62	.47	.....	.....	.....	1.74
			0.96	.53	.03	− .20				
3889.0	*H*(8)	.....	.77	0.96	.82	0.89	.78	0.77	0.36	0.58
			.88	1.13	.93	1.03	0.87	0.86	0.26	
3895.7	*Fe*	.....	.75	0.48	.27	0.19	.....	.....	.....	0.76
			.75	.42	.16	.06				
3898.0	*Fe*	.....	.48	.21	.10	.....	.....	.....	.....	0.57
			.46	.13	− .01					
3899.7	*Fe*	.....	.70	.56	.28	.23	.....	.....	.....	0.77
			.68	.51	.17	.11				
3900.5	Ti^+	.....	.67	.66	.46	.50	.....	.....	.....	0.40
			.75	.72	.47	.51				
3903.0	*Cr, Fe, Mo*	.....	.60	.43	.20	.19	.....	.....	.....	0.65
			.59	.38	.09	.08				
3906.5	*Fe*	.....	.60	.44	.....	.10	.....	.....	.....	0.72
			.56	.37		−0.05				
3907.5	*Fe, Sc*	.....	.25	.06	.....	.....	.....	.....	.....	0.26
			.25	.01						
3908.8	*Cr*	.....	.22	.08	.....	.....	.....	.....	.....	0.22
			.22	.04						
3909.8	*Fe, Co*	.....	.20	.08	.09	.....	.....	.....	.....	0.26
			.18	.04	.05					
3910.9	*Fe, –?*	.....	.13	.07	.05	.....	.....	.....	.....	0.21
			.12	.04	.01					
3911.8	*Sc*	.....	.20	.05	.02	.....	.....	.....	.....	0.21
			0.20	0.01	−0.03					

TABLE VII—*Continued*

λ	Source	Aug. 24	Oct. 1	Aug. 23	Oct. 2	Aug. 22	Oct. 3	Oct. 4	Oct. 5	Norm. K Sp.
3913.5	Ti^+	.....	0.56	0.54	0.40	0.36	0.18	.....	.....	0.29
			.65	.60	.43	.38	.15			
3914.3	*Fe, Ti*	.....	.32	.20	.....	.....	.....	.....	.....	0.32
			.32	.17						
3916.7	*Fe*	.....	.31	.14	.....	.....	.....	.....	.....	0.46
			.27	.06						
3917.2	*Fe*	.....	.29	.13	.....	.....	.....	.....	.....	0.40
			.25	.06						
3920.3	*Fe*	.....	.58	.48	0.16	.....	.....	.....	.....	0.64
			.56	.44	.04					
3922.9	*Fe*	.....	.60	.55	.20	.....	.....	.....	.....	0.62
			.60	.54	.13					
3927.9	*Fe*	.....	.49	.54	.20	.....	.....	.....	.....	0.41
			0.50	0.55	0.18					
3933.7	Ca^+	.....	8.55	6.51	1.57	1.42	1.16	0.96	0.62	16.28
			5.85	3.97	1.57	1.42	1.16	.96	.62	
3944.0	*Al*	0.78	0.56	0.44	0.18	.....	.....	.....	.....	0.69
		.80	.53	.40	.11					
3948.7	*Ti, Fe*	.66	.38	.16	.....	.....	.....	.....	.....	0.56
		0.70	.31	.04						
3952.6	*Fe, Fe*	1.02	.76	.....	.....	.....	.....	.....	.....	0.84
		1.10	.73							
3956.5	*Ti, Fe*	0.76	.52	.37	.....	.....	.....	.....	.....	0.56
		.85	.50	.31						
3958.2	Zr^+, *Ti*	.60	.46	.44	.....	.....	.....	.....	.....	0.44
		.68	.47	.44						
3961.5	*Al*	0.95	.55	.51	.23	.....	.....	.....	.....	0.70
		1.01	.52	.48	0.16					
3968.5	Ca^+	.....	.....	.....	1.18	1.43	0.96	.84	.53	.....
3970.1	*H*(7)	.....	.....	.....	0.90	1.01	0.82	0.66	0.43	.....
3973.6	*Ni*	0.30	.27	.18	.18	.....	.....	.....	.....	0.30
		.30	.27	.17	.17					
3981.8	*Fe, Ti*	.75	0.99	.73	.....	.....	.....	.....	.....	0.82
		.71	1.08	.70						
3989.8	*Ti, Fe*	.84	0.58	.41	.....	.....	.....	.....	.....	0.70
		.92	.53	.31						
3998.6	*Ti*	.72	.60	.50	.....	.....	.....	.....	.....	0.46
		0.86	.66	.51						
4005.3	*Fe*	1.06	.87	.64	.47	.....	.....	.....	.....	0.96
		1.12	.80	.52	.29					
4012.4	Ti^+	0.49	.59	.44	.36	.....	0.34	.....	.....	0.46
		0.51	.65	.43	.32		0.30			
4024.6	*Ti, Fe*	1.05	0.95	.64	.48	.....	.....	.....	.....	0.76
		1.24	1.05	.59	.37					
4027	.....	0.37	0.35	.19	.20	.....	.....	.....	.....	0.44
		0.33	0.30	.09	.10					
4030.7	*Mn*	1.34	1.09	.66	.47	.....	.....	.....	.....	1.50
		1.23	0.88	.32	.06					
4033.1	*Mn*	1.23	0.98	.66	.36	.....	.....	.....	.....	0.95
		1.43	1.00	.54	.12					
4034.5	*Mn*	0.93	0.80	.52	.42	.....	.....	.....	.....	1.06
		0.84	0.66	0.30	0.16					

TABLE VII—*Continued*

λ	Source	Aug. 24	Oct. 1	Aug. 23	Oct. 2	Aug. 22	Oct. 3	Oct. 4	Oct. 5	Norm. K Sp.
4035.7	*Mn*	0.54	0.37	0.23	0.16	.....	.....	.....	.....	0.34
		0.67	0.39	.19	.09					
4045.8	*Fe*	1.58	1.25	.70	.62	.....	.....	.....	.....	1.60
		1.57	1.23	.33	.22					
4054.9	*Fe, Zr, Ti*	0.67	0.56	.25	.....	.....	.....	.....	.....	0.60
		.72	.54	.10						
4057.5	*Mg*	.71	.48	.20	.....	.....	.....	.....	.....	0.66
		0.75	0.38	.00						
4063.6	*Fe*	1.69	1.03	.75	.53	.....	.....	.....	.....	1.53
		1.81	0.74	.41	.12					
4071.8	*Fe*	1.20	.87	.61	.46	.....	.....	.....	.....	1.26
		1.16	0.64	0.31	.09					
4077.7	Sr^+	1.48	1.10	1.17	.68	.....	.....	.....	.....	1.11
		1.77	1.09	1.20	0.48					
4090.....	*Fe?*	0.52	0.39	0.18	.....	.....	.....	.....	.....	0.42
		.60	.37	.06						
4092.7	*V*	.75	.58	.32	.....	.....	.....	.....	.....	0.61
		0.87	.56	0.18						
4101.8	*H*(6)	1.09	0.83	1.03	1.11	0.90	1.03	0.97	0.75	0.74
		2.01	1.01	1.48	1.69	1.15	1.48	1.33	0.77	

A few words concerning the accuracy of the total-absorption measures should be included. The only direct evidence on this point is afforded by the three plates of October 2. While these plates were of different exposure times, it was found that fourteen lines could be measured on all three. The average percentage deviation of these lines from the means of the three plates is only 7.8 per cent, with a range of from 1.5 to 17.9 per cent. This precision is quite satisfactory, although slightly misleading. At the phase of October 2 the spectrum had attained an appearance of comparative simplicity since only the stronger lines remained visible. Thus, errors due to difficulty in locating the continuous background and to blending of the wings of lines tended to be minimized. In the earlier phases, and in the normal K-type spectrum, where the lines are closely packed, we believe that errors in the total absorptions of individual lines may amount to as much as 100 per cent, or in some instances perhaps even more. These remarks apply to the general run of lines of average strength. For strong lines the percentage errors will undoubtedly be smaller.

It was obviously impossible, with the amount of material at hand,

to attempt a precise elimination of the effects of blends. On the microphotometer tracings the wings of blended lines were sketched in as accurately as possible, on the basis of the appearance of those relatively unblended, and the total absorptions measured accordingly.

DISCUSSION OF RESULTS

The relations between observed total absorption and height above the photosphere for four different types of lines are presented in Figures 6–9. In these diagrams the ordinates are the mean total

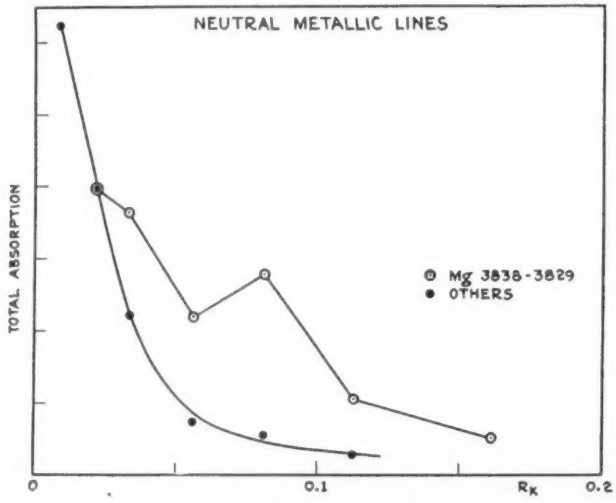

FIG. 6.—Mean total absorptions of neutral metallic lines. Ordinates on arbitrary scale; abscissae, heights of center of area of secondary above photosphere of primary.

absorptions, on an arbitrary scale, while the abscissae are expressed in terms of the radius of the primary, computed from the times of observation and the mean light-curve, Figure 3, on the assumption of central transit. For those phases in which a portion of the disk of the secondary was obscured, the abscissa is that of the center of area of the exposed part (Table VI).

Such curves, which were drawn first for a number of individual neutral metallic lines, showed considerable scatter but no systematic difference in shape depending on the atomic mass. In order to smooth out the accidental irregularities as much as possible, it was

accordingly decided to combine the observations for all such lines into one curve. The observations are most complete for the phase corresponding to October 1. Hence the observed A_B's for all the lines on that date were set equal to an arbitrary quantity, and the total absorptions at the other phases were multiplied by the factors so derived. The means taken for each date are the points shown in Figure 6. The only neutral metallic lines which seem to behave in a definitely different manner are λλ 3838, 3829 *Mg*. The mean points for these two lines are included in the figure.

The results for hydrogen are plotted in Figure 7. The measures are complete only for *Hδ* and *Hζ*, and the mean points for these two

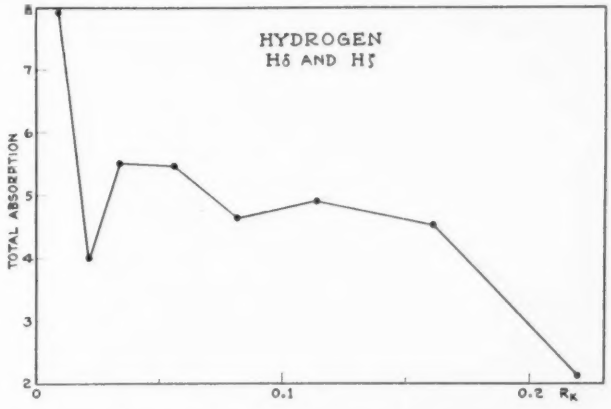

FIG. 7.—Mean total absorptions of *Hδ* and *Hζ*

lines are the ones shown. Although Table VII includes observations for several other hydrogen lines at various phases, these have not been used since their total absorptions in the normal K-type spectrum were unobtainable. The measures of these lines serve, however, to confirm the slow decrement and the order of magnitude of the total absorptions derived from *Hδ* and *Hζ*. One would anticipate somewhat more error than usual in the measurement of these lines since they are located near the bottoms of the wide Balmer lines of the secondary. While this fact doubtless accounts for some of the observed irregularity in the run of the total absorptions, there can be no doubt that the latter fall off very slowly, indeed, with increasing distance of the line of sight above the photosphere.

In the case of Ca^+, accurate measurement of H, λ 3968, has been rendered difficult by the presence of $H\epsilon$ (both components), and the several entries for this line in Table VII have not been used. The measures for K, λ 3933, are shown in Figure 8, where the total absorptions, A_B, are given in angstroms. At the phases corresponding to the first two points in this figure, the line appeared winged and presumably was composite. Hence equation (7) was applied to the corresponding A_{BK}'s to derive the A_B's. From the third point on, however, the wide wings were absent, and the line was approximately centered on a wide, barely perceptible depression in the con-

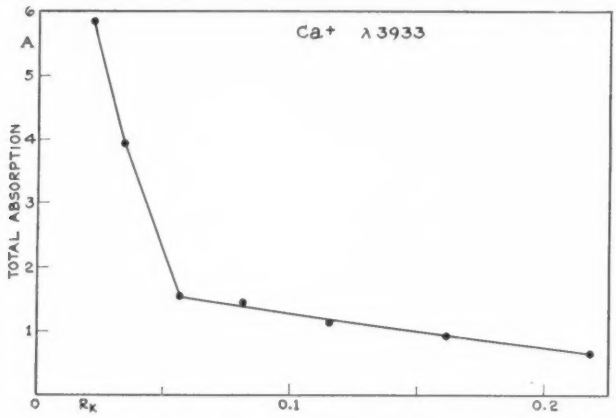

FIG. 8.—Total absorption of K (in angstroms)

tinuous spectrum, presumably the washed-out remnant of the K-type K line, the bottom of which was used as the background for measurement. Thus for the last five points of Figure 8 the A_B's were measured directly and no correction was applied.

Table VII gives seven lines in which Ti^+ is probably the predominating source. In Figure 9 five of these lines have been combined and plotted separately from the other two, λλ 3759, 3761, since there may be some real difference in the behavior of the two groups. The general characteristic of the Ti^+ lines, as compared with those of the neutral metals, is a slower decrement and a correspondingly later disappearance.

Practically all the matters discussed in the preceding paragraphs can be seen qualitatively by an inspection of Plate X, where the

wave-lengths and sources of a number of typical lines have been indicated. An interesting feature not marked on the plate should be mentioned. The second depression to the violet of $H\zeta$ (normal K-type spectrum, at the top) is probably due mostly to the head of the CN band, λ 3883. While no measures were made on it owing to its blended appearance, inspection shows that its rate of decrease and point of disappearance are quite similar to those of the neutral metallic lines.

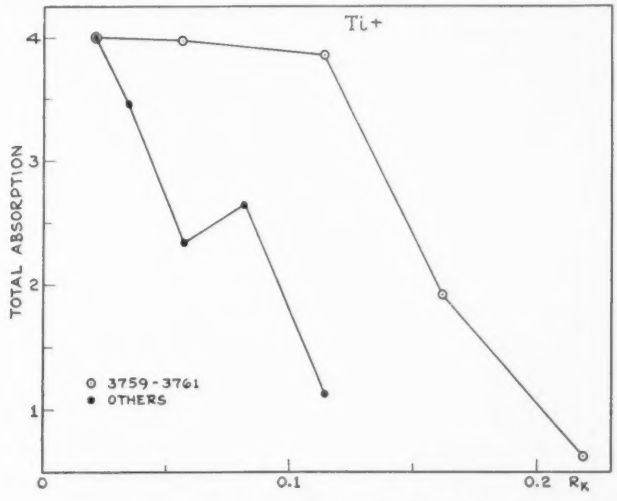

FIG. 9.—Mean total absorptions of Ti^+ lines

In order to derive the distribution of atoms in the atmosphere of ζ Aurigae it is, of course, necessary to know first of all the relation between the total absorption, A, of a line and the number of atoms, N, which are active in producing it. The situation is an extremely simple one. We have, in effect, a small, hot source of essentially continuous radiation viewed through a mass of relatively cool gas. It appears most likely, therefore, that the true contours of the absorption lines produced in the spectrum of the secondary by the atmosphere of the primary will be determined, for all practical purposes, entirely by radiation damping according to the relation $A \propto \sqrt{N}$. The thermal agitation at the low temperatures which must prevail in the atmosphere of a K4 giant can scarcely produce an ap-

preciable effect for lines having sufficient total absorption to be measurable on our plates.[14] Moreover, if the star and its atmosphere rotate as a solid body, no velocity gradient due to rotation will be produced along a chord through the atmosphere. For these reasons we shall henceforth proceed on the assumption that $A \propto 1/N$.

For the moment we consider only the neutral metallic lines. The total absorption of a line will depend first of all upon the number of atoms in the lower of the two energy states which define it—which number, in turn, is a function of the temperature and excitation potential. Thus, if there is an appreciable temperature gradient outward through the atmosphere, it would be expected that, for a given element, the numbers of atoms in levels of low and high excitation potential would decrease outward at different rates. This matter was investigated by dividing the neutral metallic lines into two groups having E.P.'s respectively greater than and less than 1 volt. There appeared to be a slight tendency for the lines of higher E.P. to fall off more rapidly than the others, as would be anticipated if there were a decrease of temperature outward. The precision of the material, however, did not seem sufficient to justify a deduction of the temperature gradient; all that can be said is that it is probably small, which, incidentally, agrees with the results for the solar chromosphere.

Since we are supposing that $A \propto 1/N$, the procedure resorted to in obtaining the mean points of Figures 6–9 is equivalent to making arbitrary changes in the factors of proportionality for the various lines. This procedure does not, however, change the ratios of the N's corresponding to a given line at different phases; hence, by squaring the ordinates of the mean points we should obtain quantities proportional to the numbers of active atoms at the corresponding phases.

This has been done and the results are shown in Figure 10. The ordinates are plotted on a logarithmic scale, and the abscissae are the same as in the preceding figures.

Consider first the points derived from the neutral metallic lines. Since they fall fairly well on a straight line, it follows that the number of atoms in the line of sight decreased exponentially with in-

[14] Struve and Elvey (*Ap. J.*, **79**, 409, 1934) have given a good discussion of this point. Their Fig. 9 is the basis of the foregoing statement.

creasing height of the latter above the photosphere. Reference to Table VII shows that the plotted points do not all have the same weight, since more lines were available at some phases than at others. The last point, in particular, would seem to have practically no weight at all, as it depends on the measures of but two lines. The situation is not quite that bad, however, since the absence of the

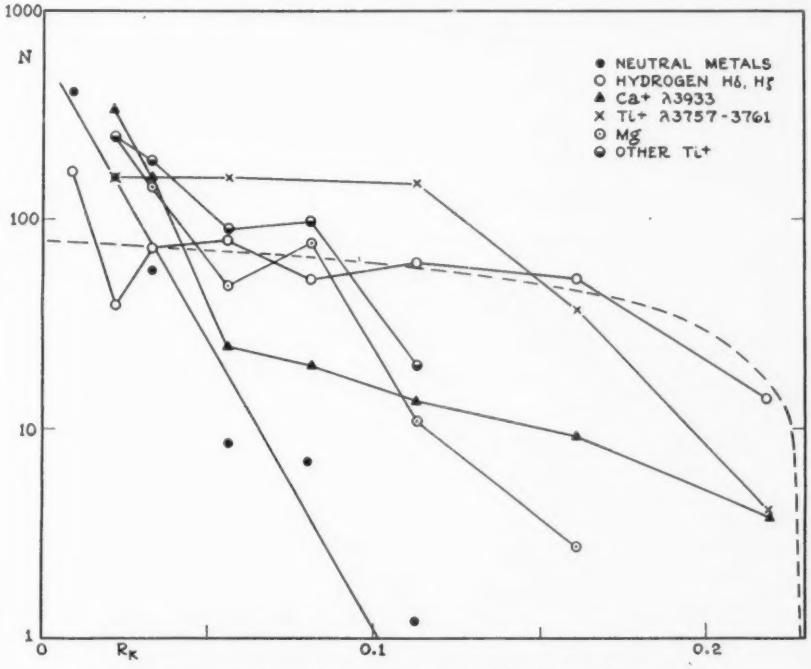

FIG. 10.—Numbers of atoms in line of sight (on arbitrary scales)

other lines simply means that very few atoms were in the line of sight at that time. The straight line drawn through the points given by the neutral metals is therefore probably a fair representation of the situation.

One interpretation of these results is as follows: Suppose the neutral metallic atoms in the atmosphere of ζ Aurigae to be in a state of gravitational equilibrium corresponding to the density distribution

$$\rho = \rho_0 e^{-\frac{\bar{m}g}{kT}h},$$

where $\bar{m}$ is the average mass of the atmospheric constituents, g the surface gravity, T the temperature, k the Boltzmann constant, and h the height above the photosphere. Integrating[15] along a chord through such an atmosphere, we find that N, the number of atoms in the line of sight, as a function of H, the distance of closest approach of the line of sight to the photosphere, is given by

$$N = \sqrt{\frac{2\pi RkT}{\bar{m}g}}\, \rho_0 e^{-\frac{\bar{m}g}{kT}H} .$$

In other words, the value of N should decrease exponentially with H, as do the observed points of Figure 10.

Assuming that our observations do imply such a density distribution, we are in a position to make a quantitative test. The simplest way probably is to compute $\bar{m}$ from the run of the measured line intensities. Taking the mass and radius of the K-type component as 15.3 and 190 times those of the sun, respectively, we find $g_\xi = 11.6$ cm/sec^2. Then we should have

$$\frac{N_1}{N_2} = e^{\frac{\bar{m}g}{kT}\Delta H} .$$

For ΔH equal to one-tenth the radius of the star, we find, from Figure 10, $N_1/N_2 = 564$. For an assumed temperature $T = 3500°$, these figures lead to $\bar{m} = 0.2 \times 10^{-24}$ gm, a mass of only about one-tenth that of the proton, 1.66×10^{-24} gm.

Naturally, we should not demand too much from such a calculation. In view of all that underlies it, a value within one or two orders of magnitude of the correct result is perhaps all that could be expected. Thus, the slope of the straight line of Figure 10 cannot be extremely accurate. Nevertheless, the observed points will not permit any change affecting $\bar{m}$ by more than about 20 per cent. Taken at its face value, the result found for $\bar{m}$ would imply an atmosphere

[15] D. H. Menzel, *Pub. Lick Obs.*, **17**, 242, 1931. Parenthetically, it may be noted that the rigorous integration in this case leads to $N \propto K_1[a(x_1+R)]$, in Menzel's notation, as was pointed out to us by Professor H. Bateman. This result does not differ very greatly from the approximate one.

partially supported by radiation pressure, in which only the fraction μ of the mass is held up by gas pressure, and having the density distribution $\rho = \text{const.} \times e^{-\frac{\mu \bar{m} g}{2kT} h}$.[16]

The most serious source of error in the computation is, however, the assumption of a central transit during eclipse. If this is not correct, the computed mass and radius, and hence the surface gravity, will differ from their true values, although within reasonable limits these factors will not make a great change in $\bar{m}$. If, however, the eclipse is not central, the scale of abscissae in Figure 10 is wrong, and the change in $\bar{m}$ may be important. Thus, for example, if we retain the same mass and radius as above, but imagine that the transit takes

TABLE VIII

ϕ'	R_K	M_v
0°	13.4×10^{12} cm	−3.06
20	14.3	3.21
40	17.5	3.61
60	26.8	4.56
80	77.4	−6.86

place at a latitude of about 69° (as seen projected on the disk), we obtain $\bar{m} = m_p = 1.66 \times 10^{-24}$ gm. Hence there is some range in the possible values of $\bar{m}$, but not a great deal, if we are to keep the dimensions of the star consistent with those deduced from the spectroscopic parallax.

The absolute magnitude has been estimated by Adams, Joy, and Humason from our three best plates taken during totality. They find, in the mean, $M_v = -2.5$ and consider that the error in this value can scarcely exceed 1 mag. In Table VIII, ϕ' is the apparent

[16] E. A. Milne, *Handbuch der Astrophysik*, **3**, Part I, 180, 1930. An alternative explanation of our result might be found in turbulence of the atmosphere, as was suggested by McCrea (*M.N.*, **89**, 718, 1929), and observed in certain stars by Struve and Elvey, *op. cit.* Macroscopic motions in the outer layers of the Ca^+ envelope might be invoked as an explanation of the large scatter in the observed radial velocities of the K line previously noted. If turbulence does play an important rôle in the atmosphere of ζ Aurigae, it is, of course, quite possible that our assumed law, $A \propto \sqrt{N}$, is incorrect. It is perhaps worth noting that if we adopt the other extreme, $A \propto N$, our value of m becomes one-half of that stated above.

latitude of the points of ingress and egress and R_K the corresponding radius computed from equation (1). The M_v's are calculated for $T = 3500°$ from the R_K's by means of the equation[17]

$$M_v = \frac{29{,}500}{T} - 5 \log \frac{R}{R_\odot} - 0.1 .$$

If we are to remain within 1 mag. of the M_v deduced by Adams, Joy, and Humason, it is clear that ϕ' cannot exceed about 30°, from which it follows that $\bar{m} < m_p$. This seems to be as far as it is profitable to carry the discussion at the present time.

Attention should be directed to the striking parallelism exhibited by the curves in Figure 10 for *Mg* λλ 3838, 3829 and for the five weaker Ti^+ lines. The upward slope between the third and fourth points on these curves, corresponding to the observations of October 2 and August 22, is found also in those of the neutral metals and is apparently real. If so, the explanation is probably to be found in a real difference in the distributions of the atoms in question on these two dates. That this may indeed be the case is rendered more probable by the fact that the extent of the Ca^+ envelope differed widely between the eclipses of 1931–1932 and 1934, as has already been noted by Beer.[11] In view of these irregularities and of the apparent difference between weak and strong Ti^+ lines, we shall not attempt to deduce a density gradient for the latter or for *Mg*.

In Figure 10 the hydrogen lines exhibit the slowest decrement of all, thus implying a slow decrease of ρ outward. As a first attempt at interpreting the measures, it was assumed that the star was surrounded by a shell of hydrogen of uniform density. If the outer radius of the shell is taken as 1.23 times that of the star, the dashed curve shown in the figure is obtained. The excellent agreement with the observed points was entirely unexpected and seems to us to be one of the most surprising results of this entire investigation. It is greatly to be regretted that clouds prevented us from continuing our observations of egress in order to see whether the hydrogen lines continued to decrease at the rate shown by the computed curve.

The observations of Ca^+ in Figure 10 are reproduced on a differ-

[17] Russell, Dugan, and Stewart, *Astronomy*, **2**, 732, 1926.

ent scale in Figure 11 for comparison with those of Beer.[18] If our first two observations of the K line are correct, there is a rather sudden decrease in the density gradient at a height of about $0.05R$ above the photosphere. This calls to mind at once Milne's[19] theory of chromospheric equilibrium. Milne supposes that the Ca^+ chromo-

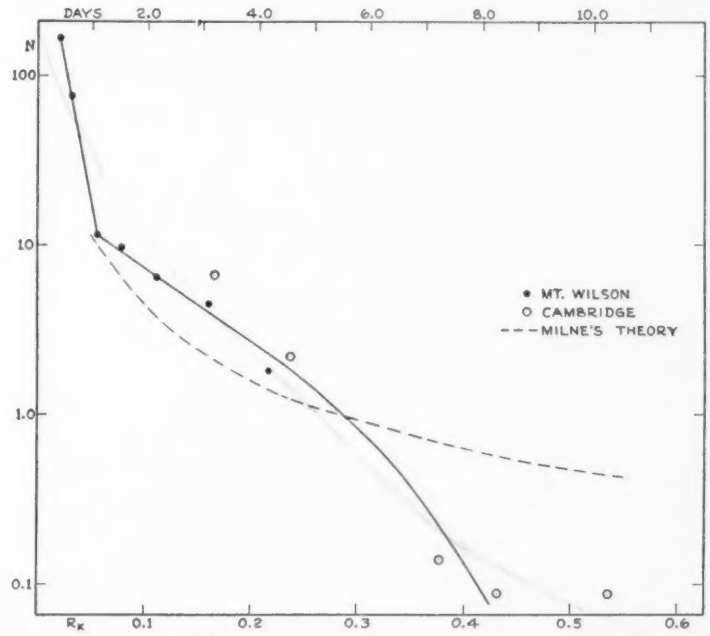

FIG. 11.—Number of Ca^+ atoms in line of sight (on arbitrary scale)

sphere of the sun is supported entirely by radiation pressure and arrives at the density distribution $\rho \propto (h+h_0)^{-2}$ (h = height). Taking $h=0$ to correspond to the photosphere, he is able to evaluate the constant h_0. These results have been criticized by Menzel[20] on the grounds that (1) the calculated pressure at the base of Milne's layer is incompatible with that which must exist in the reversing layer; (2) the predicted gradient and density at the base are too low; (3) the observed emission from the base of the chromosphere during

[18] The writers obtained three spectrograms on October 11, at a phase just short of Beer's last observation, but are unable to find any trace of a sharp K line on them.

[19] Summarized in *op. cit.*, p. 173.

[20] *M.N.*, **91**, 628, 1931.

total eclipse is at least ten times greater than that to be expected theoretically.

In the present instance it is tempting to suppose that the sharp bend in the curve at a height of about $0.05R$ marks the point at which the density distribution changes over to the chromospheric type of Milne. This supposition may readily be tested by comparing the observed run of N with H with that computed from the theory. Integrating rigorously Milne's density distribution along a chord at height H above the surface of the sphere which marks the lower limit of Milne's layer, we find

$$N \propto \frac{R-h_0}{(R+H)^2-(h_0-R)^2}+\frac{2(R+H)^2}{[(R+H)^2-(h_0-R)^2]^{3/2}}\tan^{-1}\frac{\sqrt{(R+H)^2-(h_0-R)^2}}{H+h_0}, \quad (9)$$

where R is the radius of the lower surface of Milne's layer. The dashed curve in Figure 11 has been computed from equation (9) with the radius of the photosphere taken as unity, $R=1.05$, and $h_0=0.05$ (for convenience in computation). Since the density decrement decreases with increasing h_0, a larger value of h_0 will cause N to fall off at a still slower rate outward than that shown by the calculated curve of Figure 11. Accordingly, we conclude that the observations of the Ca^+ envelope surrounding ζ Aurigae are in disagreement with the predictions of Milne's theory of chromospheric equilibrium. Although we cannot in the present case estimate the magnitude of h_0, as has been done for the solar chromosphere, it is clear that this uncertainty does not affect the general state of affairs outlined above.

An important point remains still to be discussed, namely, is it safe to assume that the atmosphere of ζ Aurigae is typical of normal K-type giants? This question must be considered in two ways. First, we know from the 1931–1932 observations of Guthnick and Schneller and from those of 1934 by Beer and from our own that the Ca^+ envelope about the star is widely variable in extent. This fact raises the question as to how nearly static we may consider the atmosphere to be during the interval covered by an eclipse. Practically nothing is known concerning the rate or frequency of such changes. The only evidence is that previously noted, which indicates that an apparently real change occurred in the distribution of certain of the atmos-

pheric constituents between August 22 and October 1. Second, what effect, if any, does the secondary have upon the structure of the atmosphere of the primary? The complete investigation of this matter would be difficult. As a beginning, however, it may be somewhat illuminating to include a calculation of the influence of the radiation of the B-type star upon the ionization of the Ca^+ envelope of the primary.

Pannekoek[21] has derived an equation which permits this to be done. His equation may be written

$$\log \frac{x}{1-x} = -\frac{5040I}{T_B} + \tfrac{3}{2} \log T_K + \log T_B + \log \beta - \log P - 6.50 ,$$

where x is the fraction of the substance ionized, I the ionization potential in volts, T_B the effective temperature of the companion, T_K the temperature of the gas, which we take to be the same as that of the K-type star, and P the electron pressure in atmospheres. β is $d\hat{\omega}/4\pi$, where $d\hat{\omega}$ is the solid angle subtended by the companion at the point at which the ionization is to be computed. For $i = 90°$, the distance between the two stars at the time of eclipse is 579×10^6 km, whence $\beta = 2.6 \times 10^{-5}$. For $P = 10^{-8}$ atm., $T_K = 3{,}500°$, and $T_B > 15{,}000°$, assumed as reasonable values, the equation shows, first, that no neutral calcium will be present in the envelope of the primary. For the second ionization, $I = 11.8$ volts, and we find the results given in Table IX.

TABLE IX

SECOND IONIZATION OF *Ca* IN ζ AURIGAE

T_B	$1-x$
20,000°	0.000
15,000	0.005
10,000	0.345

Since the H and K lines are observed, we know that at least a moderate fraction $(1-x)$ of the Ca^+ must not be further ionized. Accordingly, if $P = 10^{-8}$, it is clear that $T_B < 15{,}000°$, or, conversely, if $T_B > 15{,}000°$, $P > 10^{-8}$.

[21] *Handbuch der Astrophysik*, **3**, Part I, 289, 1930.

In conclusion we wish to acknowledge the courtesy of Dr. Stebbins and Dr. Huffer and of Dr. Oosterhoff in placing their photometric data at our disposal before publication. We also owe our thanks to Dr. Stebbins for suggestions used in combining these data. To several members of the staff we owe thanks for their co-operation in obtaining spectra; especially to Dr. van Maanen, who kindly placed the latter half of three of his nights at the 60-inch telescope at our disposal for this investigation. Acknowledgments are also due Dr. D. H. Menzel for several suggestions from which we have profited.

CARNEGIE INSTITUTION OF WASHINGTON
MOUNT WILSON OBSERVATORY
February 1935

PHOTOGRAPHIC MAGNITUDES OF ζ AURIGAE DURING THE 1934 ECLIPSE*

By P. TH. OOSTERHOFF

ABSTRACT

Photographic magnitudes of ζ Aurigae during the recent eclipse were derived from plates taken with the 10-inch refractor and Schraffierkassette. On the descending as well as on the ascending branch of the light-curve a set of observations was obtained. The epoch of minimum is found to be J.D. 2427692.70±0.15 (M.E.). The interval between maximum and minimum light is of the order of 1.5 days. The inclination of the orbital plane remains uncertain. On the assumption of central eclipse the ratio between the diameters of the K- and B-type components would be 0.038.

As ζ Aurigae is a variable of exceptional interest and the photometric data obtained during former eclipses are rather scarce, its photographic magnitudes during the 1934 eclipse were observed with the 10-inch refractor of the Mount Wilson Observatory. Since the predicted epoch of minimum and the total duration of the eclipse were uncertain by a few days, the variable was observed on as many consecutive nights as possible in order not to miss the most interesting phases of the light-variation. In consequence, the observing conditions on several occasions were very unsatisfactory. In general, the altitude of the variable was unfavorable, especially during the earlier observations. The observations were made with the Schraffierkassette,[1] set to give images 0.14×0.14 cm. The exposures were 2 minutes, on Eastman 40, 5×7 inch plates, some of which were taken by Messrs. F. E. Ross, W. H. Christie, and H. Wright, to whom I wish to express my acknowledgment.

The variable and the five comparison stars (Table I) were measured with a thermoelectric photometer provided with a diaphragm such that only the central part of each star image was included. The ratio $Q=(S_s-S_0)/(S_f-S_0)$ was computed for each star, S_s being the scale reading for the star, S_f that for the clear film near the star image, and S_0 the reading when all light was shut off. Values of Q for the comparison stars, plotted against provisional photographic

* *Contributions from the Mount Wilson Observatory, Carnegie Institution of Washington*, No. 518.

[1] *Mt. W. Contr.*, No. 476; *Ap. J.*, **78**, 313, 1933.

magnitudes taken from the *Henry Draper Catalogue*, defined the reduction-curve, which proved to be linear for the range in magnitude covered by the comparison stars. Improved magnitudes of the comparison stars derived by means of the deviations from these curves are given in the last column of Table I. The scale and zero point of the adopted magnitudes are the same as those for the H.D. values. The comparison stars are all fainter than the variable at its maximum light, but no brighter stars were available in the field.

The derived magnitude of the variable during maximum light therefore depends on an extrapolation of the reduction-curve, which

TABLE I

COMPARISON STARS

Comp. Star	Pg m	
	H.D.	Adopted
BD+43°1043	5.25	5.25
BD+40 1000	5.46	5.43
BD+42 1081	5.62	5.66
BD+43 1116	5.96	5.90
BD+40 1032	5.98	6.03

was assumed to be linear over the total range of the scale readings. Since errors of the order of a few hundredths of a magnitude may have been introduced by this procedure, the observations during the eclipse are probably of higher accuracy. Correction for differential extinction, which varied from 0.00 to −0.07 mag., gave the final magnitudes listed in Table II. Values connected by brackets were derived from the same plate. The observations are shown graphically in Figure 1.

The mean error of a single observation computed from the deviations of the comparison stars is ±0.024 mag. The magnitudes of the variable during the total eclipse, constant brightness being assumed, give ±0.026 mag. Measures of the variable outside the eclipse, on the other hand, constant brightness again being assumed, give ±0.036 mag., an increase which is probably due to the extrapolation of the reduction-curve.

The value of the mean error and the small number of observations made each night indicate that the fluctuations in the measures are

TABLE II

PHOTOGRAPHIC OBSERVATIONS OF ζ AURIGAE, 1934

Date	J.D.	Phase	Pg *m*	Date	J.D.	Phase	Pg *m*
1934	2427000+	days		1934	2427000+	days	
Aug. 14	664.94	−27.76	5.01	Sept. 25	706.88	+14.18	5.55
15	665.96	26.74	.03		.89	14.19	.56
16	666.98	25.72	.07	26	707.88	15.18	.54
17	667.94	24.76	.07				.55
	.95	24.75	.07	27	708.89	16.19	.54
18	668.97	23.73	.03				.53
20	670.96	21.74	.07	28	709.87	17.17	.54
			.07				.56
21	671.96	20.74	.06	29	710.81	18.11	.47
	.97	20.73	.07		.89	18.19	.50
22	672.95	19.75	.09		.99	18.29	.54
	.99	19.71	.11	30	711.80	19.10	.29
23	673.95	18.75	.42		.90	19.20	.28
	.99	18.71	.42		.96	19.26	.26
24	674.91	17.79	.54		712.03	19.33	.25
	.92	17.78	.51	Oct. 1	.81	20.11	.07
25	675.94	16.76	.55				.04
	.95	16.75	.53		.92	20.22	.06
26	676.95	15.75	.50				.08
			.48		.98	20.28	.13
27	677.93	14.77	.46				.06
			.51	2	713.82	21.12	.06
28	678.95	−13.75	.55				.08 .10
			.54		.91	21.21	.02
Sept. 11	692.92	+ 0.22	.53		.92	21.22	.04 .02
	.93	0.23	.53				
12	693.90	1.20	.53				
			.51	3	714.83	22.13	.04 .04
13	694.92	2.22	.53				
	.93	2.23	.51		.91	22.21	.06
14	695.93	3.23	.54		.96	22.26	.06 .09
	.94	3.24	.55				
17	698.90	6.20	.51		.97	22.27	.09
	.91	6.21	.50		715.01	22.31	.15
18	700.02	7.32	.50 .49		.02	22.32	.14 .17
19	.94	8.24	.54 .54	4	.81	23.11	.07 .06
20	701.94	+ 9.24	.49		.82	23.12	.10
			5.48		.92	+23.22	5.08

mostly errors of observation, although an unusual run in the magnitudes for October 3 suggests the possibility of a real change in the variable on that date.

As compared with the observations of Hopmann[2] during the eclipse of 1931–1932, the present observations, apart from changes caused by the eclipse, show a remarkable constancy in the light of the variable. Hopmann found irregular long-period changes in his blue magnitude outside the eclipse, as well as during eclipse, the

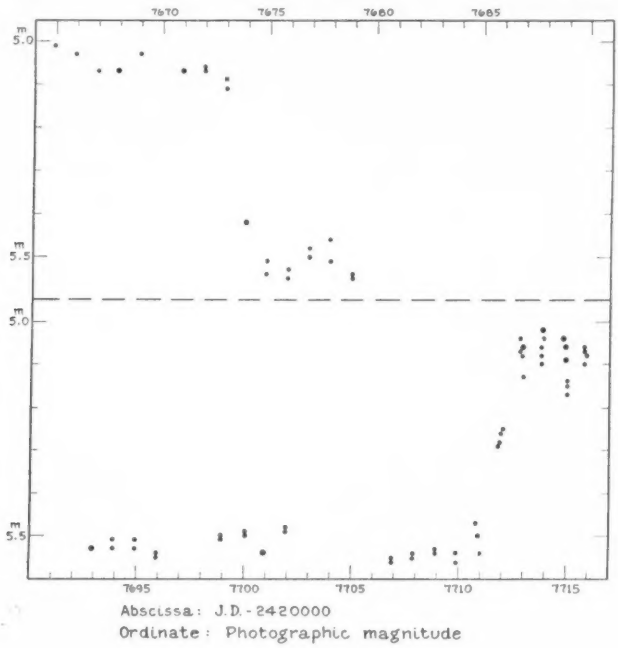

FIG. 1

amplitude of which amounted to more than 0.2 mag. He used, however, a single comparison star, η Aurigae, and therefore could not decide to which of the two stars the fluctuations should be ascribed. Dr. C. M. Huffer informs me that from recent photoelectric measures he suspects η Aurigae to be a variable.[3]

Hopmann's observations of BD+41°1044 (var. 60, 1933)[4] also have a bearing on this question. With η Aurigae as a comparison object, he found this star to be a variable of the RR Lyrae type with a period of about 0.10 day. BD+41°1044 also appears on our

[2] *Mitteilung der Sternwarte Leipzig*, No. 1, 1933.

[3] *Ap. J.*, **81**, 292, 1935.

[4] *Zs. f. Ap.*, **6**, 385, 1933.

plates and has been measured. It is somewhat fainter than the faintest comparison star used, but a linear extrapolation of the reduction-curve seems even more justified than in the case of ζ Aurigae. Practically no variation in the light was found. On the assumption of constant brightness, the mean error of a single observation was found to be ±0.047 mag., which, although considerably larger than the error for the comparison stars, is of a quite different order from the value resulting from Hopmann's blue-filter measures, viz., ±0.19 mag. Since we cannot reach any definite conclusion from these observations, accurate photometric measures of both η Aurigae and BD+41°1044 will be of much interest.

Our light-curve of ζ Aurigae yields the following quantities:

Mean Pg *m* during maximum	$5^{m}07$
Mean Pg *m* during total eclipse	5.52
Amplitude	0.45

The most interesting parts of the curve, namely, the descending and ascending branches, show only a few observations. No detailed light-curve can be obtained at a single observatory. To derive such a curve, measures made at observatories in very different longitudes must be combined. Nevertheless we may learn something from the few points obtained. Although it is uncertain whether the observations on J.D. 2427672 indicate a beginning in the decrease in brightness, there is no doubt that at least one set of observations has been secured on each branch. If we take the branches to be linear, the slowest rate of change in the magnitude permitted by our observations is 0.10 mag. in 0.32 day, the total time between maximum and minimum being 1.44 days. Since the actual rate of change at the very beginning of the eclipse and just before totality begins must be less than the average, the foregoing value should be increased by an unknown amount. The value given was obtained by superposing the mirror image of the ascending branch on the descending branch. The four observations on the ascending branch agree well with this result. Although they cover 0.23 day, the difference between the first and the last magnitudes is only 0.04±0.04 mag. The branches may be somewhat steeper than the calculation indicates, but it seems

improbable that the whole change should take place within 0.5 or 0.6 day, as was assumed by Guthnick and Schneller.[5]

From these figures the following approximate values have been derived:

Duration of eclipse	39^d7
Duration of totality	36.8
Epoch of minimum*	J.D. 2427692.70+0.15 (estimated M.E.)

* K. Walter derives J.D. 2427692.926 (*A. N.*, **253**, 375, 1934).

The phase of each observation relative to this epoch of minimum is given in Table II.

Because of the many uncertainties involved, it is not believed that a reliable value for the inclination of the orbital plane, i, can be derived from these photometric data. For this reason also the ratio of the diameters of the K- and B-type components remains uncertain. For $i=90°$, that is, for central eclipse, the value of r_B/r_K would be 0.038. If the branches of the light-curve are steeper than assumed or if $i<90°$, this ratio will be smaller.

It is a pleasant duty to express my thanks to Dr. W. S. Adams for his permission to use the equipment of the Mount Wilson Observatory.

Carnegie Institution of Washington
Mount Wilson Observatory
February 1935

[5] *Sitz. Preuss. Akad. d. Wiss., Phys. Math. Klasse*, X, 1932.

THE EMISSION LINE λ 4511 IN LATE-TYPE VARIABLES*

By A. D. THACKERAY[1]

ABSTRACT

The appearance in *emission* in M and S variables of the line λ 4511 (previously identified as the indium resonance line λ 4511.31) is suggested as due to the *coincidence in wave-length of Hδ* (λ 4101.75) *with the other In resonance line* (λ 4101.72). The behavior of λ 4511 relative to *Hδ* during the cycle of variation is not at variance with the hypothesis provided *either that* ionization at light-maximum is sufficient to remove most of the *In* atoms out of the neutral state or that atoms in the metastable state $^2P_{\frac{3}{2}}$ are more likely to reach the ground state $^2P_{\frac{1}{2}}$ by collisions than to absorb λ 4511.

An emission line λ 4511 observed in many late-type variables has been tentatively identified by Joy[2] and Merrill[3] as *In* λ 4511.31 ($5^2P_{1\frac{1}{2}}-6^2S_{\frac{1}{2}}$), but confirmation is difficult owing to the fact that the other member λ 4101.72 of the indium resonance doublet is masked by *Hδ* λ 4101.75, which appears in emission in all late-type variables. The coincidence in wave-length tempts one to suggest that the hydrogen emission stimulates the *In* atoms out of the ground state $5^2P_{\frac{1}{2}}$ to emit λ 4511 later in a manner similar to the excitation of *O* III radiation by *He* II in nebulae, recently very satisfactorily explained by Bowen.[4] This case is of special interest in that both *Hδ* and λ 4511 vary in intensity throughout the cycle of light-variation, and if the explanation in terms of fluorescence is correct, one would expect the intensity of λ 4511 to depend intimately upon that of *Hδ*, and to some extent also upon the continuous spectrum at λ 4511. The behavior of the two lines in M and S variables as found from plates kindly loaned to the writer by Dr. Merrill and Dr. Joy is summarized below.

* *Contributions from the Mount Wilson Observatory, Carnegie Institution of Washington*, No. 517.

[1] Fellow in astronomy on the Commonwealth Fund.

[2] *Mt. W. Contr.*, No. 311, p. 35; *Ap. J.*, **63**, 315, 1926. Mean wave-length in *o* Ceti 4511.50 (I.A.).

[3] *Mt. W. Contr.*, No. 399, p. 34; *Ap. J.*, **71**, 318, 1930. Mean wave-length in M variables 4511.43, in S variables 4511.40.

[4] *Pub.* A.S.P., **46**, 146, 1934.

1. The intensity-curve of $H\delta$ in M and S variables follows closely that of the light-curve, always reaching maximum intensity at or near maximum light. For convenience we divide the stars into two groups—*a* and *b*—according to the behavior of $H\delta$. In group *a*, including S variables (R Cyg and R Gem) and the M stars *o* Ceti, U Ori, and χ Cyg, the curve is unsymmetrical, the rise to maximum being very rapid compared with the descent to minimum. In group *b* the curve is roughly symmetrical.

	Star	Type	$\frac{M-m}{p}$	Mean Intensity			
				λ 4511		$H\delta$	
				Before	After	Before	After
a	χ Cyg	M6pe	.41	0.7	1.7	15	19
a	U Ori	M8e	.35	.....	1.4	.....	21
	R Gem	Se	.35	0.3	2.3	4.0	7.6
	R Cass	M7e	.39	1.4	1.4	23	22
	R Leo	M8e	.43	1.0	1.7	11.5	15
b	R Hya	M7e	.49	1.8	0.9	19	15
b	W Hya	M8e	.51	3.0	2.0	17	11
b	T Cass	M8e	.56	2.7	1.0	13.5	9.5

2. λ 4511 is invisible or weak before maximum in *a* stars, reaching greatest intensity about phase +60 days; in *b* stars the line has two maxima, before and after maximum light. The appearance before maximum is very unusual for emission lines apart from the hydrogen lines.

3. In *b* stars, λ 4511 weakens or disappears at maximum, the weakening being greatest for stars with large magnitude range. There is no appreciable weakening in W Hya, which has an unusually small range (2.8 mag.). The line was visible in *o* Ceti at the peculiarly faint maximum of February, 1924.

4. λ 4511 appears if anything stronger in S than M stars, while $H\delta$ is certainly weaker.

5. The line has been observed only in emission, never absorption, and only in Se and Me variables of type later than M5.

6. The mean relative strengths of λ 4511 at equivalent epochs

before and after maximum seem to follow roughly that of $H\delta$ as shown in the tabulation (p. 468). Intensities are visual estimates and are necessarily very rough.

7. The continuous spectrum in the region of λ 4511 is generally brighter in the stars of group *a* than in those of group *b*, particularly *o* Ceti and S stars. In some stars it weakens after maximum.

8. Joy[5] finds that in *o* Ceti λ 4511 shows smaller velocity displacements than the hydrogen and low-temperature lines and that the cyclic variations in displacement are shown to less degree than by other emission lines.

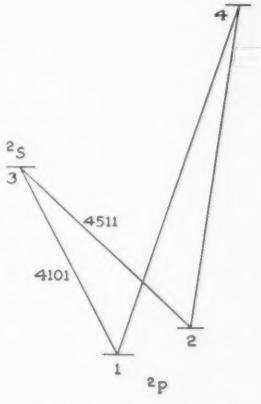

FIG. 1.—Grotrian diagram of indium resonance lines.

Several points suggest that the source of λ 4511 emission is different from that of other emission lines. The weakening or disappearance of the line at phase o when $H\delta$ is most intense does not necessarily invalidate the suggested process since maximum phase of late-type variables is always accompanied by the weakening of low-temperature lines, and appearance of enhanced lines; *In*, with its low ionization potential (5.76 volts), would be highly ionized at maximum phase.

Thus the behavior of λ 4511 relative to $H\delta$ in both M and S variables is not at variance with the present hypothesis provided the change of ionization during the light-phase is sufficient to remove most of the *In* atoms from the neutral state. It is significant in this respect to note that λ 4511 follows the intensity of $H\delta$ most closely in W Hya where the range is smallest, and presumably the ionization does not change so much.

Let us consider the transitions in detail. Denoting as in Figure 1 three states $^2P_{\frac{1}{2}}$, $^2P_{1\frac{1}{2}}$, ^2S by 1, 2, 3, respectively, let n_1, n_2, n_3 be the number of atoms per cubic centimeter in each of the states. Simple calculation shows that if the incident radiations I_{13}, I_{23} of frequency ν_{13}, ν_{23} are in the ratio $f:1$, and transitions between the three states only are considered, a steady state will be reached with a concentration of atoms in the state 2 with $N_2=fn_1$. Since the transition 2→1

[5] *Op. cit.*

is forbidden, no cyclic transition is possible between states 1, 2, 3, but if we consider the ionized atom as state 4, then a cyclic transition through the four states in the direction of emission of λ 4511 will result. Calculation is rendered difficult by ignorance of relative probabilities of ionization and absorption, and of recombinations in the states 1, 2. We ignore the other transitions from the 5^2P state since they involve frequencies in the far ultra-violet which will be weak in late-type stars.

For simplicity, neglect transitions between states 3, 4 (the lifetime of the excited state 3 being small) and let

$$P_{14}=P_{24}=yP_{23}\,, \qquad 2P_{41}=P_{42}\,,$$

where Prs = probability of transition from state r to s in unit time. We have

$$P_{32}=2P_{31}\,, \qquad fP_{23}=P_{13}\,.$$

The conditions that the number of transitions leaving any state balances the number of transitions ending on that state lead immediately to[6]

$$\frac{n_1}{1+y}=\frac{n_2}{2(f+y)}=\frac{n_3\dfrac{P_{32}}{P_{23}}}{2f+\frac{4}{3}y+\frac{2}{3}fy}\,,$$

whence

$$\alpha=\frac{\text{No. of transitions } 3\to 2}{\text{No. of transitions } 2\to 3}=\frac{n_3P_{32}}{n_2P_{23}}=1+\frac{y(f-1)}{3(f+y)}\,.$$

Although $\alpha>1$ will clearly give a cyclic transition ($1\to 3\to 2\to 4\to 1$), Woolley[7] has shown that α must be greater than 2 for production

[6] More generally, assuming

$$P_{24}=rP_{14}=yP_{23}\,,$$

$$P_{42}=2rP_{41}\,,$$

then

$$\alpha=1+\frac{y(f-1)}{f(1+2r)+3y}\,.$$

[7] *M.N.*, **94**, 637, 1934. Dr. Woolley has pointed out in a letter that this expression shows that however bright $H\delta$ emission may be ($f\to\infty$), the condition $\alpha>2$ cannot be fulfilled unless $y>3$; thus, on this hypothesis, fluorescence is dependent on very strong ionization or some strong ultra-violet transition.

of a bright line owing to the fact that emission takes place in all directions, while absorption is mainly of photospheric radiation from below. We see that $a > 1$, provided $f > 1$ and $y > 0$ and provided recombination from the ionized state is possible. Further, a increases with both f and y. The strength of $3 \rightarrow 2$ emission depends partly on a, which measures the preponderance of the cyclic transition, and partly on the number of neutral atoms. To account for the weakening of λ 4511 at maximum we have to assume that ionization reduces the number of neutral atoms sufficiently to overbalance the effect of the increase in a. The difference is one of a weak cyclic transition by a large number of atoms, and a strong one by few atoms.

The comparative strength of λ 4511 relative to $H\delta$ in S stars is a difficulty, since evidence from zirconium oxide bands and strong enhanced lines points to higher temperatures and lower densities than in M variables,[8] so that we expect the ionization of *In* to be higher. The difficulty remains, however, whether the line is formed by the suggested process of fluorescence or not, since the evidence for its low-temperature characteristics seems to be established from its behavior in the M cycle, and from the fact that it has never been observed in stars of earlier type than M5. Strong ionization, represented by large y in our expression, will, as we have seen, speed up the cyclic transition and can only weaken the line if it decreases the number of neutral atoms sufficiently through difficulty of recombination. If we suppose conditions in S stars to favor recombination (as well as ionization) to a greater extent than in M stars, we can see how increased ionization would have less effect on the number of neutral atoms and might actually strengthen the emission of λ 4511. This is not perhaps as unlikely a hypothesis as it might seem at first, for Merrill[9] has pointed out certain anomalies in S stars which indicate that conditions must be particularly favorable to production of emission lines (e.g., the simultaneous appearance of Fe^+ 4583 and the low temperature line *Mg* 4571).

An alternative explanation is possible in terms of collisions en-

[8] Merrill, *Mt. W. Contr.*, No. 325; *Ap. J.* **65**, 23, 1927.

[9] *Mt. W. Contr.*, No. 325, p. 17; *Ap. J.*, **65**, 39, 1927.

hancing the otherwise forbidden transition of $2 \rightleftarrows 1$.[10] If we consider only the three states 1, 2, 3, and let

$$P_{21} = 2P_{12} = y'P_{23} ,$$

we find

$$a = 1 + \frac{y'(f-1)}{f+3y'} .$$

In this case we expect a *minimum* of y' at maximum light since collisions would be rarer in the low-pressure atmosphere associated with this phase; thus the weakening or disappearance of λ 4511 at maximum light would be accounted for. Moreover, difference in composition might easily provide a larger y' in S than M stars, since the collision area of atoms depends largely on the foreign gases present. We note that in this case, as $f \to \infty$, the condition $a > 2$ leads to $y' > 1$; thus, comparing the two hypothetical cycles, the probability of collision ($2 \rightleftarrows 1$) need be only one-third as great as that of ionization ($2 \rightleftarrows 4$) to provide fluorescence.

If increased ionization at maximum phase of M variables causes the disappearance of λ 4511, we might expect the line to appear in dwarf stars showing bright hydrogen lines where the ionization is presumably much lower. With this in view, an examination has been made of Mount Wilson plates of the dwarfs WB 16^h906, WB $10°234$, and YY Gem (component C of α Gem), all of which show hydrogen emission, but λ 4511 does not appear. This is not surprising, for the hydrogen decrement in these stars is normal, $H\delta$ being faint and certainly much weaker than the continuous spectrum at λ 4511, so that conditions are unfavorable to fluorescence of λ 4511 through $H\delta$ radiation.

It should be remarked that although the rarity of indium is to some extent an objection to its identification with λ 4511, the production of an emission line by cyclic transitions would need far fewer atoms than that of a normal absorption line where absorption and emission nearly balance. With only a few atoms fluorescent emission may be made as intense as we please simply by speeding up the cycle of transitions. The fact that λ 4511 has only been observed in emis-

[10] Note that state $2(=\,^2P_{\frac{1}{2}})$ is metastable.

sion in M stars certainly gives support to the hypothesis that it is due to fluorescent excitation.

If the observed λ 4511 emission represents *Hδ* radiation absorbed by *In* atoms, we might expect a corresponding absorption line within the *Hδ* profile at λ 4101.72. The strength of this absorption would, however, depend on the relative distribution of *H* and *In* atoms in the atmosphere, and it is not likely to be great unless *In* lies entirely above the layers emitting *Hδ*. It is probable that neutral indium is present in only the lowest layers and the *H* emission extends to the highest, as in the solar chromosphere, in which case little or no absorption should be observed. In other words, λ 4511 emission represents fluorescence in the lower levels of *Hδ* radiation which has been emitted downward from the higher levels.

In conclusion, we may say that although the emission line λ 4511 cannot yet be identified with certainty as due to indium, the observational data are not unfavorable to the hypothesis that it is produced by fluorescence set up by the coincidence in wave-length of *Hδ* (λ 4101.75) with the *In* resonance line (λ 4101.72). Photometric measures of line intensity would help in putting the observations on a more rigorous quantitative basis. Visual examination of plates suggests that the factor *f* is normally as great as 10 and probably considerably greater.

The writer is indebted to the Commonwealth Fund for the opportunity to work at Mount Wilson Observatory and acknowledges with thanks the helpful criticisms of Dr. Theodore Dunham, Jr., and Dr. R. v. d. R. Woolley.

CARNEGIE INSTITUTION OF WASHINGTON
MOUNT WILSON OBSERVATORY
February 1935

NOTE ON DISPERSING AND CONDENSING TENDENCIES IN A VISCOUS, COMPRESSIBLE GAS*

By GUSTAF STRÖMBERG

ABSTRACT

Certain conditions for general and local expansion and condensation in a viscous, compressible gas have been formulated. Applying them to the formation of the galaxy, we find that both expansion and contraction may occur. The stars are formed in the non-rotating, cool, and dense parts of the system. The original nebula had a much greater extension and mass than the system of stars that finally developed.

The question whether a gas freely hovering in space tends to disperse or to condense, generally or locally, is of great importance in cosmological theories, since it is generally assumed that the stars and the planets have been formed from a very tenuous primordial gas. In particular, it has been found that the original simple form of Laplace's theory for the formation of the solar system must be abandoned, since secondary condensations could not have been formed unless the local density exceeded a fairly large fraction of the mean density of the system. Thus, in order that Neptune might condense from the solar nebula, the density at the place and time of its formation must have been at least 0.36 of the mean density, whereas the local density at Neptune's present distance from the sun could at the most have been only of the order of a thousandth part of the mean density.[1]

It is obvious that the temperature of the gas plays an important rôle in determining whether the gas condenses or contracts. Lindblad[2] has called attention to one type of condensation caused by sublimation of a gas on small particles, even if the gas itself is at a fairly high temperature. In the following we shall try to formulate some factors which determine the tendencies in a viscous, compressible gas, on the supposition that the time scale is sufficiently long.

* *Contributions from the Mount Wilson Observatory, Carnegie Institution of Washington*, No. 520.

[1] Jeffreys, *The Earth* (2d ed.; Cambridge, 1929), pp. 14–15; Moulton, *Ap. J.*, **11**, 126, 1900.

[2] *Nature*, **135**, 133, 1935.

It is clear that a condition for the growth of a condensation is that in the particular region the gravitational forces acting inward must be greater than the centrifugal forces and the pressure gradients acting outward. This gives us Poincaré's condition[3] for the growth of an incipient condensation,

$$\rho > \frac{\omega^2}{2\pi f}, \tag{1}$$

where ρ is the local density, ω the local angular velocity, and f the gravitational constant. If the gas from which the solar system was formed rotated as a solid, as is nearly always assumed, we can find the value of ω at the time of the formation of a planet, and thus evaluate the condition for the formation of a planet like Neptune as given at the beginning.

In *Mt. Wilson Contr.* Nos. 492 and 503[4] the writer has shown that a number of facts about stellar and planetary motions can be explained if we assume that the primordial gas had the properties of a viscous, compressible fluid, in which the angular velocity, at least at great distances from the center, decreased outward. If local condensations were started, they would ultimately tend to move "inward," that is, toward regions of smaller gravitational energy.

If the gas did not rotate as a rigid body, we should, in addition to the systematic changes in angular velocity, expect local irregularities in ω at an early stage of development, since the time required for viscous forces to equalize angular velocities is proportional to the square of the linear dimensions of the system. Further, since condensations, once having been started and a stable state of motion also having been established, tend to move "inward," the planets must have been "born" at much greater distances from the sun than they are now. Both these circumstances make it probable that, at an early stage of the evolution of the solar system, there existed regions in which ω was practically zero. If the density of such a region happened to be slightly above that in the adjacent parts and its temperature not greater than that of the surroundings, concentration in the primordial gas would start in the region and gradually grow in

[3] *Leçons sur les hypotheses cosmogoniques* (Paris, 1911), pp. 22–23.

[4] *Ap. J.*, **79**, 460; **80**, 327, 1934.

mass. Viscous forces would slowly change ω, but Poincaré's condition could well remain satisfied during the subsequent development. This general reasoning applies, of course, equally well to the formation of stars.

Important information can be deduced from the virial theorem, which can be written in the form

$$\tfrac{1}{2}\frac{d^2I}{dt^2}=\int(2T+G)dm\,, \tag{2}$$

where I is the moment of inertia, and T and G are the kinetic and gravitational energies, both reduced to unit mass. T is a sum of two parts,[5] the mechanical kinetic energy and the heat energy. T is always positive, G is always negative. It is clear that the sign of dI/dt, after a sufficiently long time has elapsed, is the same as that of d^2I/dt^2. If the former is positive, the system generally expands; if negative, it contracts.

We shall assume that in the prestellar state of the gas there is no subatomic source of energy within the system. Since some of the kinetic energy will be converted into radiation by the collisions, which are essential for the applicability of the hydrodynamical laws,[4] a certain part of the internal energy will be lost to the surrounding space. We denote by E the rate at which this loss occurs. The law of conservation of energy then gives

$$\frac{D}{Dt}\int(T+G)dm=-E\,. \tag{3}$$

From (2) and (3),

$$\tfrac{1}{2}\frac{d^3I}{dt^3}=-\int\frac{DG}{Dt}\,dm-2E\,. \tag{4}$$

If the system expands, dI/dt is positive, and the integral in (4) is also positive. Since E is positive, d^3I/dt^3 is negative and exercises a retarding effect on the expansion.

[5] In *Mt. W. Contr.* No. 503 I used in the virial theorem the mechanical kinetic energy instead of the total kinetic energy T. Hence I neglected the changes in heat energy in the expression for the third time derivative. This oversight was called to my attention by Professor Lindblad. The deductions from the virial theorem are here given in a more complete form. We must further note that the effect of inelastic collisions is not taken into account in the virial theorem.

If the system contracts, dI/dt is negative, and also the integral in (4); d^3I/dt^3 may then be positive or negative, according to the relative size of the two terms on the right-hand side in equation (4). If the energy lost in the form of radiation is sufficiently large, d^3I/dt^3 will be negative, the contraction will in the end proceed at an accelerated speed, until liquefaction or sublimation occurs, or until subatomic energy begins to be liberated, causing ultimately a bar to further contraction.

If the system is contracting and has an angular momentum differing from zero, the motions can, at least in certain simple cases, be expected ultimately to be continuous and approximately steady. As shown in *Mt. Wilson Contr.* No. 503, we have then

$$-\int \frac{DG}{Dt}\, dm = \Phi\,, \tag{5}$$

where Φ is the dissipation function, which is positive as long as there is still internal gross motion in the system.

If a system of nebulae has started from a common system of gas, large portions may be detached, forming a number of subsystems. Each subsystem may expand or contract, but the general system would show a tendency to expansion if a sufficiently large part of the initial energy was in the form of kinetic energy of motion.

But in many cosmological studies we are not concerned with what happens to the system as a whole; we want to know what happens within those parts which eventually are left behind after high-speed molecules and portions of high mass motion have escaped. In particular, are we interested in the motions of the condensations, which are less affected by pressure gradients than the gas around them. Hence for similar motions perpendicular to the gradient of gravitational energy a condensation will move relative to the surrounding gas in the direction of decreasing gravitational energy. In the residual system dI/dt must be permanently zero or negative; d^2I/dt^2 and d^3I/dt^3 must therefore also be zero or negative. From equations (4) and (5) it then follows that, if the system has rotation and the motions in the residual system are ultimately continuous and steady, $2E$ must be greater than or equal to the dissipation of energy Φ. The dissipation of energy tends to disperse the residual system by heat-

ing it, while the loss of energy by radiation tends to contract the system by cooling it. On account of the motion of condensations relative to the surrounding gas, the system of condensations may congregate; a small part of the intervening gas may yet escape, but most of it must condense on the bodies until no gas is left over.

Eddington's[6] statement that "in the end viscosity triumphantly establishes the law of motion it is striving for—only there is nothing left to obey it" refers to a system in which the internal molecular and gross motions are so large that it completely "evaporates." But we must remember that bodies may be formed in the residual system which finally escape the effects of viscosity by gradually acquiring uniform rotation, and by moving in a gas of negligible density. The present result is analogous to Lindblad's[7] statement that "the Milky Way is an effect of the cooling of the stellar gas by the evaporation of its swift molecules." "Stellar gas" here means a gas consisting of stars as molecules. In *Mt. Wilson Contr.* No. 503, in referring to the prestellar gas I described the effect by stating that "viscous forces produce at the same time a scattering and a condensation; we confine our study to the contracting system." Condensations originated in the cooler and denser parts of minimum angular velocity in the original nebula, *which had a much greater extension and mass than the system of bodies finally developed.*

In the case of the expanding envelope of gas surrounding a nova, condensations with velocities less than that of escape can well be formed, even if most of the gas permanently escapes. If the system has rotation, the bodies formed will ultimately move in circles in a common plane of motion, and the residual system of bodies will therefore have very small extension perpendicular to this plane. This may be the way in which planetary systems are formed.

CARNEGIE INSTITUTION OF WASHINGTON
MOUNT WILSON OBSERVATORY
February 1935

[6] *The Rotation of the Galaxy* (Halley Lecture; Oxford, 1930), p. 29.

[7] *M.N.*, **95**, 20, 1934.

THE SPECTROGRAPHIC ORBIT OF W URSAE MINORIS*

By ALFRED H. JOY and O. L. DUSTHEIMER[1]

ABSTRACT

The orbit of the brighter component of the eclipsing variable W Ursae Minoris has been determined from eleven spectrograms. The resulting elements are: $e=0.0$ (assumed), $\gamma=-7.7$ km/sec., $k=105.5$ km/sec., $a \sin i=2{,}470{,}000$ km, mass function $=0.21\odot$. The spectral type is A4 and the spectroscopic absolute magnitude is $+2.2$. The mass, density, and absolute dimensions of the components have been estimated with the assistance of Dugan's photometric orbit and Eddington's mass-luminosity curve.

The variability of the eclipsing binary W Ursae Minoris ($\alpha=16^h34^m.8$, $\delta=+86°26'$; 1900) was discovered independently by T. H.

TABLE I

OBSERVATIONS OF W URSAE MINORIS

Plate	J.D.	Phase	Vel.	O−C
	2420000+		km/sec.	km/sec.
γ 16643	5781.7083	1.2719	+100	+ 2
17221	6016.9653	0.0677	− 36	− 2
17234	6019.0417	0.4429	−114	− 1
17331	6048.9423	1.4238	+ 80	− 3
17372	6075.9708	1.2338	+ 89	− 8
17377	6076.9167	0.4785	−109	+ 2
17428	6105.7590	0.4011	−115	− 2
17465	6111.9597	1.4983	+ 70	+ 5
17475	6130.8660	1.6919	+ 6	+10
17479	6131.7361	0.8608	− 11	− 8
17727	6222.7340	1.6972	− 1	+ 5

Astbury[2] and C. R. Davidson[3] in 1913. Four photometric solutions, two photographic and two visual, have been made.[4]

Eleven spectrograms have been obtained with the 60-inch re-

* *Contributions of the Mount Wilson Observatory, Carnegie Institution of Washington*, No. 521.

[1] Of Baldwin-Wallace College.

[2] *A.N.*, **194**, 414, 1913.

[3] *Ibid.*, **195**, 416, 1913.

[4] Martin and Plummer, *M.N.*, **78**, 644, 1918; M. B. Shapley and I. E. Woods, *H.B.*, No. 844, 3, 1927; D. B. McLaughlin, *A.J.*, **36**, 113, 1926; R. S. Dugan, *Princeton U. Obs. Contr.*, No. 10, 15, 1930.

flector and 9-inch camera. The spectrum of the brighter component only can be seen. Although the expected rotation effect (60 km/sec. from limb to limb) is comparatively small, the lines are not well defined. In this respect the spectrum resembles that frequently found among stars of low luminosity. The type is estimated to be A4n and the absolute magnitude determined from the spectrum is +2.2.

The observations for radial velocity are given in Table I. The phases are computed from Dugan's elements

$$\text{Min.} = 2424999.604 \text{ G.M.T.} + 1.70116E .$$

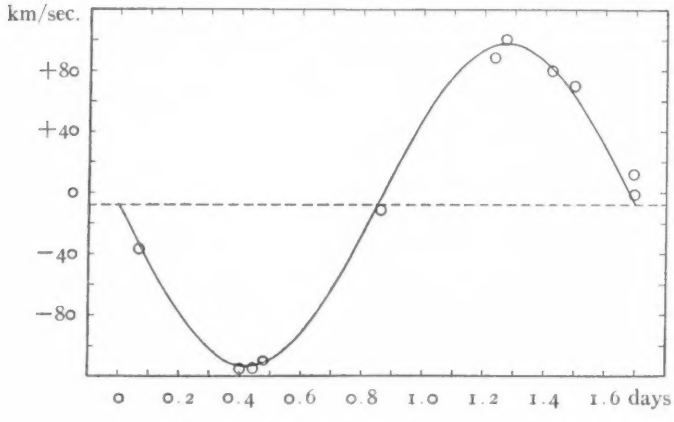

FIG. 1.—Velocity-curve of W Ursae Minoris

The spectrograms have been measured by both observers. From five to fifteen lines have been used for each plate, but, on account of the character of the spectral lines, the results should receive low weight.

The velocity-curve is shown in Figure 1, where the individual observations are plotted. The residuals are given in the last column of Table I. If a circular orbit be assumed, the approximate elements are

$$\gamma = -7.7 \text{ km/sec.}$$
$$k = 105.5 \text{ km/sec.}$$
$$a \sin i = 2{,}470{,}000 \text{ km}$$
$$\frac{m_2^3 \sin^3 i}{(m_1+m_2)^2} = 0.21\odot$$

The photometric solutions indicate that the brighter star is the larger and that its light is cut off at primary minimum by a smaller, fainter companion whose surface brightness is about one-sixth that of the principal star. The difference in visual brightness of the two stars is 2.4 mag. The eclipse is probably partial and the inclination of the orbit 83°. The radii of the stars, in terms of the relative orbit, are 0.38 and 0.33 according to Dugan's "uniform" solution. With the aid of these photometric results we find

Radius of primary orbit	2,490,000 km
Absolute magnitude of secondary	4.6 mag.

Since the spectrum of the smaller star cannot be observed even at the maximum phase of eclipse, we must resort to indirect methods for an estimate of the masses, densities, and linear dimensions. For the

TABLE II

ESTIMATED DIMENSIONS OF W URSAE MINORIS

Radius of primary orbit	2,490,000 km
Radius of secondary orbit	3,520,000 km
Radius of relative orbit	6,010,000 km
Radius of large star	2,300,000 km (3.3⊙)
Radius of small star	2,000,000 km (2.9⊙)
Density of large star	0.046⊙
Density of small star	0.049⊙

brighter star with absolute visual magnitude 2.2 and type A4, Eddington's mass-luminosity relation indicates a mass of 1.7⊙. The mass of the fainter star is then found from the mass function to be 1.2⊙. We can now compute the linear dimensions of the relative orbit and determine the size of the stars and their densities (Table II). The parallax resulting from the spectroscopic absolute magnitude is 0″.005.

CARNEGIE INSTITUTION OF WASHINGTON
MOUNT WILSON OBSERVATORY
March 1935

NOTES

ON THE COLOR TEMPERATURE OF NOVA HERCULIS

ABSTRACT

Color temperatures are derived from the spectrophotometric gradients of ten spectra. The mean value, uncorrected for atmospheric extinction, is $T = 10{,}500°$ K.

Observations of the color temperature of this object were begun soon after its discovery and have been continued to date. The purpose of this note is to present these measures, which are approximate but which may be of interest at the present time.

Spectra of the nova were secured with the single-prism spectrograph, employing a very wide slit. Immediately before or after exposure to the nova, the spectrum of α Coronae Borealis was photographed upon the same plate. Each plate was standardized for spectrophotometric measures in the calibrating spectrograph of this observatory, and the usual precautions were taken in regard to equality of exposure times and development technique. The emulsions used were Eastman 33 and Wratten and Wainwright Panchromatic.

The plates were measured in a manner similar to that outlined by the Greenwich observers in their color temperature work.[1] The gradient of the continuous spectrum of the nova relative to that of α Coronae Borealis was determined from tracings of the spectra made with a Moll microphotometer, using a vacuum thermocouple. The color temperature of the comparison star was taken as 18,000° K, in accordance with the revised zero point of the Greenwich system.[2]

The results are listed in Table I, with the dates and spectral regions used. These temperatures are not considered to be of great precision, but should indicate values of the correct order. The greatest source of error probably lies in the difficulty of distinguishing the

[1] Observations of color temperatures of stars, made at Greenwich, 1932.

[2] *M.N.*, **94**, 488, 1934.

continuous spectrum from the many emission bands present. For the interval covered by the observations three spectral regions were chosen as being relatively free from emission, as follows: (1) the region between $H\epsilon$ and $H\delta$, denoted in the table by 4000 A; (2) the region between 4700 A and $H\beta$, denoted by 4800 A; and (3) the region between 6000 A and $H\alpha$, denoted by 6200 A. The gradients which determine the color temperatures were derived only from these spectral regions.

TABLE I

COLOR TEMPERATURES OF NOVA HERCULIS

Date (G.C.T.)	Spectral Regions	T_c	Wt.	Remarks
1934 Dec. 30.448	4000–4800 A	11,700° K	1	
1935 Jan. 4.461	4000–6200	10,900	1	
23.444	4000–4800	7,800	½	Clouds during exposures
24.474	4000–4800	13,000	1	
30.492	4000–6200	11,700	1	
Feb. 6.478	4000–4800–6200	10,200	2	Mean of two plates
13.470	4000–4800–6200	10,000	2	Mean of two plates
27.445	4000–4800	7,900	1	

The observations are not corrected for atmospheric extinction, such correction awaiting the determination of atmospheric absorption at Ann Arbor. The observations were made, as far as possible, so that small differences in zenith distances existed between the nova and the comparison stars. It should be noted that all the temperatures will be raised by the application of this correction. The weighted mean of the observations gives the result

$$T_c = 10{,}500^\circ\text{K} \pm 370^\circ ,$$

the probable error being derived from the internal agreement of the observations. There appears to be some decrease in temperature after January 4, but the evidence is not conclusive. Extinction corrections will, however, increase this tendency. Comparison with other results can only be indicated at present. Balanowsky[3] reports a color temperature, on December 24, of 6500° K relative to Vega, but the adopted temperature of the comparison star is not stated.

[3] *A.N.*, **254**, 155, 1935.

Meyermann[4] states that the nova, on January 15, had a lower color temperature than the comparison star ι Herculis (B_3).

Since February 27, color temperature observations of the nova have been continued with respect to ι Herculis. When the color temperature of the latter is determined on the Greenwich system, these observations will be expressed as color temperatures.

R. M. PETRIE

THE OBSERVATORY
UNIVERSITY OF MICHIGAN
March 20, 1935

SPURIOUS CORRECTION OF RADIAL VELOCITIES IN THE *CAPE ANNALS*

ABSTRACT

Attention is called to spurious corrections applied to the measures of radial velocities made with the Hartmann comparator at the Cape Observatory.

In Volume **10,** Part VIII, of the *Annals of the Cape Observatory* an error occurs affecting Section A, "The Spectroscopic Determination of the Constant of Aberration and of the Solar Parallax." In this section a correction has been made for differences in the scales of the plates measured on the Hartmann comparator. This correction is referred to on page 6: "In the measurements for the derivation of the constant of aberration, however, the small differences in scale from plate to plate were allowed for," and on page 13: "The fifth column gives the factor, by means of which differences in scale were allowed for, as explained below."

The formulae for the derivation of the scale-correction factor are given on pages 13–14. This correction is based on a misunderstanding of the principle of the Hartmann spectrocomparator. As is well known, the measures are made in terms of micrometer movements of a standard plate. It is the scale of the standard plate alone which matters and which has to be accurately determined.

The plate to be measured against the standard is optically adjusted to appear in the microscopes as of the same scale as the stand-

[4] *Ibid.*, p. 158.

ard plate in any one field of view. As the standard plate alone is moved the measures are in terms of the standard plate and any difference of scale in the two plates is eliminated optically. Naturally if, say, corresponding iron lines are made to appear coincident in the center of the field at one end of the stretch of spectrum to be measured, they will not coincide at the other end of the stretch of spectrum if the actual scales of the two plates are not identical, and no optical adjustment will make them coincide. That is quite impossible. The micrometer movement of the standard plate required again to bring corresponding lines into coincidence is a measure of the difference of length of the stretch of spectrum to be measured. This has nothing whatever to do with the optical adjustment of the two spectra so that they appear to be of the same scale. The scale-correction factor on page 13 is therefore superfluous and introduces an error into the computations. It was not applied to the major portion of the work on radial velocities appearing in the same volume.

JOSEPH LUNT

November 7, 1934

NOTE ON THE FOREGOING PAPER BY DR. LUNT

Shortly after the publication of *Cape Annals*, Volume **10**, Part VIII, Dr. Lunt drew my attention to the fact that the scale corrections applied to the measures made with the Hartmann comparator and given in Section A were incorrect in theory. I am in full agreement with this. It is obvious that the comparator can be used to compare two plates with widely different scales and that the difference in scale will necessitate a progressive micrometer shift of the standard plate to bring about coincidence in successive regions of the spectrum; this progressive shift is entirely independent of the precise optical adjustment of the two spectra by which they appear of the same scale in the microscope eyepiece.

The plates to which the corrections were applied had been measured, as explained (*op. cit.*, p. 10), many years before and the corrections were applied at that time. The extreme range of temperature was only about 10° F.; the corrections were, therefore, in all cases very small. Though they actually determine the difference in scale

between the standard plate and the comparison plate, any such difference is automatically compensated for in the design of the comparator and no corrections need be applied.

The important matter is whether the application of these corrections produces any appreciable effect on the final value of the constant of aberration. It might seem at first sight that there would be a systematic effect due to a possible small systematic change in scale between summer and winter. Though the effect for any individual star would tend to be systematic, the effect becomes of an accidental nature for a series of stars well distributed in right ascension, for the corrections to the sun in the case of two stars observed at the same season of the year, whose right ascensions differ by twelve hours, are approximately equal in magnitude but opposite in sign.

An approximate estimate which I made while at the Cape by using a mean correction for each star at each epoch satisfied me that the final effect on the deduced value of the aberration constant was negligible and that a more detailed examination was not necessary.

H. SPENCER JONES

INDEX TO VOLUME 81

SUBJECTS

AUTHORS